Mechanistic Load Restriction Decision Platform for Pavement Systems Prone to Moisture Variations

National Road Research Alliance

MnDOT Contract 1034192 Task 4: Sensitivity Analysis and Framework Refinement

Prepared by:

S. Masoud Mousavi
Majid Ghayoomi
Eshan V. Dave

Department of Civil and Environmental Engineering
University of New Hampshire

Published by:

Minnesota Department of Transportation
Research Services & Library
395 John Ireland Boulevard, MS 330
St. Paul, Minnesota 55155-1899

TABLE OF CONTENTS

LIST OF FIGURES

LIST OF TABLES

CHAPTER 1: INTRODUCTION

1.1 RESEARCH PROJECT ABSTRACT AND OBJECTIVES

Excess moisture in aggregate base and subgrade soil has detrimental impacts on longevity and serviceability of pavements. Seasonal ground water level fluctuations, inundations due to storms and post-storm recess, frost penetrations and freeze-thaw effects lead to continuous moisture hysteresis and change of stress states in pavement foundation. Current analysis and design procedures rely on approximate empirical approaches, which renders their ability to incorporate moisture-dependency and to conduct real-time and forecasted pavement capacity and load restriction analyses. A load restriction decision platform is proposed to provide a reliable and mechanistically-informed tool for pavement engineers to assess pavement performance and make traffic allowance decision during and after periods of excessive moisture. This platform encompasses three core attributes: (1) A mechanics-based model that correctly captures soil and base response to saturated and unsaturated soil states. It will be validated using actual field pavement tests such as MnROAD and can be further enhanced through the use of physically modelled scaled pavement sections; (2) a system-based approach to integrate impacts of various stressors (soil moisture state, vehicular loads and volume, climatic conditions etc.), current pavement conditions, subgrade properties, hydro-geology, and short-term climate forecast. Due to large number of variables and their inter-dependencies, a system dynamics modelling approach can holistically capture all significant variables and provide a user-friendly system for pavement load restriction decision making; and (3) a policy-informed decision-platform that incorporates inputs from transportation agencies and users to facilitate its implementation and to realize the cost-effectiveness of such mechanistic approach.

1.2 SUMMARY OF RESEARCH METHODOLOGY (SCOPE)

This project is developing a mechanistic pavement load restriction decision framework using system dynamics approach. The main outcome of this project will be a toolkit for pavement engineers to make decisions regarding load restrictions due to seasonal soil moisture variations as well as during post-flooding instances. The use of system-based approach is necessary to integrate impacts of various stressors (soil moisture state, vehicular loads and traffic volume, climatic conditions etc.), current pavement conditions, subgrade properties, hydro-geology, and short-term climate forecast. Due to a very large number of variables and their inter-dependencies, a system dynamics modelling approach can holistically capture all significant variables and provide a user-friendly tool for pavement load restriction (both in current time and for future forecasting) decision making. This research is divided into 10 tasks. The study initiated with development of an initial memo to quantify research benefits and potential implementation steps (Task 1) and literature review (Task 2). This was followed with development of the system dynamics framework to mechanistically evaluate pavement load restrictions (Task 3). The next steps in this research are to simultaneously undertake tasks of conducting sensitivity analysis of the system dynamics model (Task 4) and developing a user-friendly toolkit that can be readily implemented for a pavement load restriction decision process (Task 5). This report details the research activities of Task

4. Using information from MnROAD (and other agency data if made available to researchers) on pavement sub-surface moisture states and pavement surface deflections (from FWD testing), researchers will calibrate and validate the toolkit in Task 6. Task 8 will finalize the quantification of research benefits and provide guidance on implementation of the research products. Task 7 is out of state travel for researchers to present findings of this project at the annual meeting of the Transportation Research Board and Tasks 9 and 10 will develop and revise the final report for the study.

This report serves as the primary deliverable for Task 4 (Sensitivity Analysis and Framework Refinement) of the study.

1.3 ORGANIZATION OF THE REPORT

This report is organized in 6 chapters. The subsequent six chapters review the developed system dynamics model and the sensitivity analysis of the developed model. This includes a brief overview of the developed system dynamics model for evaluating pavement response to traffic loading during moisture variations (chapter 2) that was previously discussed in Task 3 report in detail, the methodology for sensitivity analysis (chapter 3), local sensitivity analysis to identify the important parameters (chapter 4), and global sensitivity analysis to identify main contributors in overall system response (chapter 5). Lastly, a summary is provided in chapter 6 that highlights the key findings from the proposed system dynamics framework and briefly describes the on-going and upcoming research tasks in this study.

CHAPTER 2: Overview of the Developed System Dynamics Framework

2.1 INTRODUCTION

A System dynamics-based approach was adopted in this study to integrate and understand complex interaction of key factors affecting the overall performance of flexible pavements prone to moisture variations. The model was developed to simulate the real time behavior of pavement systems due to moisture variations. Three main structures including hydrological, geotechnical, and pavement response structures were identified to be crucial in order to develop the System dynamics model (SDM). A detailed discussion on components and variables required to model each structure and the interaction between them was provided in task 3 deliverable report. This chapter briefly review the developed SDM and its key components in simulating moisture movement and pavement system performance during moisture variations. In addition, the improvements in the framework since Task 3 report are discussed in this chapter.

2.2 DEVELOPED SYSTEM DYNAMICS FRAMEWORK

Figure 2-1 presents the three major structures of the SDM and the interaction between them and their variables. The first step in the mechanistic analysis of pavement response to moisture variations is the simulation of moisture movement in pavement layers. This is performed through the hydrological structure. The hydrological structure consists of two main components; (1) climate information and (2) unsaturated soil hydraulics. The climate information provides material and information data that controls water flux into and out of the soil surface (i.e., flows associated with water infiltration and discharge). A summary of the input variables associated with the climate information is provided in Table 2-1.

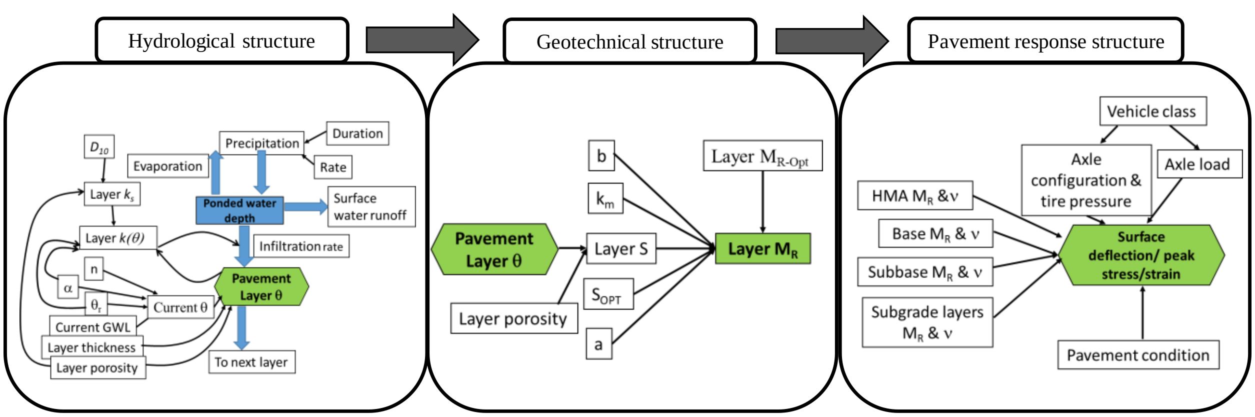

Figure 2-1: A conceptual schematic of the SDM structures and their variables.

Table 2-1: A summary of the variables associated to climate information.

Climate information	Variables	Note
Precipitation	Rate (P_r) and duration (P_d)	Can be input based on real or forecast precipitation time history
Evaporation	Rate (E_r)	Can be input based on real or forecast evaporation time history
Ponded water	Height of accumulated water above natural subgrade (H_P)	Can be input based on real or forecast climate condition
Surface water runoff	Rate (SR_r)	Zero for pavements located on "flat natural ground" with poor drainage system, otherwise equals precipitation minus infiltration and evaporation

The second component in hydrological structure of the SDM is the unsaturated soil hydraulics. This component includes the variables and governing equations related to estimation of initial pavement layers' moisture content, moisture movement in unsaturated pavement layers, and their time dependent moisture content. The initial moisture content of the layers is estimated based on layers' soil water retention curve (SWRC) data and initial ground water level (GWL) where GWL is defined as the depth of ground water from subgrade soil surface. It is noteworthy that the infiltration process in this study was assumed to occur through pavement shoulders. Since the permeability of aggregate base and subbase layers are typically much higher than natural subgrade soil, the infiltration of water through these layers may result in ponding of water above subgrade layer. Therefore, the degree of saturation in these layers is governed by both water infiltration in these layers and ponded water height above the subgrade. Accordingly, the aggregate base and subbase layers' degree of saturation are calculated based on the weighted average of the inundated portion and the unsaturated portion of each layer. The moisture movement in subgrade soil is governed by its hydraulic properties including saturated and unsaturated hydraulic conductivity and moisture content. The methodology and governing equations for simulating moisture movement in unsaturated subgrade layers and estimating their time dependent moisture content were elaborated in Task 3 and Task 2 deliverables reports (Ghayoomi et al. 2019; Mousavi et al. 2020). A summary of input parameters for unsaturated soil hydraulic component of the hydrological structure is provided in Table 2-2.

The second structure in the SDM is the geotechnical structure. The geotechnical structure incorporates the time dependent moisture content of pavement layers estimated from the hydrological structure to estimate their resilient modulus. This is performed by using Equation 2-1 which estimates unbound pavement layers' resilient modulus (M_R) based on their resilient modulus at the optimum degree of saturation ($M_{R\text{-}OPT}$) (Zapata et al. 2007).

$$\boldsymbol{log\left(\frac{M_R}{M_{R-OPT}}\right) = a + \frac{b-a}{1+exp\left[ln\left(-\frac{b}{a}\right)+k_m(S-S_{OPT})\right]}}$$

Equation 2-1

where S_{OPT}= degree of saturation at optimal water content (in decimals); a= minimum of log ($M_R/M_{R\text{-}OPT}$); b= maximum of log-log ($M_R/M_{R\text{-}OPT}$); and k_m= regression parameter. Table 2-3 summarizes the required input values for geotechnical structures and their values.

Table 2-2: Required input parameters for simulation of moisture infiltration through the SDM.

Parameters	Description	Note
K_s	Pavement layer saturated hydraulic conductivity	Required for base, subbase, and subgrade. Can be estimated based on empirical equations.
α_{vG} and n_{vG}	van Genuchten 1980 SWRC fitting parameters	Required for subgrade.
θ_r	Pavement layer residual volumetric water content	Required for base, subbase, and subgrade.
θ_s	Pavement layer saturated water content	Required for base, subbase, and subgrade.
Initial GWL	Initial ground water level	-
Th_{Base}	Base thickness	-
$Th_{Subbase}$	Subbase thickness	-

Table 2-3: Required input parameters in the geotechnical structure of the SDM.

Parameters	Value/note
a	=-0.3123 for coarse grained soils =-0.5934 for fine grained soils
b	=0.3 for coarse grained soils =0.4 for fine grained soils
S_{OPT}	Depends on soil type/initial conditions. Can be estimated based on empirical equations.
k_m	6.8157
$M_{R\text{-}OPT}$	Can be estimated based on pavement layer type and properties, or obtained from field/lab tests

Lastly, the pavement response structure incorporates the results of hydrological and geotechnical structures along with traffic load information to predict pavement response in terms of surface deflection time history. The input variables required to estimate pavement response include those related to mechanical pavement layers properties and traffic loading. A summary of these parameters is presented in Table 2-4.

Table 2-4: Required input parameters in the pavement response structure of the SDM.

parameter	Note
Asphalt concrete resilient modulus ($M_{R,AC}$)	Depends on pavement current condition
Asphalt Concrete thickness Th_{AC}	-
Layer Poisson's ratio (ν)	Required for each pavement layer
Tire pressure	Depends on vehicle type
Wheel load	Depends on vehicle type

2.3 SUMMARY

This chapter reviewed the structures and components of the developed system dynamics model for evaluation of surface deflection of flexible pavement systems during moisture variations. In general, 32 input variables are required to estimate surface deflection of a flexible pavement system during moisture variations. These variables are subject to uncertainty, so sensitivity analysis is an important task for understanding the significance of each parameter on the SDM output and the reliability of simulation results. Following chapters describe comprehensive sensitivity analyses and statistical modeling to address this challenge.

CHAPTER 3: Methodology for Sensitivity Analysis

3.1 INTRODUCTION

Accurate estimation of pavement performance during moisture variations relies on a sound understanding of the key contributing parameters and their interaction in the system. However, the collection of accurate information about all contributing parameters, such as subgrade hydraulic conductivity, may not be feasible. Large number of variables and their interaction within the system, and high uncertainties in their values warrant a detailed understanding of the significance of various uncertainties on the performance of flexible pavements. This can be addressed by sensitivity analysis which shed light on how variations in output (i.e., surface deflection) can be apportioned to different source of variations (e.g., subgrade hydraulic conductivity). Furthermore, sensitivity analysis not only determines the significance of each parameter on the model output, but it also helps to develop intuition about model structure and guides the data collection efforts based on significance of the parameter of interest. In other words, the sensitivity analysis could identify the need for additional data collection for the parameters that significantly impact the output behavior (Saltelli et al. 2008).

Uncertainties in physical phenomena are often analyzed using two major sensitivity analyses approaches; (1) local sensitivity analysis method (LSA), and (2) global sensitivity analysis (GSA) (Tang et al. 2007; Wei 2013). The LSA techniques are also referred as to univariate sensitivity analysis and commonly investigate the individual effects of each input parameter while other parameters are maintained at a reference value. Although these methods require relatively low computational demand, the sensitivity results are dependent on and may only be valid for the select reference values. For the systems with high number of variables, such as flexible pavement systems, nonlinear interactions among variables may become more significant. The local sensitivity analysis methods, however, are not able to capture this. On the other hand, global sensitivity analysis methods use a multivariate analysis approach and consider a wide range of variables and the high-ranking interaction between them. Considering that a large number of input parameters are involved in the SDM, GSA methods require a significantly large number of simulations to reliably identify the significance of each parameter. However, this is not computationally feasible. In order to address this challenge, an LSA was first performed to understand the significance of each input parameter in overall system behavior (i.e., surface deflection time history). Then, the most significant parameters were identified and refined to conduct a GSA. Following sections describe the methodologies for performing LSA and GSA in this study.

3.2 METHODOLOGY FOR SDM SENSITIVITY ANALYSIS

Sensitivity analysis of a system response requires identification of independent input variables contributing to the overall system behavior. Therefore, the first step in sensitivity analysis was to identify independent input parameters in the SDM. Then, possible range of each input parameter was determined by using published information or assigning logical values. The next step was to use a sampling strategy to conduct simulations for the select range of the variables. Depending on the sensitivity analysis method (i.e., LSA versus GSA) several numbers of simulation were performed using the programed SDM in Vensim

Pro® and the response was obtained in terms of surface deflection time histories. Since the behavior of the surface deflection is dependent on time, the evaluation of the sensitivity of response to select parameters was evaluated in terms of time dependent behavior and selected "performance measure indices". The performance measure indices determine the key performance attributes during a moisture variation event (e.g., peak surface deflection during and after moisture variation event). Lastly, the results were statistically analyzed using regression method and each parameter was ranked based on its significant importance. The following sections provide relevant information about above mentioned steps.

3.2.1 Selection of Input Parameters and Their Ranges

The primary goal of this section is to identify the least number of interdependent variables and their ranges to run sensitivity analysis and to assign reference values for local sensitivity analysis. In general, 32 input variables were identified in the SDM. These include variables associated with the (1) climate data, (2) unsaturated soil hydrology, (3) geotechnical structure, and (4) pavement response structure. For climate data, precipitation rate, duration, and evaporation rate were considered as independent variables for the sensitivity analysis. Surface water runoff which results in removal of excess moisture from the pavement foundation (i.e., AC, aggregate base, and subbase layers) was considered to be zero in this study. Table 3-1 summarizes the range of climate data input variables.

Table 3-1: A summary of the climate input parameters and their ranges considered for sensitivity analysis.

Variables	Ranges	Reference value
Precipitation rate (P_r)	0 to 0.1 m/hour (~0 to 4 inch/hour)	0.05 m/hour (~ 2 inch/hour)
Precipitation duration (P_d)	5 to 20 hours	10 hours
Evaporation rate (E_r)	0.0001 to 0.001 m/hour (~ 0.004 to 0.04 inch)	0.005 m/hour (0.2 inch/m)

The parameters required for unsaturated soil hydrological component and geotechnical structure of the SDM are to be selected for aggregate base and subbase, and subgrade soil. In this study, it was assumed that the base and subbase layers consist of granular material. Table 3-2 presents the reference values and the ranges of parameters for aggregate base and subbase layers.

Table 3-2: Base and subbase variables and their reference values.

Parameters	Description	Range	Reference value
$K_{s,Base}$	Base hydraulic conductivity	12 to 160 m/hour (472 to 6300 inch/hour)	50 m/hour (~1968 inch/hour)
$K_{s,Subbase}$	Subbase hydraulic conductivity	4 to 40 m/hour (157 to 1574 inch/hour)	12 m/hour (~472 inch/hour)
Th_{Base}	Aggregate base thickness	0 to 0.5 m (~20 inch)	0.3 m (~12 inch)
$Th_{Subbase}$	Subbase thickness	0 to 0.3 m (~0 to 12 inch)	0.1 m (~4 inch)
$a_{base}= a_{subbase}$	Equation 2-1 fitting parameters	-	-0.3123
$b_{base}= b_{subbase}$	Equation 2-1 fitting parameters	-	0.3
$S_{OPT-Base}$	Base optimum degree of saturation	-	0.45
$S_{OPT-Subbase}$	Subbase optimum degree of saturation	-	0.5
$M_{R-OPT,Base}$	Base optimum resilient modulus	200 to 300 MPa (~ 29 to 43 ksi)	250 MPa (~36 ksi)
$M_{R-OPT,Subbase}$	Subbase optimum resilient modulus	100 to 200 MPa (~14 to 29 ksi)	150 MPa (~22ksi)

Among the required input parameters for simulation of moisture movement in unsaturated subgrade layers, saturated hydraulic conductivity and van Genutchen (1980) SWRC model's fitting parameters are interdependent. In order to define independent parameters and their ranges for subgrade, these variables were estimated based on fundamental soil properties. Due to difference in material properties of fine-grained and coarse-grained soils, two types of subgrade soils were considered, and two sets of sensitivity analysis were performed, accordingly. The subgrade soil for the first set was assumed to be a coarse-grained soil (such as, fine sand) and the second set assumed a fine-grained soil with variable plasticity (representative of clayey or silty soil).

For the first set of sensitivity analysis, the hydraulic conductivity of sand was estimated based on its void ratio (e) and effective grain diameter (D_{10}); according to Equation 3-1 presented in Table 3-3. Parameters a_{vG} and n_{vG} were assumed to be linearly related to D_{10} where a_{vG}= 5 m^{-1} at D_{10}= 0.07, a_{vG}= 25 m^{-1} at D_{10}= 0.42, n_{vG}= 1.7 at D_{10}= 0.07, and n_{vG}= 3.7 at D_{10}= 0.42. Further, subgrade optimum resilient modulus ($M_{R-OPT,Subgrade}$) was assumed to be linearly correlated to its void ratio where $M_{R-OPT,Subgrade}$= 50 kPa at e= 0.8 and $M_{R-OPT,Subgrade}$= 150 kPa at e= 0.4. It should be noted that these assumptions are not intended to and may not provide an accurate estimation of the SWRC parameters and $M_{R\text{-}OPT,Subgrade}$. However, they can establish a logical interdependency between these parameters and soil properties for the purpose of sensitivity analysis. Table 3-4 presents the reference values and the ranges of parameters for the coarse-grained subgrade soil.

Table 3-3: Empirical relations for estimation of hydraulic conductivity of fully saturated soils.

Reference	Equation number	Hydraulic conductivity (cm/s)	Notation	Remarks
(Chapuis 2004)	Equation 3-1	$k_s = 2.46[D_{10}^2 \frac{e^3}{(1+e)}]^{0.78}$	e= void ratio of soil D_{10}= effective grain diameter	Applicable for uniform gravel and sand and non-plastic silty sands
(Mbonimpa et al. 2002)	Equation 3-2	$k_s = C_p \frac{\gamma_w}{\mu_w} \frac{e^{3+x}}{(1+e)} \frac{1}{\rho_s^2 w_L^{2\chi}}$	γ_ω=unit weight of water (kN/m3) μ_ω= Water dynamic viscosity (Pa·s) ρ_s= Density (kg/m^3) of solids W_L= Liquid limit (%) x= $7.7w_L^{-0.15}$-3	Applicable for plastic soils, $\gamma_\omega \approx 9.8$, $\mu_\omega \approx 10^{-3}$, C_p=5.6, χ=1.5

Table 3-4: Subgrade variables and their reference values for the first set of the sensitivity analysis.

Subgrade soil type/Parameters	Description	Range	Reference soil/value
Sand	SW/SP/A-1b/A-3	Fine to medium sand	Fine sand
$D_{10\text{-}subgrade}$	Subgrade effective grain diameter	0.07 to 0.42 mm (~0.003 to 0.017 inch)	0.24 mm (~0.01 inch)
$e_{Subgrade}$	Subgrade void ratio	0.45 to 0.75	0.6
$K_{s,Subgrade}$	Subgrade saturated hydraulic conductivity	correlated to e and D_{10} (See Equation 3-1)	2 m/hour (~78 inch/hour)
α_{vG}	-	Linearly correlated to D_{10}	15
n_{vG}	-	Linearly correlated to D_{10}	2.7
$a_{Subgrade}$	Equation 2-1 fitting parameters	-	-0.3123
$b_{Subgrade}$	Equation 2-1 fitting parameters	-	0.3
$S_{OPT\text{-}Subgrade}$	Subgrade optimum degree of saturation	-	0.6
$M_{R\text{-}OPT,Subgrade}$	Subgrade optimum resilient modulus	linearly correlated to $e_{subgrade}$	100 MPa (~14.5 ksi)

For the second set of sensitivity analysis, the hydraulic conductivity of silt/clay was estimated based on its void ratio (e) and liquid limit (w_L); according to Equation 3-2 presented in Table 3-3. Parameters a_{vG} and n_{vG} were assumed to be linearly related to soil w_L where a_{vG}= 0.5 m^{-1} at w_L = 40, a_{vG}= 2 m^{-1} at w_L = 5, n_{vG}= 1.1 at w_L = 40, and n_{vG}= 1.5 at w_L = 5. Further, subgrade optimum resilient modulus ($M_{R\text{-}OPT,Subgrade}$) was assumed to be linearly correlated to its void ratio where $M_{R\text{-}OPT,Subgrade}$= 10 kPa at e= 1.5 and $M_{R\text{-}OPT,Subgrade}$= 100 kPa at e= 0.5. presents the reference values and the ranges of parameters for the fine subgrade subgrade soil.

Table 3-5: Subgrade variables and their reference values for the second set of the sensitivity analysis.

Subgrade soil type/Parameters	Description	Range	Reference soil/value
Clay/Silt	ML-CL/A-4 to A-6	Low plasticity silt/clay	ML
$w_{L,subgrade}$	Subgrade liquid limit	5 to 40	20
$e_{Subgrade}$	Subgrade void ratio	0.6 to 1.4	1
$K_{s,Subgrade}$	Subgrade saturated hydraulic conductivity	correlated to w_L and e (See Equation 3-2)	1.8×10^{-5} m/hour (~0.0007 inch/hour)
α_{vG}	-	Linearly correlated to w_L	1
n_{vG}	-	Linearly correlated to w_L	1.3
$a_{Subgrade}$	Equation 2-1 fitting parameters	-	-0.59
$b_{Subgrade}$	Equation 2-1 fitting parameters	-	0.4
$S_{OPT\text{-}Subgrade}$	Subgrade optimum degree of saturation	-	0.85
$M_{R\text{-}OPT,Subgrade}$	Subgrade optimum resilient modulus- linearly correlated to $e_{subgrade}$	-	55 MPa (~8 ksi)

The ground water depth from subgrade soil surface was assumed to range between 1 to 5 m for the sensitivity analysis and was assumed to be located at 3 m for the reference model. The reference values and the ranges of the parameters considered for the pavement structure analysis is shown in Table 3-6.

Table 3-6: Pavement response structure variables ranges and their reference values.

parameter	Range	Reference value
$M_{R,AC}$	700 to 7000 MPa	3000 MPa
Th_{AC}	0.05 to 0.5 m	0.15 m
AC Poisson's ratio (ν_{AC})	0.3 to 0.4	0.35
Base Poisson's ratio (ν_{Base})	0.25 to 0.4	0.3
Subbase Poisson's ratio ($\nu_{Subbase}$)	0.25 to 0.4	0.3
Subgrade Poisson's ratio ($\nu_{Subgrade}$)	0.3 to 0.5	0.4
Tire pressure	-	550 kPa
Wheel load	20 to 90 kN	45 kN

3.2.2 Univariate and Multivariate Sensitivity Simulations

Selection of an appropriate sampling methodology is the next step in sensitivity analysis after determination of independent parameters and their ranges. There are several sampling strategies such as random sampling using Monte Carlo (MC) simulation and Latin Hypercube Sampling (LHS). Monte Carlo simulation randomly assign N points for the selected ranges of the variables. However, this method relies on pure randomness of the input and may be inefficient in capturing the response ranges (i.e., requires a large number of simulations to minimize sampling error). On the other hand, LHS method spread the sample points more evenly across all possible values. The LHS method was used in this study for the sensitivity simulations. The simulation assumed a random uniform distribution for the ranges of input variables. For the univariate sensitivity simulations, each parameter was changed while the other parameters were kept at the reference values reported in Section 3.2.1. A minimum of 20 simulations were performed for each parameter using Vensim Pro® Sensitivity Simulation tool and the results were obtained in terms of surface deflection time history for each simulation. The multivariate sensitivity analysis was performed by simultaneously changing select variables using LHS method. This included 2000 simulations for each set of sensitivity analysis (i.e., coarse-grained subgrade and fine-grained subgrade).

3.2.3 Selection of Performance Measure Indices

After performing each set of simulations, the sensitivity simulation data including values of the model parameters and surface deflection time histories were obtained for each simulation run. Further, Vensim Pro® shows the confidence bounds for select variable and simulation run. For example, Figure 3-1 presents the estimated asphalt concrete (AC) surface deflection time history assuming reference values for the coarse-grained subgrade and Figure 3-2 illustrate 50%, 75%, 95%, and 100% confidence bounds for the analysis of sensitivity of AC surface deflection to subgrade D_{10}.

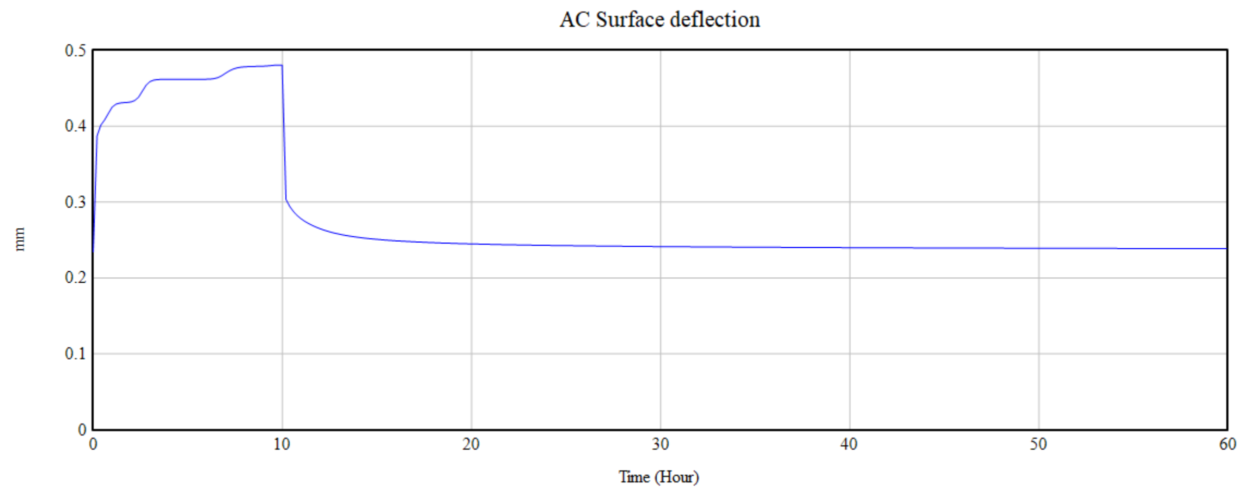

Figure 3-1. AC surface deflection time history of the coarse-grained subgrade reference model.

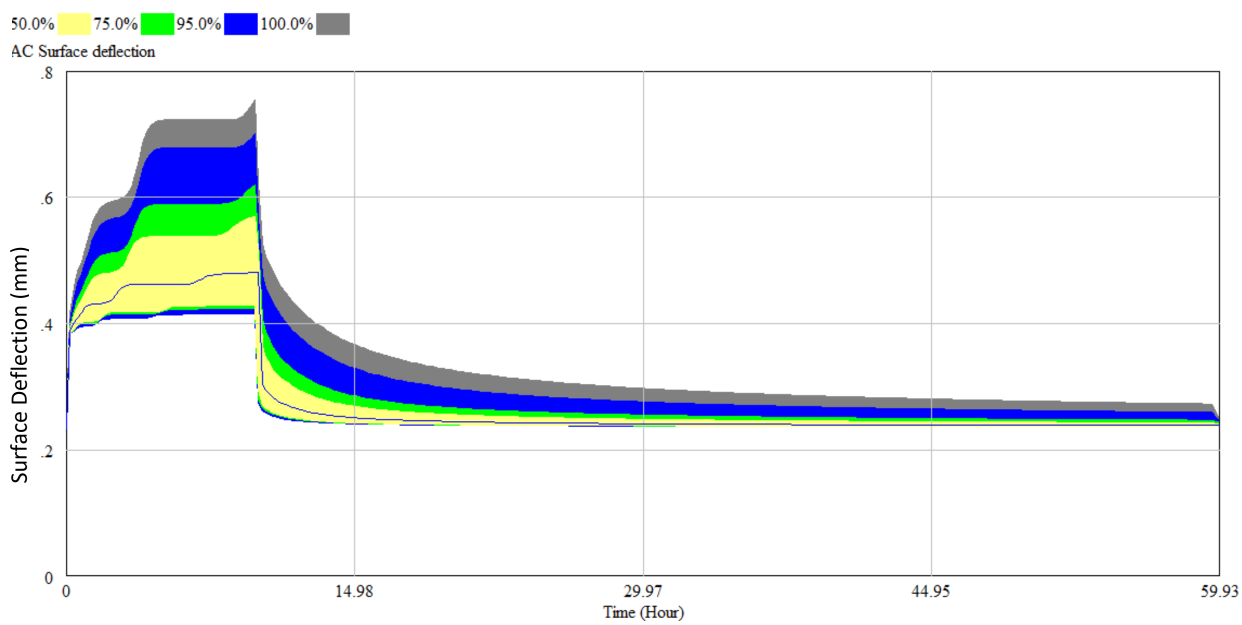

Figure 3-2. Sensitivity of AC surface deflection (mm) to subgrade D_{10}. Results show surface deflection time histories for 50%, 75%, 95%, and 100% Confidence bounds.

While the results in terms of time history provide useful information about the time dependent performance of the flexible pavement under moisture variation, further analysis is required to statistically quantify the significance of each parameter on pavement performance. In this regard, the time dependent performance of pavement was evaluated using four key performance index measures including (1) peak surface deflection (δ_p), (2) Peak to initial surface deflection ratio (δ_p/δ_0), (3) time to peak surface deflection (t_P), and (4) Recovery time ($t_{Rec.}$). The peak surface deflection shows the maximum surface deflection that the pavement would experience during a moisture variation event. The peak to initial surface deflection ratio is the ratio of the peak surface deflection to the surface deflection right before precipitation (i.e., Hydrostatic condition). Time to peak surface deflection shows the time required to reach the peak surface deflection and lastly, the recovery time measures the time that it takes to reach 80% recovery from the peak surface deflection. The recovery is defined as the ratio of current surface deflection to the peak minus the initial surface deflection.

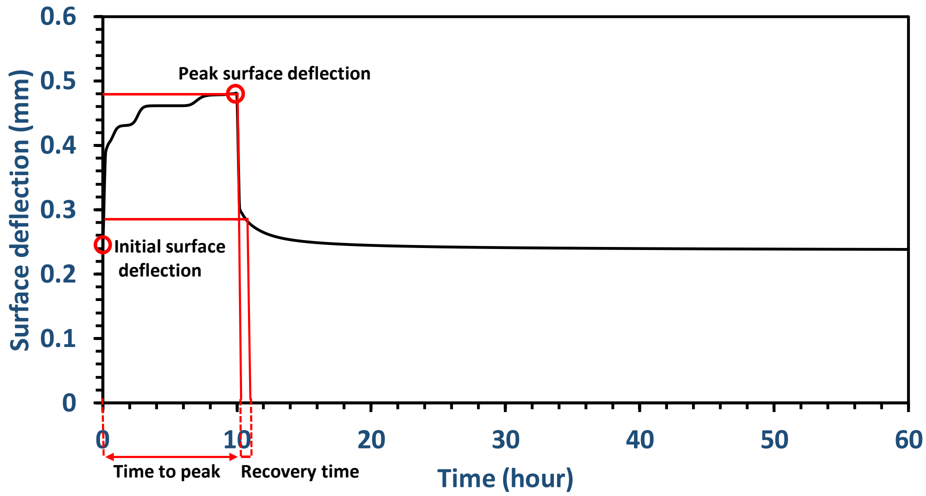

Figure 3-3. Performance measures used for sensitivity analyses.

3.2.4 Statistical Analysis

The extracted data for sensitivity simulations including values of input parameters and key performance measures were used for statistical analysis. In this study, linear regression method was utilized to comparatively evaluate the importance of each input parameter for each performance measure. In this regard, the data were analyzed using JMP software and standard regression coefficients including PValue, LogWorth, and t-ratio were used for statistical comparison of the significance of the effect of each parameter on the given performance measure.

CHAPTER 4: LOCAL SENSITIVITY ANALYSIS

4.1 INTRODUCTION

The local sensitivity analysis is intended to investigate the impact of uncertainty in individual variables on the system performance. This included two sets of sensitivity simulations for coarse-grained and fine-grained soils. The results were interpreted in terms of surface deflection time histories and performance measure indices introduced in Chapter 3. Following sections describe the local sensitivity analysis results for each set of simulations.

4.2 LOCAL SENSITIVITY ANALYSIS FOR COARSE-GRAINED SUBGRADE

4.2.1 Reference model response

Simulation of moisture variation impact on pavement surface deflection was performed using the developed SDM and the reference model values presented in Chapter 3. The results are shown in Figure 4-1. According to this figure, 10 hours of precipitation initially resulted in a dramatic increase in the AC surface deflection followed by a gradual increase in surface deflection. This is followed by a relatively quick recovery of surface deflection after the end of precipitation. The main reason for such behavior is the high hydraulic conductivity of the pavement layers which resulted in movement of the excess moisture out of the pavement layers.

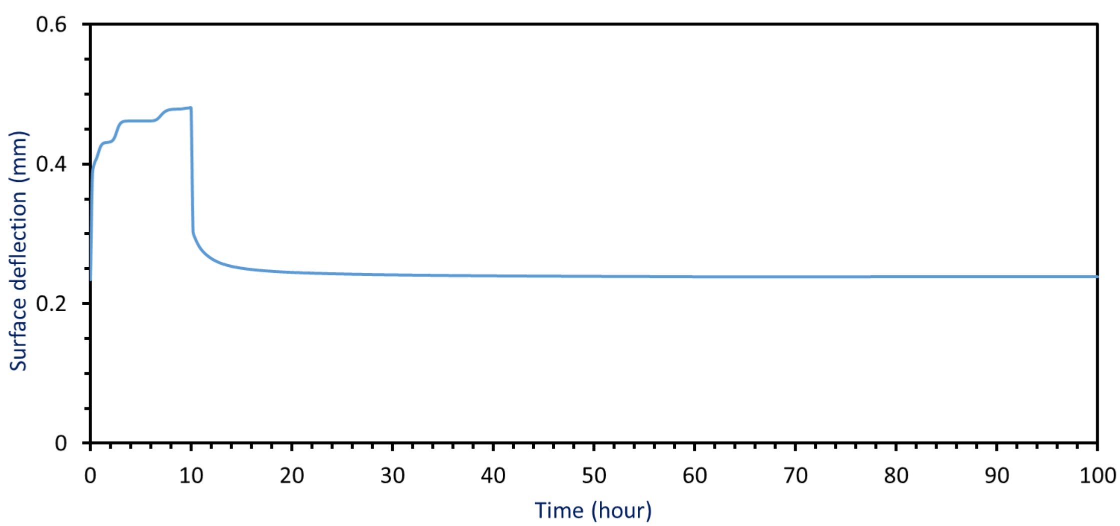

Figure 4-1. AC surface deflection time history of the coarse-grained subgrade reference model.

4.2.2 Univariate sensitivity simulation results

Univariate simulations were performed by changing an independent parameter while maintaining the other parameters at the reference model value. The reference model values and the ranges of each parameter for sensitivity simulations were reported in Chapter 3. The simulation results are interpreted and discussed in terms of key performance measures.

Sensitivity of peak surface deflection (δ_p):

Figure 4-2 presents the variations of peak surface deflection with subgrade D_{10}. Sensitivity simulations indicated that a reduction in D_{10} from the reference model value can considerably increase the peak surface deflection experienced during the moisture variation event (Figure 4-2a). According to Figure 4-2b, a 60% reduction in D_{10} resulted in almost 46% increase in δ_p, compared to the value for reference model. However, the impact of D_{10} on δ_p became less pronounced for D_{10} values higher than the reference value. For example, a 60% increase in D_{10} from the reference model resulted in only 12% reduction in δ_p (Figure 4-2b). These results suggest that for relatively medium to coarse sand particles, an increase in particle size has less significant impact on the pavement performance during moisture variation events. However, a decrease in particle size can potentially elevate the chance of damage to pavement structure.

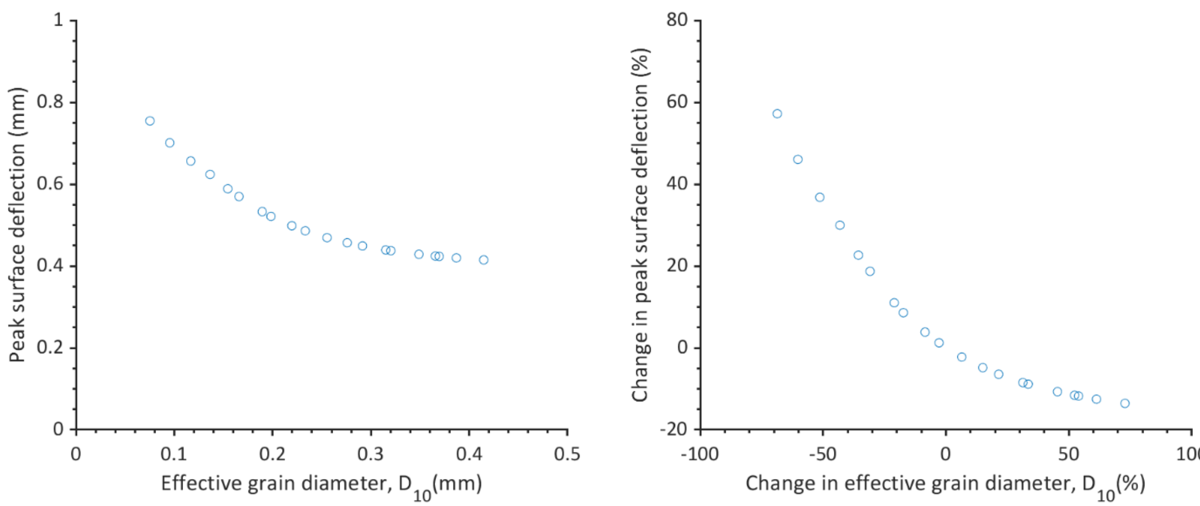

(a) (b)

Figure 4-2. Sensitivity of peak surface deflection to the variations of subgrade D_{10}. (a) Peak surface deflection versus D_{10} ; (b) change in peak surface deflection versus change in D_{10}.

The sensitivity of δ_p to subgrade void ratio was analyzed by changing void ratio values from 0.45 to 0.75. These values correspond to relative density, D_r= 12.5% and 87.5%, respectively, for the given soil. Figure 4-3 presents the sensitivity simulation results in terms of percent change in δ_p versus percent change in void ratio relative to the reference model values. The results indicate that a reduction in void ratio increases δ_p. The main reason for this observation is that in the SDM, the subgrade soil void ratio would impact both subgrade resilient modulus and its hydraulic conductivity. Although a soil with lower void ratio would have higher resilient modulus at a given moisture content, it would have lower hydraulic conductivity. This would result in poor drainage of water and potentially, elevation of excess moisture in pavement structural layers. Thus, higher surface deflection observed for the soil can be attributed to its lower hydraulic conductivity which result in poor drainage of water and inundation of pavement structural layers.

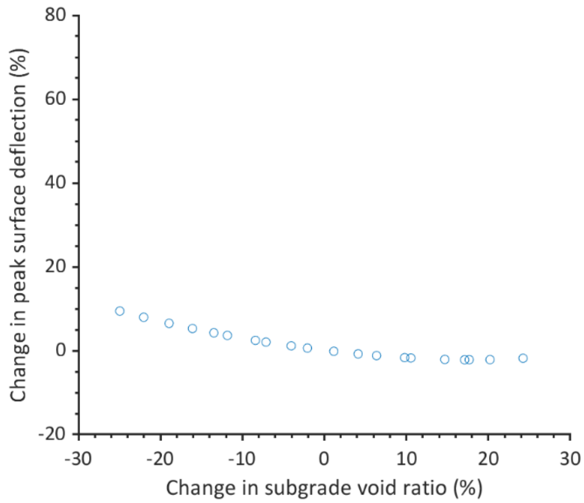

Figure 4-3. Sensitivity of peak surface deflection to the variations of subgrade void ratio.

Figure 4-4 illustrates the change in δ_p with precipitation rate and duration. Results indicate that while a change in precipitation rate is likely to have a substantial impact on pavement surface deflection, a change in its duration between the ranges tested in this study (i.e., 5 to 15 hours) is less likely to impact the magnitude of δ_p. The main reason for such observation is high hydraulic conductivity of the subgrade soil. In general, if the hydraulic conductivity of soil is higher than the precipitation rate, it is expected that the subgrade soil reaches the steady state infiltration at a given degree of saturation. In this case, an increase in precipitation duration would not impact the steady state degree of saturation of soil. However, a change in precipitation rate can alter the steady state infiltration rate and consequently the soil's degree of saturation.

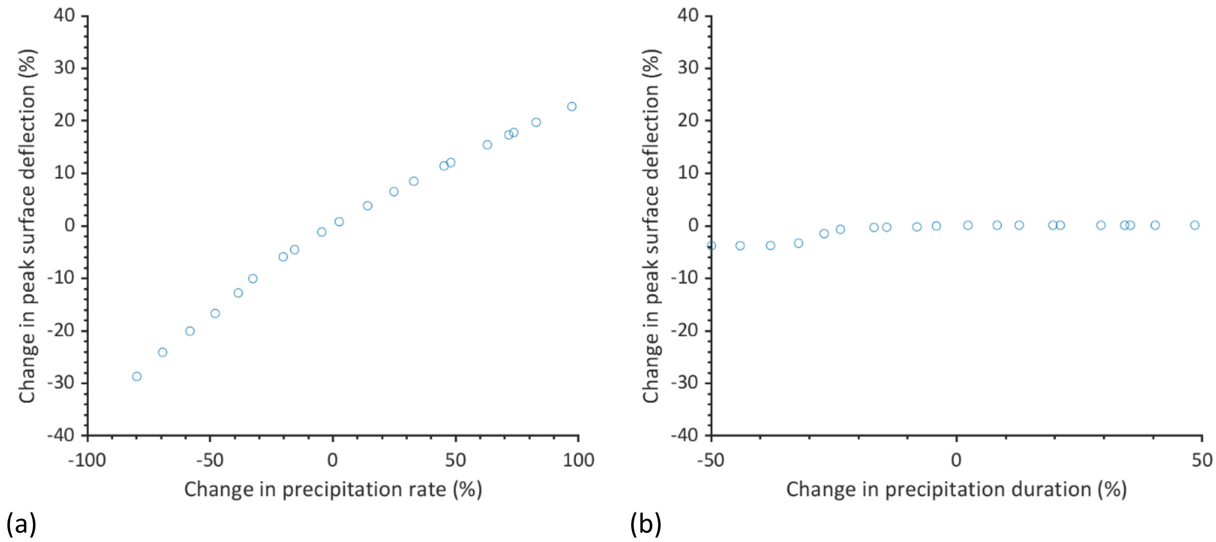

Figure 4-4. Sensitivity of peak surface deflection to the variations of precipitation (a) rate and (b) duration.

Figure 4-5 shows the results of sensitivity simulations for base and subbase optimum resilient modulus ($M_{R\text{-}OPT,Base}$ and $M_{R\text{-}OPT,Subbase}$, respectively). Results indicate that $M_{R\text{-}OPT,Base}$ and $M_{R\text{-}OPT,Subbase}$ are inversely proportional to δ_p. The comparison of $M_{R\text{-}OPT,Base}$ versus peak surface deflection curves and those of subbase indicate that a change in $M_{R\text{-}OPT,Base}$ would have higher impact on peak surface deflection than $M_{R\text{-}OPT,Subbase}$. Similar observations were also made for the comparisons of the impact of base and subbase thicknesses on peak surface deflection (Figure 4-6).

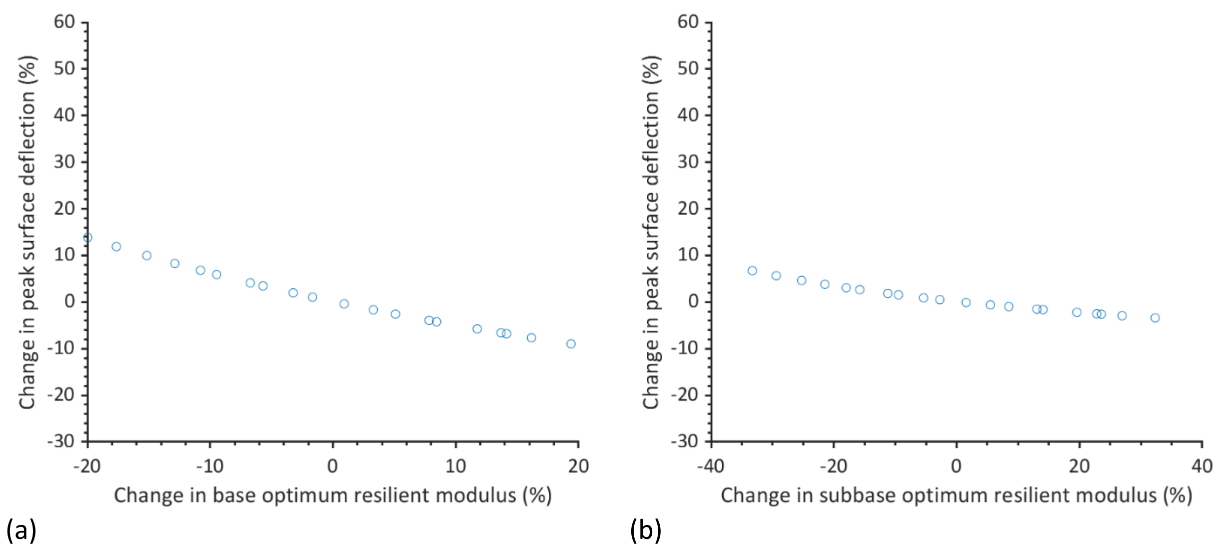

Figure 4-5. Sensitivity of peak surface deflection to the variations of (a) base and (b) subbase optimum resilient moduli.

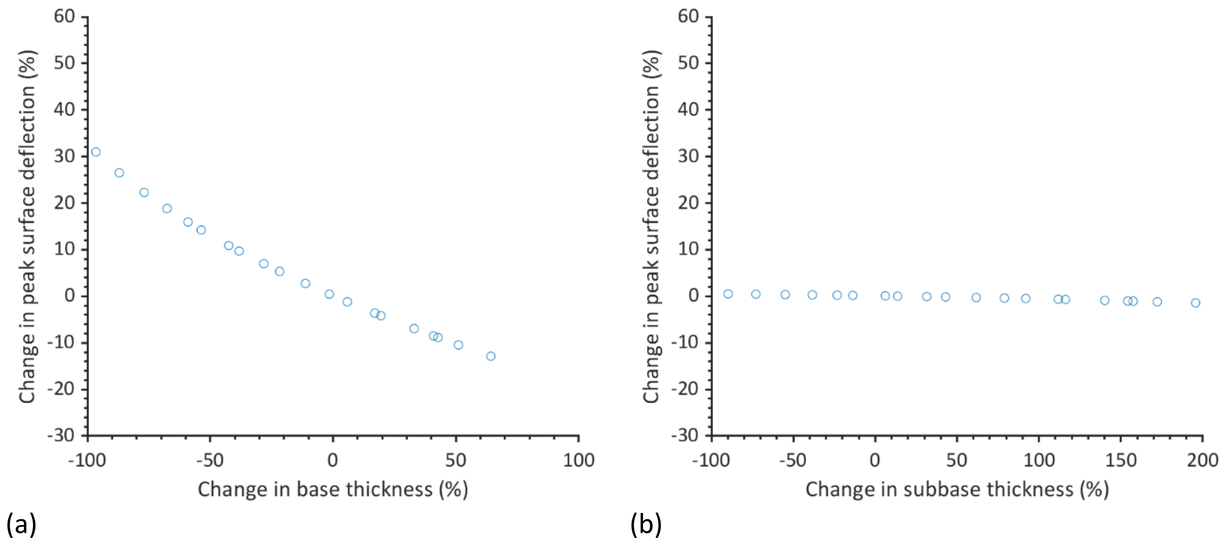

Figure 4-6. Sensitivity of peak surface deflection to the variations of (a) base and (b) subbase thicknesses.

Figure 4-7 presents variations in δ_p with changes in aggregate base and subbase hydraulic conductivities ($K_{s,Base}$ and $K_{s,Subbase}$, respectively). Results indicate a nonlinear relationship between peak surface deflection and $K_{s,Base}$ and $K_{s,Subbase}$, where reduction in the hydraulic conductivity increases the peak surface deflection. The results also indicate that peak surface deflection is more sensitive to change in aggregate base hydraulic conductivity than subbase.

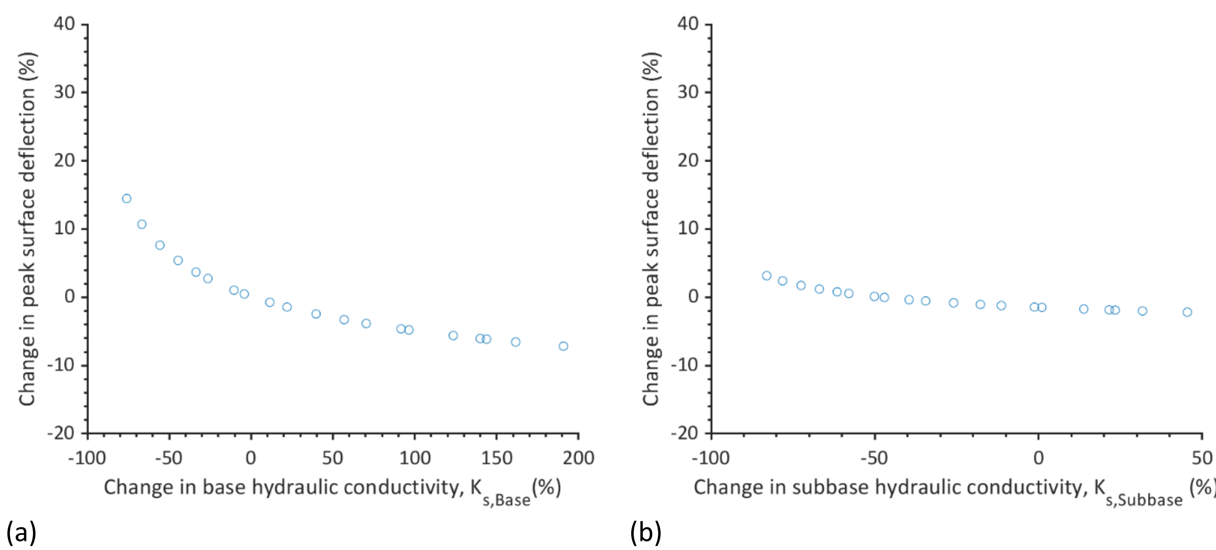

Figure 4-7. Sensitivity of peak surface deflection to the variations of (a) aggregate base and (b) subbase hydraulic conductivities.

Figure 4-8 presents the results of δ_p sensitivity simulations to changes in asphalt concrete resilient modulus ($M_{R,Ac}$) and thickness (Th_{AC}). Results show that a decrease in $M_{R,Ac}$ or Th_{AC} leads to a substantial increase in δ_p during a moisture variation event. However, peak surface deflection is more sensitive to a change in Th_{AC} than $M_{R,Ac.}$

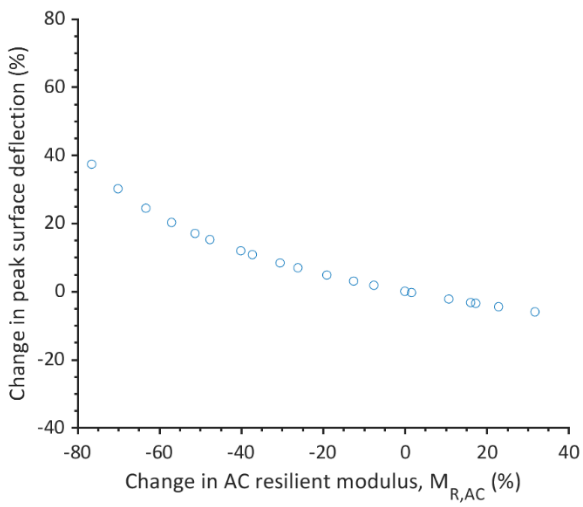

(a)

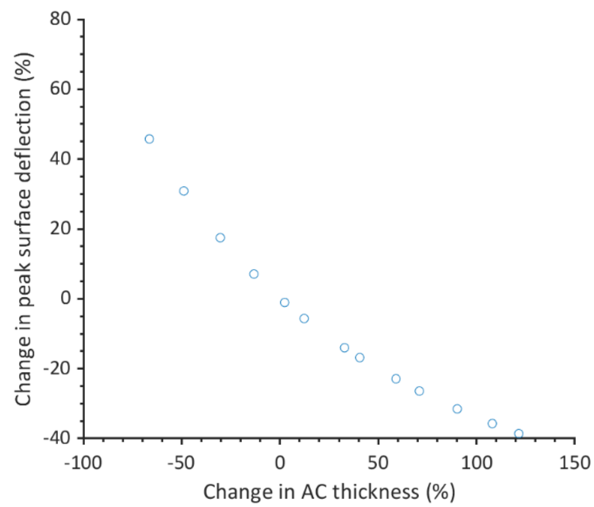

(b)

Figure 4-8. Sensitivity of peak surface deflection to the variations of (a) $M_{R,AC}$ and (b) Th_{AC}.

Figure 4-9 presents the variations of peak surface deflection with change in wheel load. Results indicate a substantial impact of wheel load on the peak surface deflection.

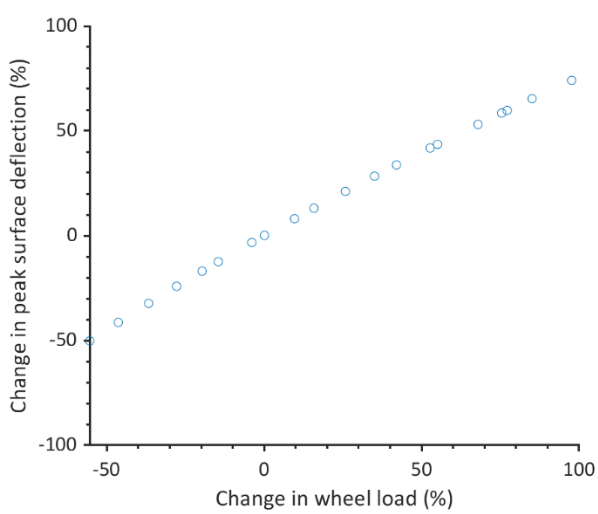

Figure 4-9. Sensitivity of peak surface deflection to the variations of wheel load.

For the ranges of GWL and layers' ν, and the reference model considered in this study, the sensitivity analyses indicated minimal impact of these variables on the δ_p. Results of sensitivity simulations for these parameters are shown in the Appendix.

Sensitivity of peak to initial surface deflection ratio (δ_p/δ_0):

Although peak surface deflection provides a good information about the impact of a certain variable on general performance of pavement, it provides little information on the extent of its impact during moisture variation compared to initial condition. For example, increase in $M_{R,AC}$ reduces both initial (i.e., before precipitation) and the peak surface deflection during moisture variation event. Therefore, peak surface deflection provides no information about the extent to which a change in $M_{R,AC}$ would impact pavement performance relative to the initial condition. For this purpose, the normalized peak to initial surface deflection defined in this study provides a better measure of the impact of a certain variable on the change in surface deflection during moisture variation events. This can be confirmed by comparing the results for sensitivity of δ_p and δ_p/δ_0 to $M_{R,AC}$ shown in Figure 4-10. According to this figure, while an approximately 80% reduction in $M_{R,AC}$ from the reference value (i.e., 3000 MPa) resulted in almost 40% increase in δ_p (Figure 4-10a), 80% reduction in $M_{R,AC}$ resulted in only a slight reduction in δ_p/δ_0.

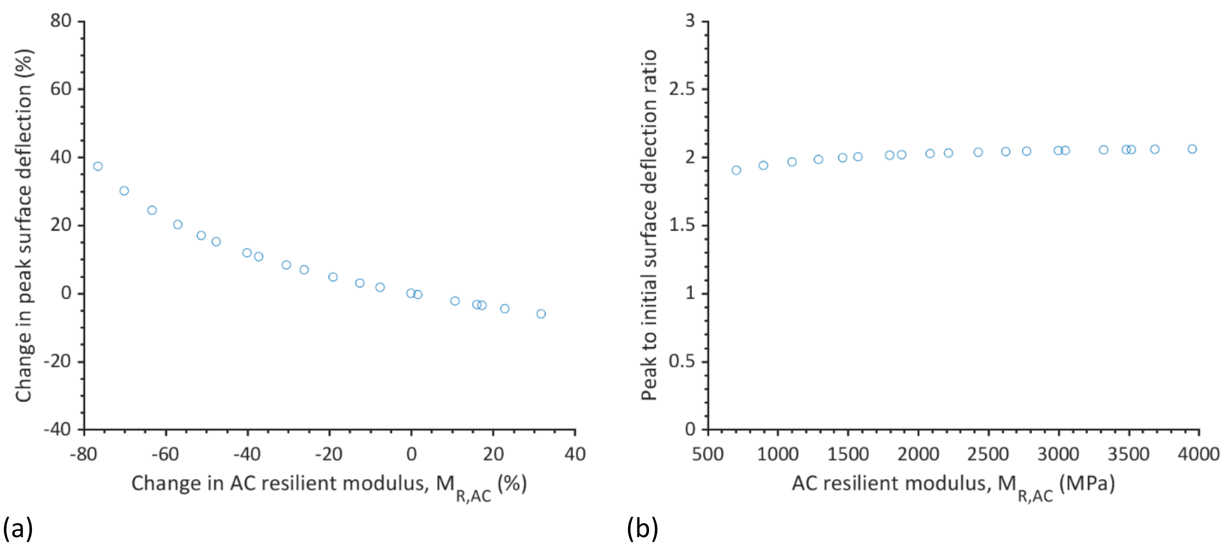

Figure 4-10. Comparison of δ_p and δ_p/δ_0 as the performance measure index; (a) sensitivity of δ_p and (b) Sensitivity of δ_p/δ_0 to $M_{R,AC}$.

Figure 4-11 illustrates the variation of δ_p/δ_0 with subgrade D_{10} and e. This figure shows similar trends between δ_p/δ_0–D_{10} and δ_p/δ_0–e curves to what were observed in δ_p–D_{10} and δ_p–e curves in Figure 4-2 and Figure 4-3, respectively. According to the results presented in Figure 4-11a, if two pavement systems with different subgrade D_{10} of 0.4 and 0.1 mm are subjected to a precipitation event, the one having the smaller D_{10} would experience a surface deflection approximately 200% higher than that of hydrostatic condition (before precipitation). On the other hand, for the pavement system with subgrade D_{10} of 0.4 mm, the same precipitation event would lead to only 60% increase in initial surface deflection. Since D_{10} and e are directly proportional to soil hydraulic conductivity, the results presented in Figure 4-11 indicate that a change in hydraulic conductivity of subgrade can considerably impact the extent to which an extreme climatic event can damage the pavement structure.

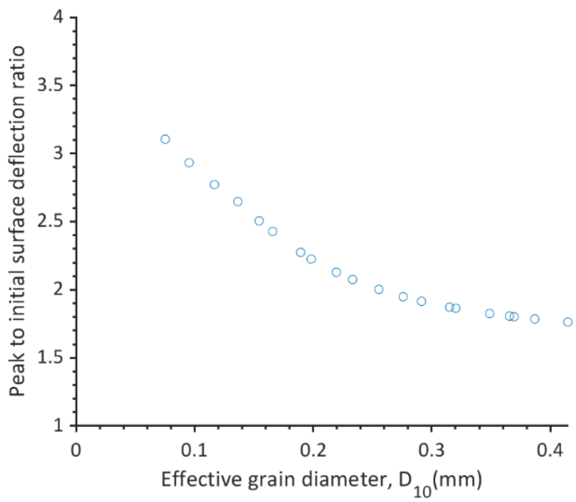

(a)

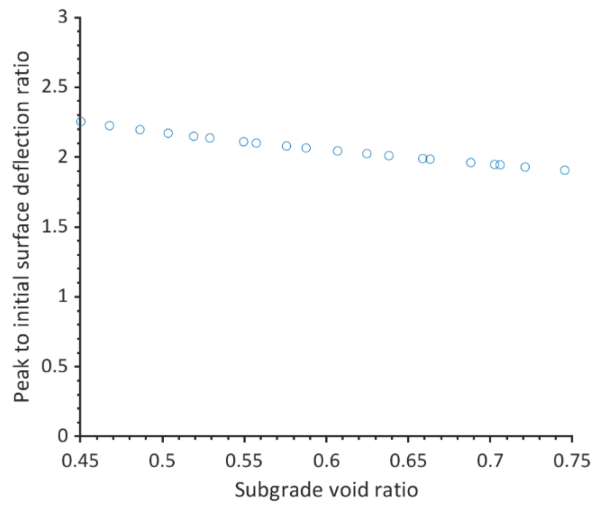

(b)

Figure 4-11. Sensitivity of δ_p/δ_0 to variation in subgrade (a) D_{10} and (b) e.

Results of analysis of sensitivity of δ_p/δ_0 to aggregate base and subbase saturated hydraulic conductivity yields similar conclusions to the subgrade saturated hydraulic conductivity. As it is shown in Figure 4-12, reduction in $K_{s,Base}$ or $K_{s,Subbase}$, can adversely impact the potential effects of a precipitation event on the integrity of a pavement system.

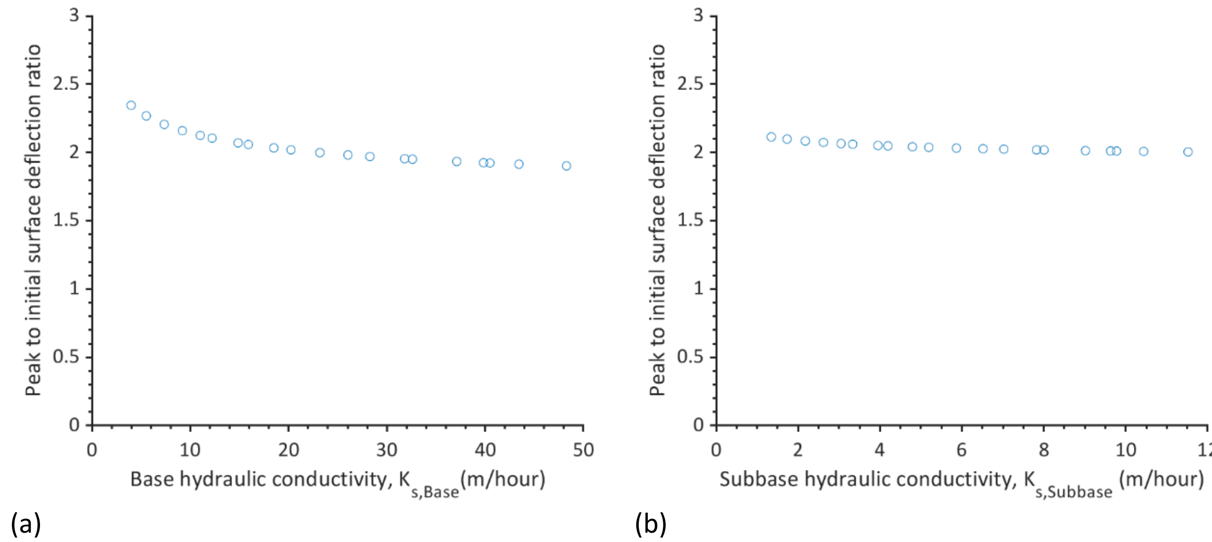

Figure 4-12. Sensitivity of δ_p/δ_0 to variation in saturated hydraulic conductivity of (a) aggregate base and (b) subbase.

Figure 4-13 presents the variation of δ_p/δ_0 with the precipitation rate. Results of sensitivity analysis show a substantial impact of precipitation rate on δ_p/δ_0. While a precipitation event with P_r= 0.02 m/hour results in approximately 50% increase in initial surface deflection, the surface deflection would increase up to 150% of its initial value for P_r= 0.1 m/hour.

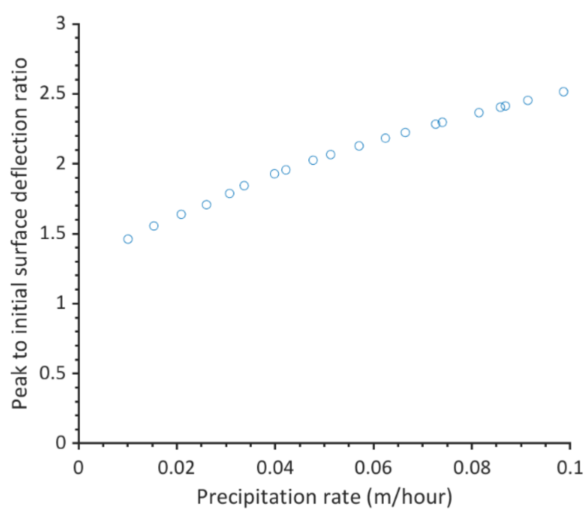

Figure 4-13. Sensitivity of δ_p/δ_0 to variation in precipitation rate.

The SDM simulations indicated that resilient moduli and thicknesses of pavement layers have minimal impact on δ_p/δ_0. This indicates that δ_p/δ_0 is mostly controlled through variables related to hydrology of the pavement system (e.g., hydraulic conductivity of layers and precipitation rate), rather than the variables that control the stiffness of the pavement system. It should be emphasized that this conclusion may hold valid only for the pavement systems with similar condition to the reference model evaluated in this study. A GSA is required to understand the significance of each variable in general condition.

Sensitivity of time to peak surface deflection (t_p):

The time to peak surface deflection indicates how quickly a pavement section reaches its highest surface deflection under a certain traffic load and during a certain precipitation event. SDM simulations for the range of variables considered in this study indicated no considerable impact of the input parameters on the t_p. For example, Figure 4-14 shows the sensitivity of t_p to subgrade D_{10}. According to this figure, the peak surface deflection occurs after approximately 10 hours from the initiation of the precipitation, which is the same as the end of precipitation period. This explains why t_p is insensitive to change in input parameters, as for the given reference model and the defined range of variables, the highest surface deflection always occurs at the end of precipitation period.

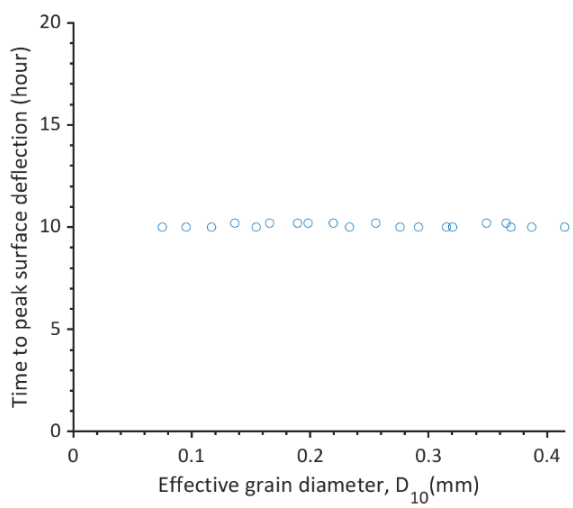

Figure 4-14. Sensitivity of t_p to variations in subgrade D_{10}.

Sensitivity of recovery time (t_R):

The recovery time reflects the time it takes for the excess moisture to redistribute within the pavement layers so that 80% of the excess surface deflection is recovered. Figure 4-15 exhibits the variations of t_R with subgrade D_{10} and e. According to Figure 4-15a, subgrade D_{10} can considerably impact the recovery time. The impact of D_{10} is more significant for D_{10} values approximately less than 0.2 mm. For D_{10}> 0.25 mm, the recovery time is less than an hour. This can mainly be due to the impact of D_{10} on hydraulic conductivity of soil. The redistribution of moisture is expected to be slower in soils with lower hydraulic conductivity. On the other hand, if the hydraulic conductivity is large enough, moisture moves almost freely within the soil and redistribution of moisture can happen relatively quickly. Similar to D_{10}, although in lower extents, an increase in subgrade void ratio resulted in reduction in recovery time (Figure 4-15b). This is because hydraulic conductivity of coarse-grained soils is more impacted by its D_{10} than void ratio.

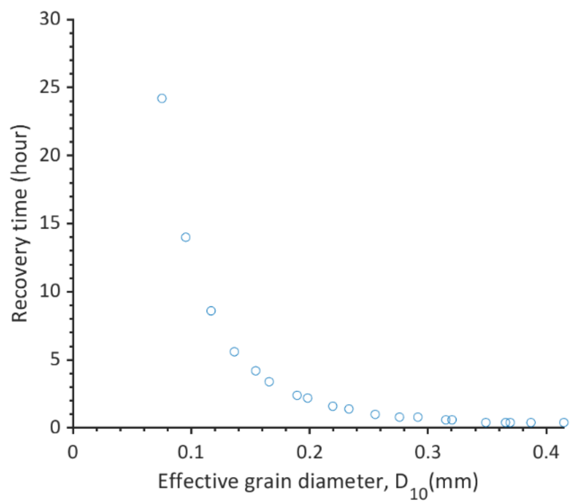

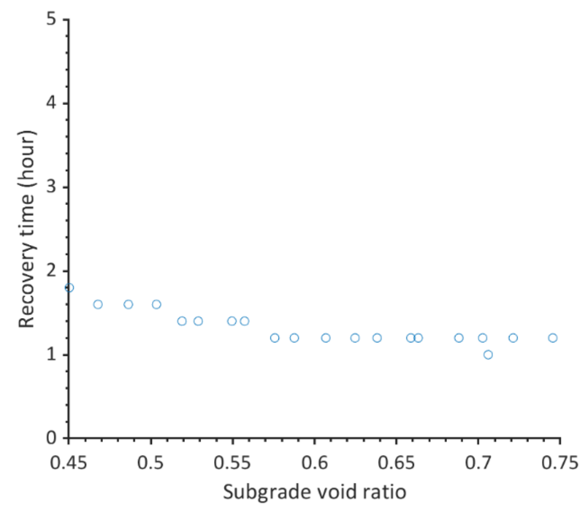

Figure 4-15. Sensitivity of t_R to variations in subgrade (a) D_{10} and (b) e.

The impact of precipitation rate and duration on t_R is presented in Figure 4-16. An increase in precipitation rate increased t_R (Figure 4-16a). This means that a longer time is required for redistribution of moisture in pavement layers for higher precipitation rates which is due to higher amount of water being accumulated in pavement layers. An increase in precipitation duration from 5 to 7 hours resulted in an increase in t_R (Figure 4-16b). However, further increase in precipitation rate did not impact t_R. This is due to a change in moisture movement from transient to steady state after 7 hours of precipitation. For steady state infiltration, the pavement layers' degree of saturation is controlled by the rate of precipitation rather than its duration. Therefore, once the steady state condition is achieved, an increase in precipitation duration has no impact on its degree of saturation and consequently the time required for redistribution of the excess moisture.

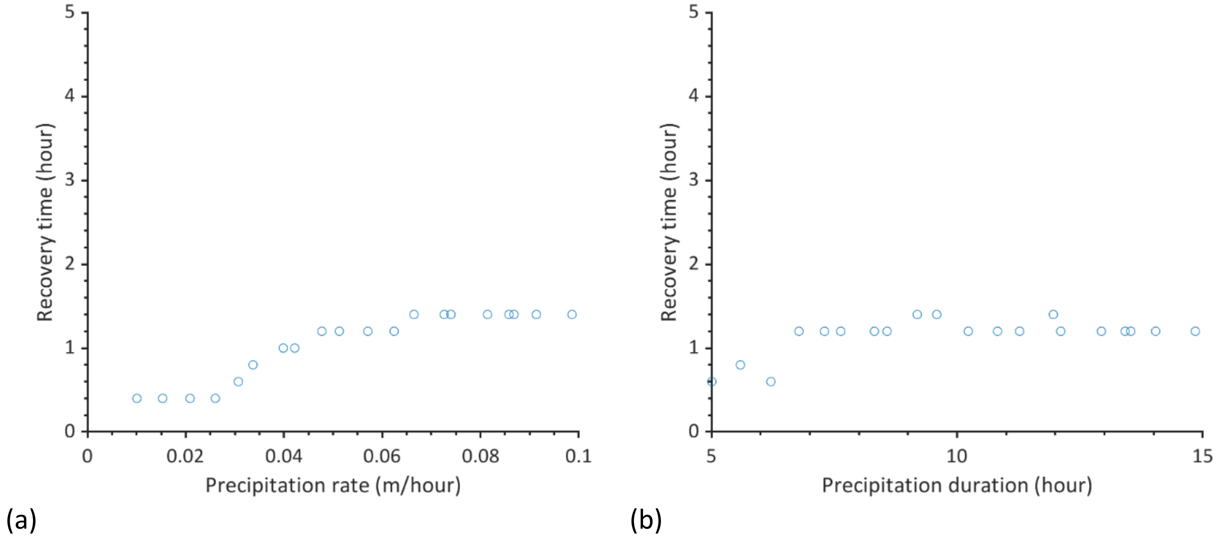

Figure 4-16. Sensitivity of t_R to variations in precipitation (a) rate and (b) duration.

Figure 4-17 presents the variation of t_R with GWL. According to this figure, t_R gradually increases as the GWL increases. For a hydrostatic condition (i.e., before precipitation) and a given depth above GWL, soil degree of saturation decreases with an increase in the depth of the ground water. Therefore, in a moisture variation event and for deeper ground water levels, redistribution of moisture may take longer for a deeper GWL than a shallower one since soil moisture content would need to go back to a lower value.

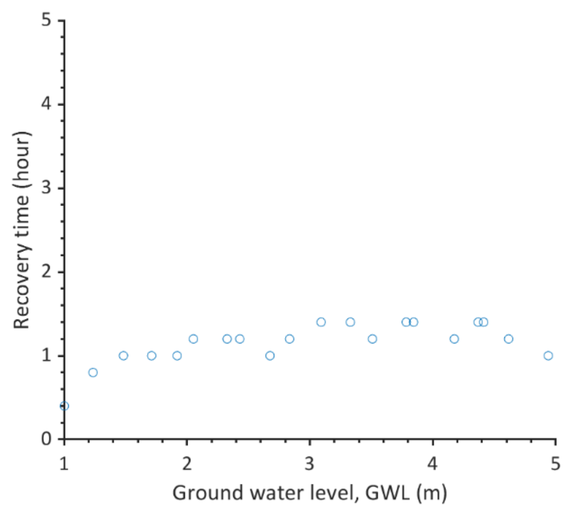

Figure 4-17. Sensitivity of t_R to variations in initial GWL.

Figure 4-18 presents results of sensitivity simulation in terms of aggregate base and subbase thickness versus t_R. An increase in either thickness of aggregate base or subbase resulted in reduction in recovery time. This is due to higher permeability of these layers that accelerated the redistribution of moisture in pavement layers. On the other hand, an increase in AC thickness or resilient modulus increase the recovery time in Figure 4-19.

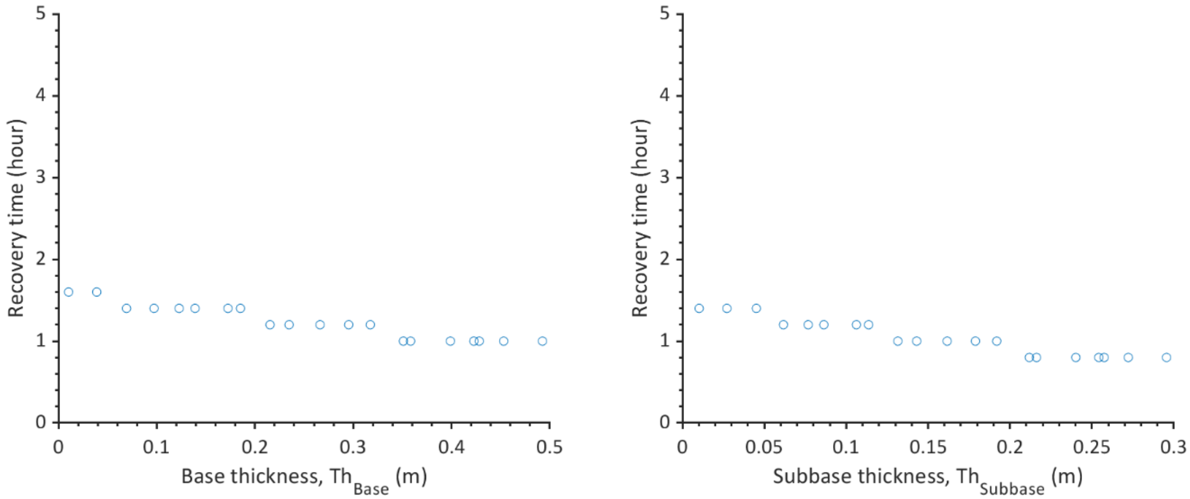

(a) (b)

Figure 4-18. Sensitivity of t_R to variations in (a) aggregate base and (b) subbase thicknesses.

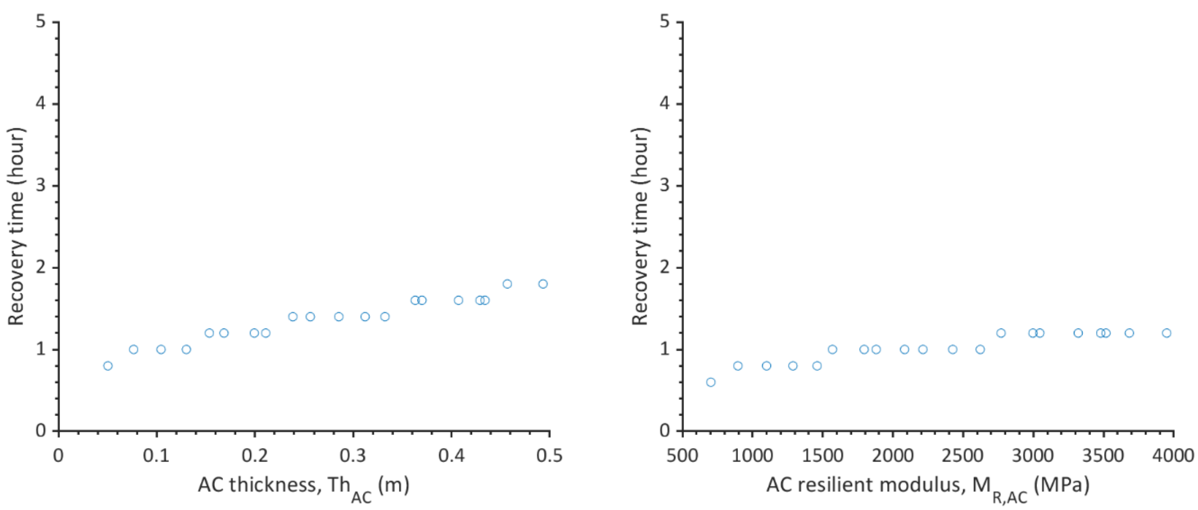

(a) (b)

Figure 4-19. Sensitivity of t_R to variations in AC (a) thickness and (b) resilient modulus.

Figure 4-20 shows the variation of recovery time with wheel load. Results presented in this figure suggest that a longer time is required for the recovery of pavements under higher wheel loads.

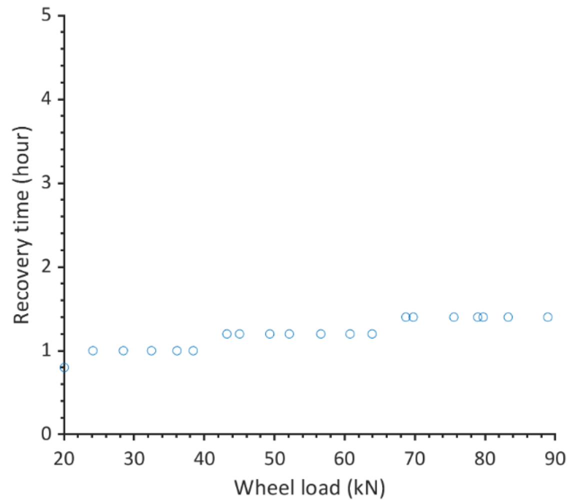

Figure 4-20. Sensitivity of t_R to variations in wheel load.

4.3 LOCAL SENSITIVITY ANALYSIS FOR FINE-GRAINED SUBGRADE

4.3.1 Reference Model Response

For this set of analysis, the subgrade reference model input parameters and their ranges were assigned based on values presented for a fine-grained subgrade in Table 3-5. Figure 4-21 presents the surface deflection time history for the fine-grained subgrade reference model (Figure 4-21a) along with the one for the coarse-grained subgrade (Figure 4-21b). Similar to the coarse-grained subgrade model, results presented in Figure 4-21a indicate a sharp increase in AC surface deflection with start of rain. This is due to inundation of subbase and base coarse material under the ponded water which resulted in a drastic reduction in their stiffness and resistance against loading. Unlike the coarse-grained subgrade reference model, the surface deflection continues to increase after when the precipitation stops. This is due to gradual saturation of subgrade layers with a very low hydraulic conductivity. Because of this, the surface deflection reaches the peak value approximately 170 hours (~one week) after the end of precipitation. The evaporation of ponded water and the infiltration and redistribution of water within the subgrade layers resulted in a gradual recovery of surface deflection. However, due to significantly lower hydraulic conductivity of fine-grained subgrade, its recovery time is considerably slower than that of the coarse-grained reference model. While the surface deflection almost completely recovers after 30 hours in coarse-grained subgrade model, the full recovery was not achieved even after 1000 hours for fine-grained subgrade reference model.

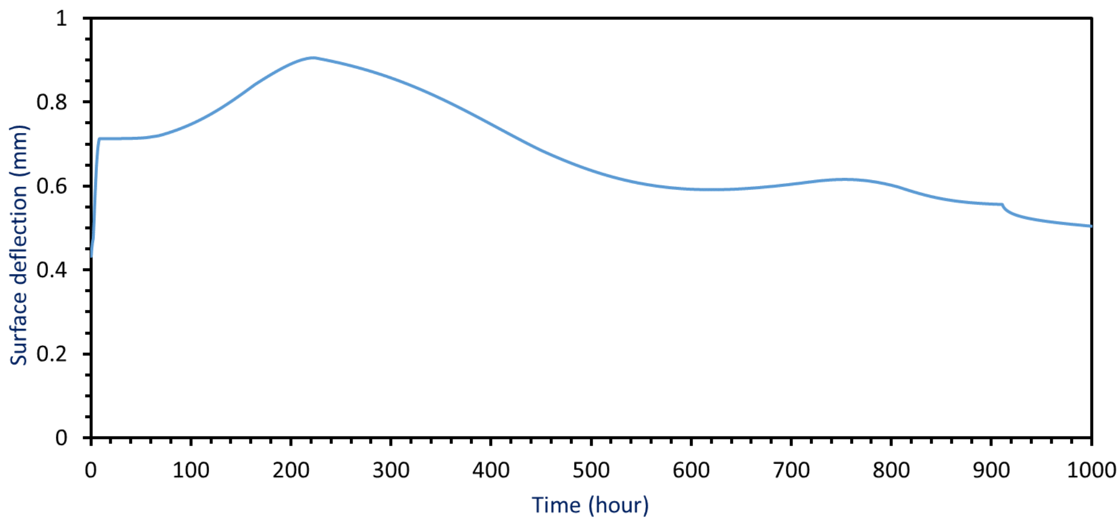

(a)

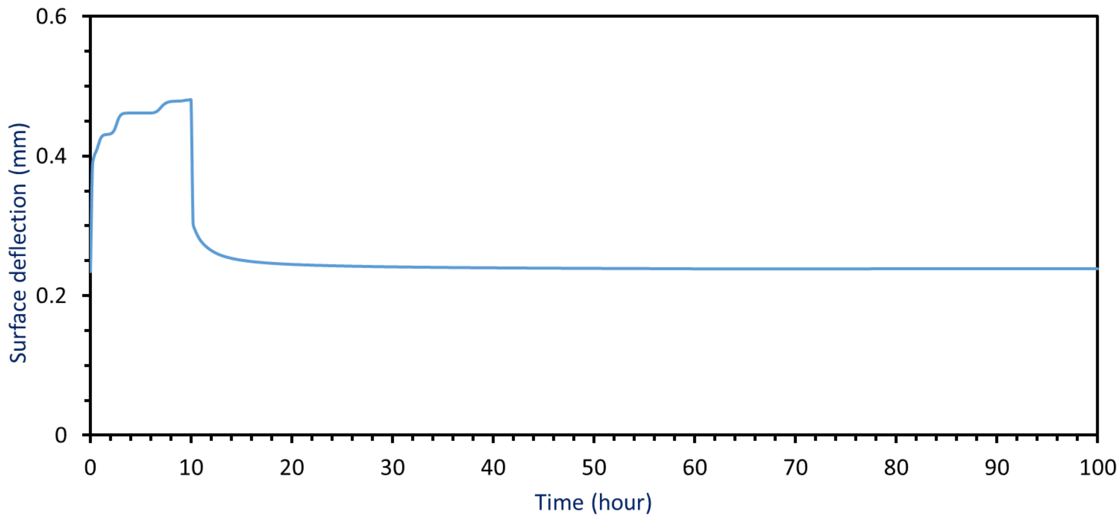

(b)

Figure 4-21. Surface deflection time history for (a) the fine-grained subgrade reference and (b) the coarse-grained subgrade reference models.

4.3.2 Univariate sensitivity simulation results

Univariate SDM simulations were performed by changing an independent parameter while maintaining the other parameters at the reference model value. The reference model values and the ranges of each parameter for sensitivity simulations were reported in Chapter 3. The simulation results are interpreted and discussed in terms of key performance measures.

Sensitivity of peak surface deflection (δ_p):

Figure 4-22 presents the variations of peak surface deflection with subgrade liquid limit and void ratio. Results indicated a highly non-linear relationship between δ_p and w_L (Figure 4-22a). This is due to the complex impact of w_L on pavement response to traffic loading. The subgrade liquid limit impacts both water retainability (i.e., SWRC fitting parameters) and hydraulic conductivity. In general, soils with higher liquid limit would have higher water retainability. Therefore, at a given depth above the GWL, it is likely that soils with higher liquid limit would have higher degree of saturation, and consequently, lower stiffness. On the other hand, lower hydraulic conductivity is expected for soils with higher w_L. The interaction of these two factors explains the nonlinearity and multiple points of inflection observed in δ_p versus w_L curve.

The peak surface deflection during precipitation was substantially affected by change in void ratio (Figure 4-22b). In general, an increase in void ratio increased the δ_p. This is in contrast with what was observed for the coarse-grained case. This is a result of the interaction of soil stiffness and hydraulic conductivity in fine-grained soils. While the effect of subgrade *e* on its hydraulic conductivity was likely to be the dominant factor affecting δ_p in a coarse-grained soil, the change in subgrade stiffness most likely plays more important role in δ_p in a fine-grained subgrade.

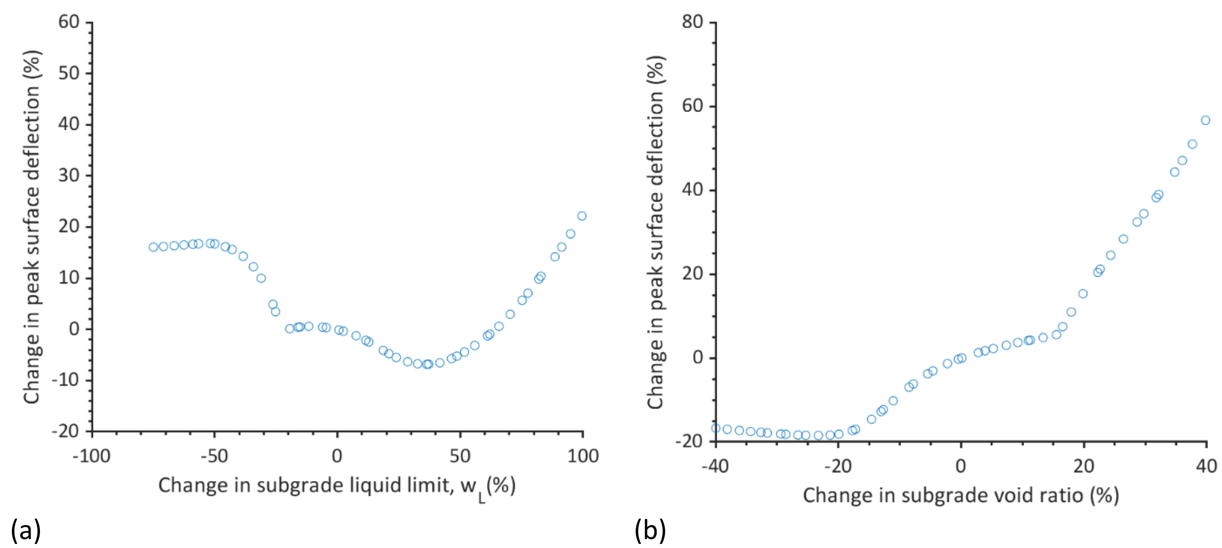

Figure 4-22. Sensitivity of peak surface deflection to the variations of subgrade liquid limit.

The results presented in Figure 4-22a and b showed several points of inflection in peak surface deflection versus w_L or *e* curves. The reason for this observation is a transition in mode of saturation in the layers. Moisture movement from a layer to another layer results in sequences of saturation and desaturation of layers. The complex interaction of hydro-mechanical properties of soil and climatic factors may change these sequences and time dependent pavement behavior. In order to better illustrate this, time histories of surface deflection for the inflection point between -20 to -30% change in w_L (i.e, w_L=16 to 17%) are reviewed in Figure 4-23. According to the results presented in this figure, due to saturation and desaturation of pavement layers, a double peak behavior is observed in the surface deflection versus time curves. The first peak is due to saturation of shallow pavement layers while the second peak is attributed to the movement of moisture to deeper soil and desaturation of aggregate base layer. While for w_L=16% the first peak controls the highest surface deflection, the highest surface deflection is controlled by the second peak when w_L=15%. This change in time dependent surface deflection behavior is expected to dramatically change the time to peak surface deflection and recovery time as will be observed in following figures.

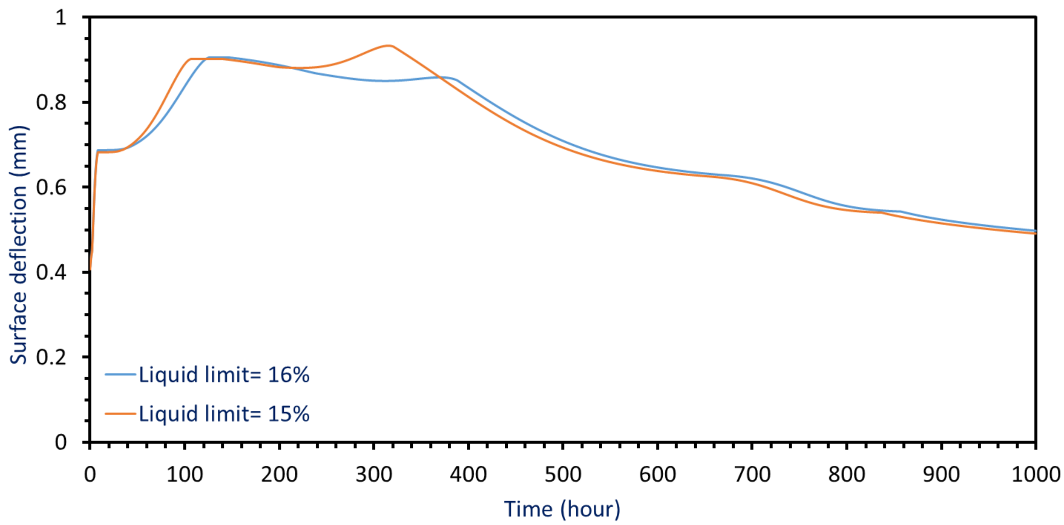

Figure 4-23. Surface deflection time histories for the fine-grained model with w_L= 16 and 17%.

Figure 4-24 illustrates variations of δ_p with precipitation rate and duration. Results indicate substantial impact of both P_r and P_d on δ_p. The trend observed in δ_p -P_r curve is almost consistent with what was observed for coarse-grained subgrade case. While in coarse-grained case, δ_p was almost insensitive to change in P_d, it was considerably increased with an increase in P_d. Higher precipitation duration allows infiltration of moisture through fine-grained subgrade layers while maintaining moisture content of the structural pavement layers at a high level.

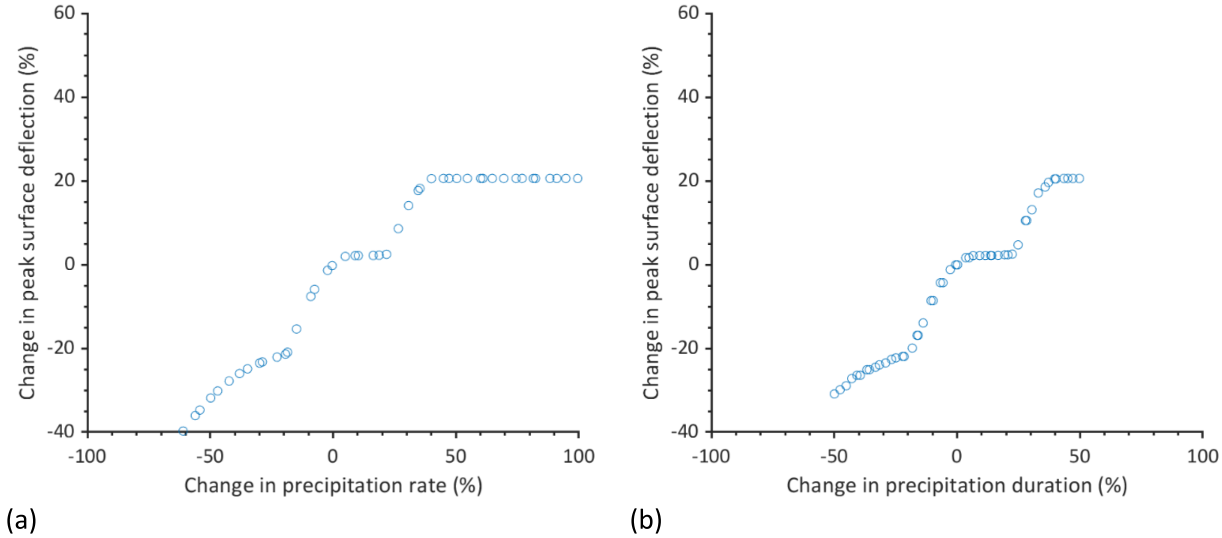

Figure 4-24. Sensitivity of peak surface deflection to the variations of precipitation (a) rate and (b) duration.

Figure 4-25 shows the results of sensitivity simulations for aggregate base and subbase optimum resilient modulus. Results indicate that $M_{R\text{-}OPT,Base}$ and $M_{R\text{-}OPT,Subbase}$ are inversely proportional to δ_p. Results showed that δ_p is more sensitive to change in $M_{R\text{-}OPT,Base}$ than $M_{R\text{-}OPT,Subbase}$. Similar observations were also made for the comparisons of the impact of aggregate base and subbase thicknesses on peak surface deflection (Figure 4-6).

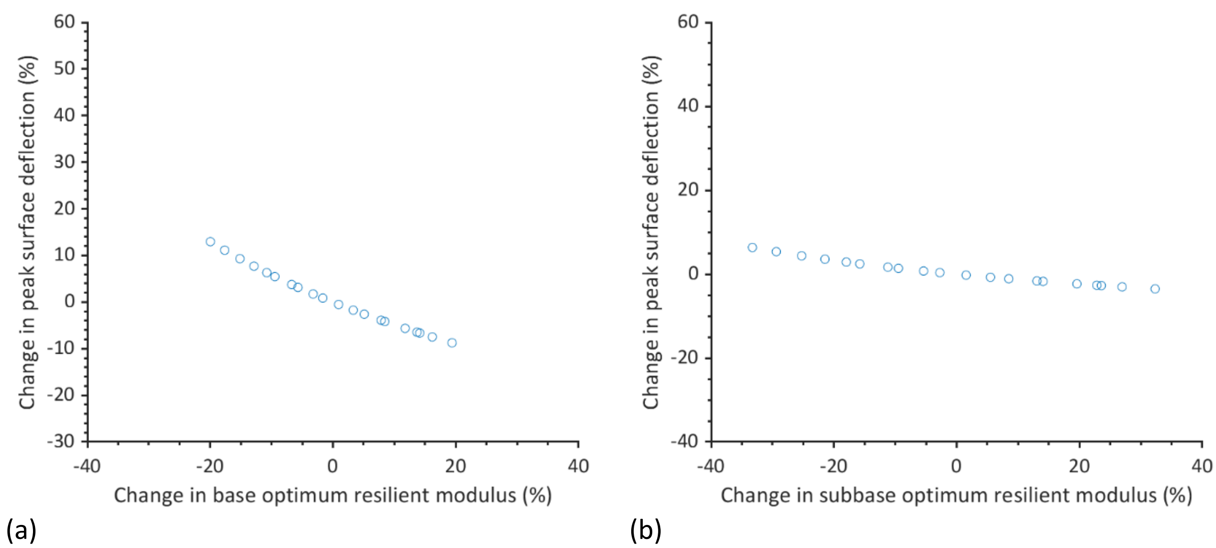

Figure 4-25. Sensitivity of peak surface deflection to the variations of (a) aggregate base and (b) subbase optimum resilient moduli.

The SDM simulations indicate a substantial impact of aggregate base and subbase thickness on δ_p (Figure 4-26). Results indicate that 50% increase in aggregate base thickness reduces the peak surface deflection by almost 30% (Figure 4-26a). Similar trend, although in lower rates were observed for aggregate subbase thickness (Figure 4-26b). A comparison between Figure 4-26 and Figure 4-7 indicates that d_p in fine-grained subgrade model is more sensitive to aggregate base and subbase thickness than in the coarse-grained subgrade model. For a pavement system with low permeable fine-grained subgrade, it is more likely that aggregate base and subbase layers become fully saturated. The high thickness of these layers above natural subgrade surface helps them to stay above the ponded water height.

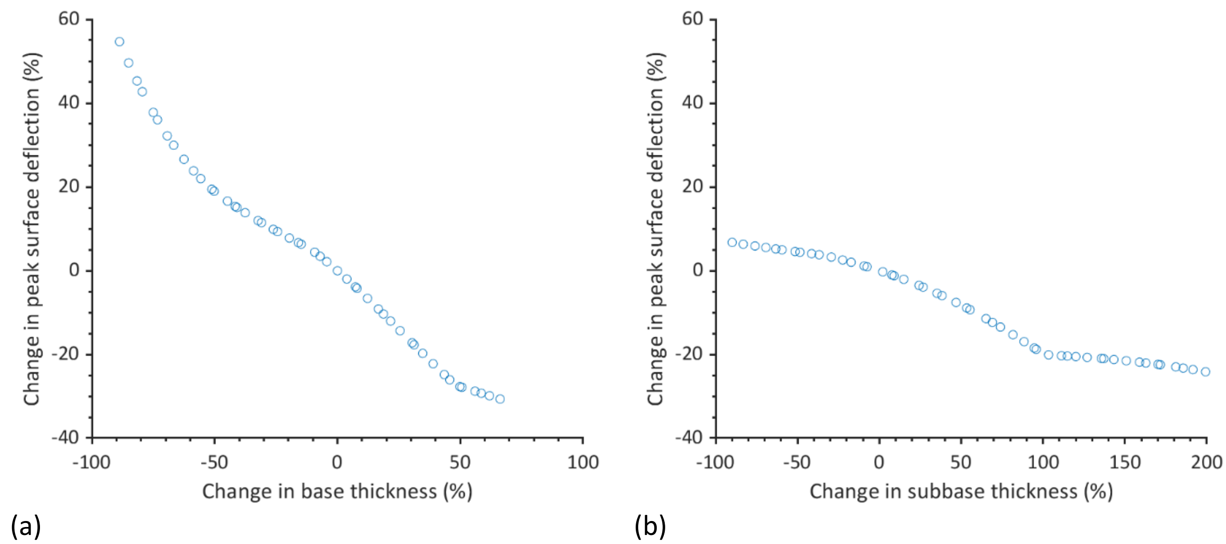

Figure 4-26. Sensitivity of peak surface deflection to the variations of (a) aggregate base and (b) subbase thicknesses.

Figure 4-27 presents the results of δ_p sensitivity simulations to $M_{R,Ac}$ and Th_{AC}. Results show that a decrease in $M_{R,Ac}$ or Th_{AC} leads to a substantial increase in δ_p during a moisture variation event. However, peak surface deflection is more sensitive to a change in Th_{AC} than $M_{R,Ac}$.

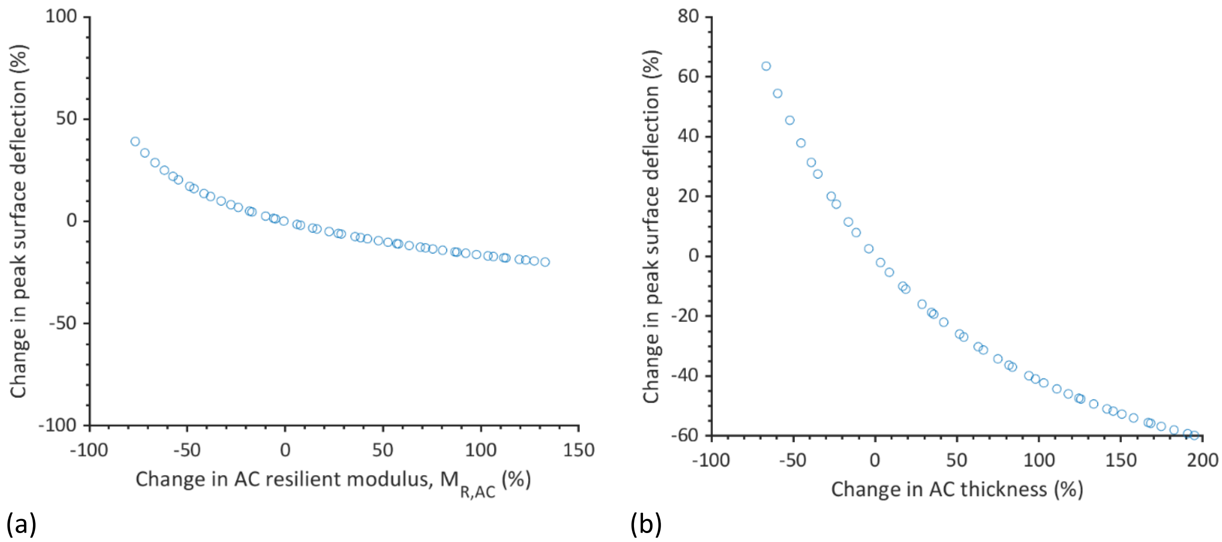

Figure 4-27. Sensitivity of peak surface deflection to the variations of (a) $M_{R,AC}$ and (b) Th_{AC}.

Figure 4-28 presents the sensitivity of peak surface deflection to initial GWL. Results show lower surface deflection as the initial GWL becomes deeper.

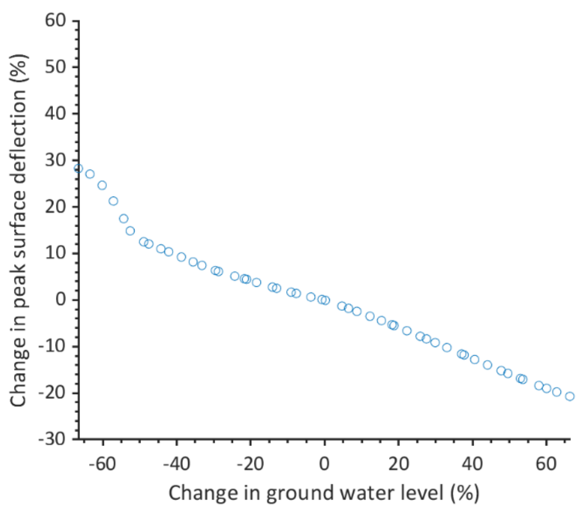

Figure 4-28. Sensitivity of peak surface deflection to the variations of initial GWL.

Figure 4-29 presents the variations of peak surface deflection with changes in wheel load. Results indicate a substantial impact of wheel load on the peak surface deflection.

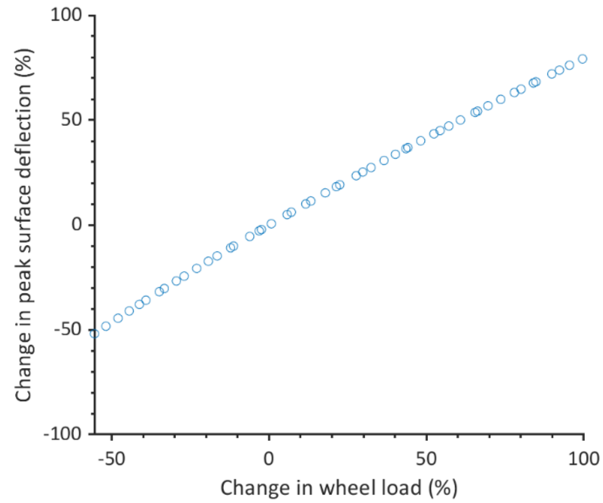

Figure 4-29. Sensitivity of peak surface deflection to the variations of wheel load.

Sensitivity of peak to initial surface deflection ratio (δ_p/δ_0):

Figure 4-30 illustrates the variation of δ_p/δ_0 with subgrade w_L and e. Results indicate considerable impacts of w_L and e on δ_p/δ_0. The ratio of δ_p/δ_0 decreased from approximately 4 to 1.5 as w_L increased from 5 to 40.

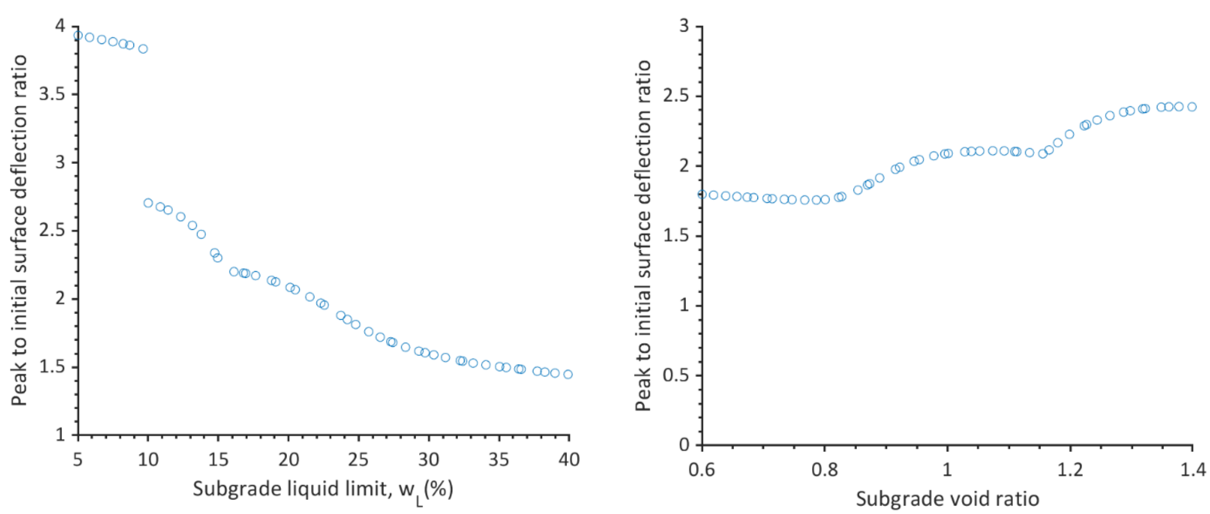

(a) (b)

Figure 4-30. Sensitivity of δ_p/δ_0 to variation in subgrade (a) w_L and (b) e.

Figure 4-31 presents the variation of δ_p/δ_0 with precipitation rate and duration. Results show similar trends as what was observed for the peak surface deflection under variable P_r and P_d. Similar observation were also made for δ_p/δ_0 versus evaporation rate (Figure 4-32).

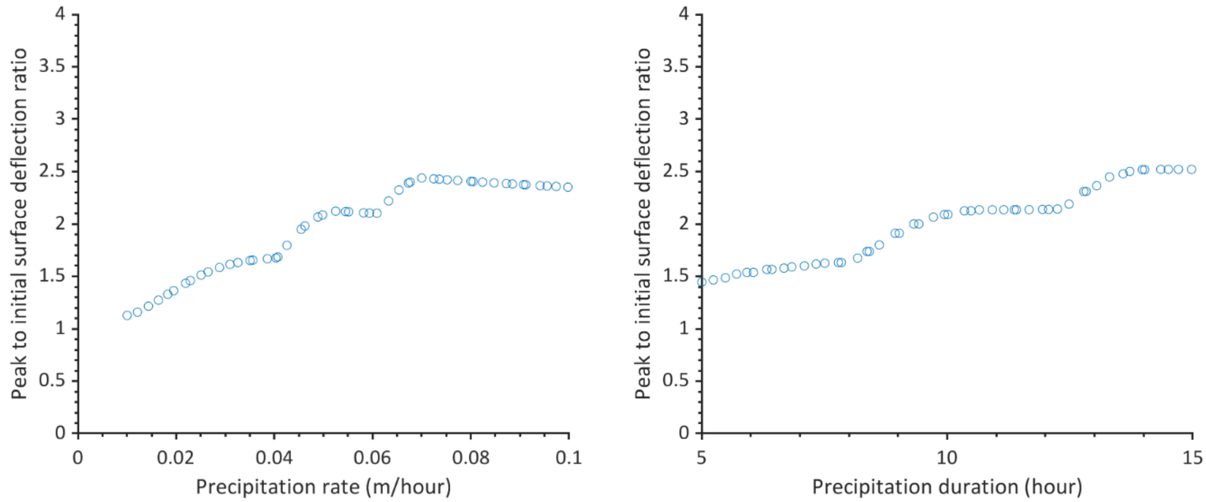

(a) (b)

Figure 4-31. Sensitivity of δ_p/δ_0 to variation in precipitation (a) rate and (b) duration.

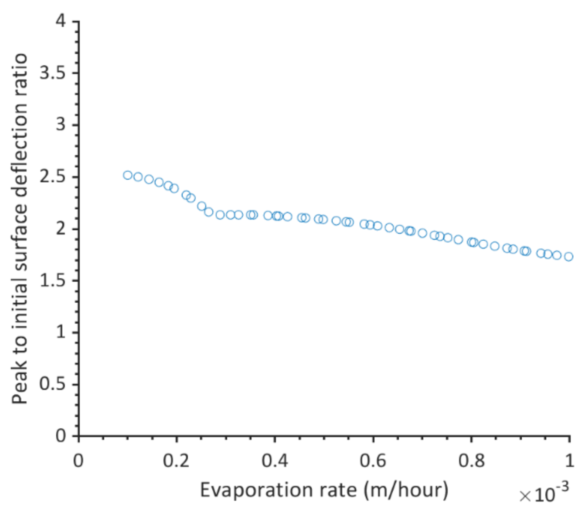

Figure 4-32. Sensitivity of δ_p/δ_0 to variation in evaporation rate.

Unlike the coarse-grained subgrade reference model, results show substantial impact of pavement layers' thicknesses on δ_p/δ_0 for fine-grained case (Figure 4-33).

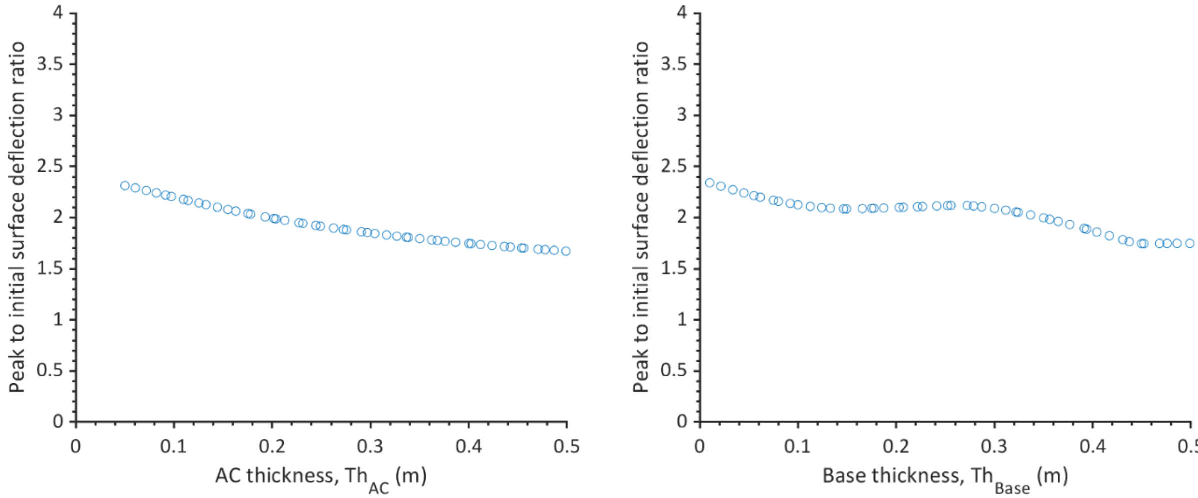

(a) (b)

Figure 4-33. Sensitivity of δ_p/δ_0 to variation in (a) AC and (b) aggregate base thicknesses.

Like the SDM simulation for coarse-grained subgrade model, resilient moduli of pavement layers had minimal impact on δ_p/δ_0. The SDM simulations for other parameters are provided in the Appendix.

Sensitivity of time to peak surface deflection (t_p):

The SDM simulations indicated a nonlinear relationship between t_p and evaporation rate, precipitation rate and duration, subgrade void ratio and liquid limit, and aggregate base and subbase thicknesses. Figure 4-34 presents, as an example, results of the analysis of sensitivity of t_p to subgrade liquid limit. The SDM simulations for other parameters are provided in the Appendix.

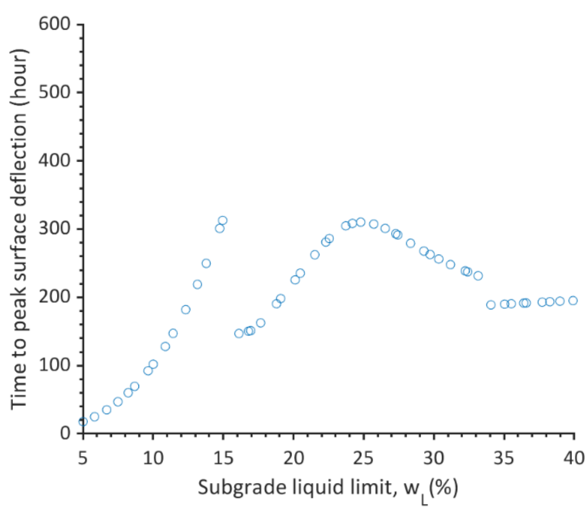

Figure 4-34. Sensitivity of t_p to variation in subgrade liquid limit.

Sensitivity of recovery time (t_R):

Figure 4-35 illustrates the variations of t_R with subgrade w_L and e. Results show high sensitivity of t_R to these parameters. According to the results presented in Figure 4-35a, t_R increase as w_L increases from 5% up to approximately 7%. However, for the liquid limit values greater than 7%, w_L is inversely proportional to t_R. This implies that the recovery time decreases as the hydraulic conductivity increases which is in contrast with what was observed for the coarse-grained case. Void ratio versus recovery time results also support this conclusion (Figure 4-35b). The change in the mechanism of excess moisture removal from the system can be responsible for this. As the hydraulic conductivity of subgrade becomes relatively very low, less water infiltrates through the subgrade and most of the moisture is removed through evaporation. As the redistribution of moisture in a fine-grained subgrade is typically very slow, this accelerates the recovery process. This can be confirmed by evaluating the sensitivity of t_R to evaporation rate (Figure 4-36). While evaporation had minimal impact on t_R for coarse-grained subgrade case, it plays a significant role in t_R of fine-grained subgrade reference model.

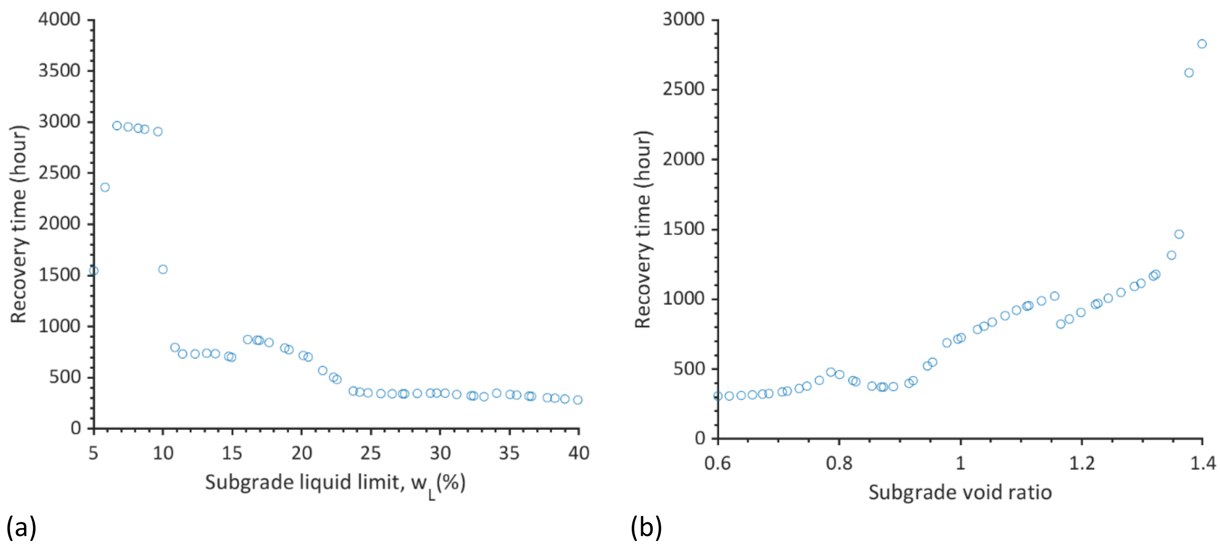

Figure 4-35. Sensitivity of t_R to variations in subgrade (a) w_L and (b) e.

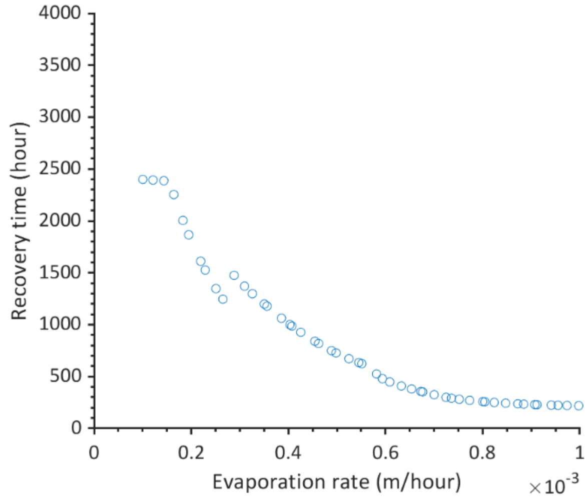

Figure 4-36. Sensitivity of t_R to variations in evaporation rate.

Results of SDM simulation for pavement structural layers thicknesses, and precipitation rate and duration indicated a considerable impact of these variables on t_R. However, similar to sensitivity analysis for coarse-grained subgrade, pavement structural layers moduli and hydraulic conductivity, traffic load, and GWL had minimal impact on the recovery time for fine-grained pavement model. The sensitivity results for these variables are provided in the Appendix.

4.4 SUMMARY AND CONCLUSIONS

Two sets of univariate sensitivity simulations, one considering a coarse-grained subgrade and one considering a fine-grained subgrade were performed to understand the significance of the SDM input variables on pavement system performance during moisture variation and under traffic loading. The pavement performance was evaluated using four performance measures, namely, peak surface deflection, peak to initial surface deflection ratio, time to peak surface deflection, and recovery time. Results of the analysis indicated that the significance of the impact of input parameters is dependent on the type of the subgrade soil. Table 4-1 qualitatively summarizes the overall significance of the impact of each input parameter on performance measures for coarse-grained and fine-grained subgrade models. It should be emphasized that the results and conclusions presented herein may only hold valid for the reference model, ranges of variables, and select relationships used for the analysis.

Table 4-1. Overall qualitative significance of the impact of SDM input parameters on the pavement performance measures from local sensitivity analysis.

Variable		Performance measure index							
		$(\delta_p)_{coarse}$[a]	$(\delta_p)_{fine}$[b]	$(\delta_p/\delta_0)_{coarse}$	$(\delta_p/\delta_0)_{fine}$	$(t_P)_{coarse}$	$(t_P)_{fine}$	$(t_R)_{coarse}$	$(t_R)_{fine}$
$D_{10,\ Subgrade}$	↑	***↓	NA	***↓	NA	-	NA	***↓	NA
$w_{L,Subgrade}$	↑	NA	**↓↑	NA	***↓	NA	***↓↑	NA	***↓
$e_{Subgrade}$	↑	*↓	***↓	*↓	*↑	-	***↓↑	*↓	***↑
P_r	↑	***↑	**↑	***↑	**↑	-	***↓↑	*↑	***↑
P_d	↑	*↑	***↑	-	**↑	***↑	***↓↑	*↑	***↑
E_r	↑	-	**↓	-	**↓	-	***↓↑	-	***↓
GWL	↑	*↓	***↓	-	*↓↑	**↑	***↓↑	*↑	*↓↑
$K_{s,base}$	↑	**↓	-	**↓	*↑	-	-	-	*↑
$K_{s,subbase}$	↑	*↓	-	*↓	-	-	-	-	-
Th_{base}	↑	**↓	***↓	-	**↓	-	***↓	*↓	***↓
$Th_{subbase}$	↑	*↓	**↓	-	*↓	-	**↓	*↓	**↓
$M_{R\text{-}opt,base}$	↑	**↓	**↓	-	-	-	-	*↑	-
$M_{R\text{-}opt,subbase}$	↑	*↓	*↓	-	-	-	-	-	-
$M_{R,AC}$	↑	**↓	***↓	-	-	-	-	*↑	-
Th_{AC}	↑	***↓	***↓	**↓	**↓	-	-	*↑	*↑
Wheel load	↑	***↑	***↑	-	-	-	-	*↑	-

[a] Coarse-grained subgrade reference model.

[b] Fine-grained subgrade reference model.

"***" indicates relatively substantial impact, "**" indicates relatively moderate impact, * indicates relatively low impact, "-" indicates minimal impact, and "↑" shows the direction of the impact on the given performance measure as a result of an increase "↑" in input variables. "↑" implies increase, "↓" implies decrease, and "↓↑" implies nonlinear behavior.

CHAPTER 5: MULTIVARIATE GLOBAL SENSITIVITY ANALYSIS (GSA)

5.1 INTRODUCTION

Univariate sensitivity simulations presented in Chapter 4 provided instructive information about the importance of each parameter and its overall contribution to pavement system behavior. However, due to complex interaction of input variables and extreme nonlinearity in response in most cases, the results may only be applicable to the reference model values. For example, while the recovery time is likely to be insensitive to evaporation for highly permeable subgrades, it is likely to be substantially impacted by evaporation for subgrades with relatively low permeability. Therefore, the interaction of evaporation and permeability of subgrade is expected to become critically important for design or evaluation of a pavement system prone to moisture variations. While a local sensitivity analysis may not be able to explain the interaction between different parameters, a global sensitivity analysis can holistically assess the significant of input variables and their interaction on critical pavement performance indicators during and after a moisture variation event. This chapter presents the results of global sensitivity analysis for coarse-grained and fine-grained subgrade cases.

5.2 GLOBAL SENSITIVITY ANALYSIS FOR COARSE-GRAINED SUBGRADE

Based on univariate sensitivity analysis results, input parameters that had low to substantial impact on the pavement performance measures during and after moisture variation event were selected for global sensitivity analysis. In addition, due to substantial impact of evaporation rate on the response of fine-grained subgrade reference model, it was considered in the multivariate simulations. The multivariate simulations included 2000 SDM simulations using LHS method for the select parameters and their ranges, as shown in Table 5-1. Results of the simulations were interpreted in terms of the four performance measure indices. Statistical analysis, using JMP software was performed to understand the significant importance of each parameter and to rank them based on their significant impact.

Table 5-1. Select input parameters and their ranges for GSA of coarse-grained subgrade model.

Parameters	Range
$D_{10, Subgrade}$	0.07 to 0.2
$e_{Subgrade}$	0.45 to 0.75
P_r	0.01 to 0.1 m/hour
P_d	5 to 15 hours
E_r	0.0001 to 0.001
GWL	1 to 5m
$K_{s,base}$	12 to 160 m/hour
$K_{s,subbase}$	4 to 40 m/hour
Th_{base}	0 to 0.5 m
$Th_{subbase}$	0 to 0.3 m
$M_{R\text{-}opt,base}$	200 to 300 MPa
$M_{R\text{-}opt,subbase}$	100 to 200 MPa
$M_{R,AC}$	700 to 7000 MPa
Th_{AC}	0.05 to 0.5 m

5.2.1 Sensitivity of δ_p to Select Parameters

Results of sensitivity analysis of peak surface deflection to variations in select input parameters for coarse-grained subgrade case are provided in Table 5-2. p-values reported in the table provides evidence to support or reject null hypothesis that the response and input parameters are not correlated. A p-value greater than 0.05 indicates strong evidence for the null hypothesis. Logarithm of worth (log(worth)) present the significance of each model effect, defined as $\log_{10}$(p value). Parameter t Ratio is the ratio of parameter coefficient in linear regression model to its standard error and it indicates the significance and direction of the impact.

According to the results presented in Table 5-2, Th_{AC} may have the most significant impact on peak surface deflection. The negative "t Ratio" value obtained for Th_{AC} indicates its inverse relationship with the peak surface deflection (i.e., an increase in Th_{AC} results in decrease in the peak surface deflection). P_r, $M_{R,AC}$, $D_{10,Subgrade}$, $M_{R\text{-}OPT,Base}$, and Th_{Base} are other parameters that would play a substantial role in estimation of the peak surface deflection. Further, similar to univariate sensitivity simulations, the results indicate that the peak surface deflection is insensitive to variations of evaporation rate between the ranges examined in this study.

Table 5-2. Summary of the analysis of the sensitivity of peak surface deflection to select input parameters for coarse-grained subgrade model.

Ranking	Variable	Log (worth)	t Ratio	p value
1	Th_{AC}	644.97	-95.4	<.0001
2	P_r	380.842	57.14	<.0001
3	$M_{R,AC}$	340.603	-52.13	<.0001
4	$D_{10,Subgrade}$	236.403	-39.67	<.0001
5	$M_{R\text{-}OPT,Base}$	217.196	-37.41	<.0001
6	Th_{Base}	198.948	-35.25	<.0001
7	$K_{s,Base}$	23.952	-10.44	<.0001
8	$M_{R\text{-}OPT,Subbase}$	21.986	-9.97	<.0001
9	$TH_{Subbase}$	20.536	-9.61	<.0001
10	$Ks_{subbase}$	17.119	-8.71	<.0001
11	P_d	14.014	7.82	<.0001
12	*Initial GWL*	8.997	6.15	<.0001
13	$e_{Subgrade}$	3.44	-3.57	0.0004
14	E_r	0.832	1.45	0.1472

5.2.2 Sensitivity of δ_p/δ_0 to Select Parameters

Results of the analyses for sensitivity of δ_p/δ_0 to variations of the select parameters indicate that precipitation rate (P_r) and subgrade effective grain diameter ($D_{10,Subgrade}$) may have the most influential effect on δ_p/δ_0 (Table 5-3). The results indicate that, as long as δ_p/δ_0 is concerned, evaporation rate may become an important contributor to the pavement system response. Further, δ_p/δ_0 is insensitive to the subbase resilient modulus variations between the ranges tested in this study.

Table 5-3. Summary of the analysis of the sensitivity of δ_p/δ_0 to select input parameters for coarse-grained subgrade model.

Ranking	Variable	Log (worth)	t Ratio	p value
1	P_r	684.758	87.8	<.0001
2	$D_{10,Subgrade}$	386.467	-53.52	<.0001
3	Th_{AC}	175.536	-31.43	<.0001
4	$M_{R,AC}$	133.721	26.7	<.0001
5	Th_{Base}	97.578	-22.28	<.0001
6	$e_{Subgrade}$	66.691	-18.03	<.0001
7	$K_{s,Base}$	59.425	-16.93	<.0001
8	*Initial GWL*	37.26	13.16	<.0001
9	$Ks_{subbase}$	29.203	-11.55	<.0001
10	P_d	26.998	11.08	<.0001
11	$M_{R\text{-}OPT,Base}$	11.626	7.06	<.0001
12	$Th_{Subbase}$	3.218	-3.43	0.0006
13	E_r	1.501	-2.15	0.0316
14	$M_{R\text{-}OPT,Subbase}$	0.089	0.24	0.8142

5.2.3 Sensitivity of t_p to Select Parameters

Results of analyses for sensitivity of t_p to variations of the select parameters indicate that precipitation duration and initial GWL may have the most substantial impact on t_p (Table 5-4). While LSA results indicated that variations of P_r, $D_{10,Subgrade}$, and $e_{Subgrade}$ may have minimal impact on t_p, the GSA results indicate that these parameters may significantly impact t_p. According to GSA results presented in Table 5-4, the rest of select parameters do not have significant impact on t_p.

Table 5-4. Summary of the analysis of the sensitivity of t_p to select input parameters for coarse-grained subgrade model.

Ranking	Variable	Log (worth)	t Ratio	p value
1	P_d	594.402	76.64	<.0001
2	*Initial GWL*	142.733	27.75	<.0001
3	P_r	89.123	-21.17	<.0001
4	$D_{10,Subgrade}$	3.56	-3.64	0.0003
5	$e_{Subgrade}$	2.814	3.17	0.0015
6	Th_{Base}	0.73	-1.32	0.1860
7	$M_{R,AC}$	0.558	1.09	0.2764
8	$M_{R\text{-}OPT,Subbase}$	0.354	-0.77	0.4426
9	$Th_{Subbase}$	0.332	0.73	0.4656
10	E_r	0.219	0.52	0.6043
11	$M_{R\text{-}OPT,Base}$	0.182	0.44	0.6579
12	$K_{s,Base}$	0.167	-0.41	0.6809
13	$K_{s,\ subbase}$	0.011	0.03	0.9761
14	Th_{AC}	0	0	0.9999

5.2.4 Sensitivity of t_R to Select Parameters

Table 5-5 presents the summary of the sensitivity of t_R to variations of the select parameters evaluated in this study. Results indicate that subgrade effective grain diameter may have the most significant impact on t_R. This might have been expected, as it was also observed in LSA results, for a pavement with coarse-grained subgrade, the redistribution of excess moisture after an extreme moisture variation event is primarily governed by its hydraulic properties. The results presented in Table 5-5 indicate that the hydraulic conductivity of aggregate base and subbase layers do not significantly impact t_R. This is mainly because these layers are assumed to be consisted of granular material with relatively high permeability, if permeabilities of these layers are reduced, their impact on recovery time will become significant.

Table 5-5. Summary of the analysis of the sensitivity of t_R to select input parameters for coarse-grained subgrade model.

Ranking	Variable	Log (worth)	t Ratio	p value
1	$D_{10,Subgrade}$	303.309	-44.87	<.0001
2	*Initial GWL*	66.572	18.01	<.0001
3	P_r	45.755	14.7	<.0001
4	Th_{Base}	35.639	-12.85	<.0001
5	$M_{R,AC}$	35.042	12.74	<.0001
6	P_d	21.283	9.76	<.0001
7	$M_{R\text{-}OPT,Base}$	12.228	7.25	<.0001
8	$Th_{Subbase}$	11.036	-6.86	<.0001
9	$e_{Subgrade}$	9.682	-6.39	<.0001
10	E_r	2.354	2.85	0.0044
11	Th_{AC}	1.484	2.14	0.0328
12	$M_{R\text{-}OPT,Subbase}$	1.309	1.97	0.0491
13	$Ks_{subbase}$	0.048	0.13	0.8955
14	$K_{s,Base}$	0.001	0	0.9986

5.3 GLOBAL SENSITIVITY ANALYSIS FOR FINE-GRAINED SUBGRADE

Similar to coarse-grained subgrade case, the GSA was investigated by performing 2000 multivariate simulations using the SDM. The select parameters and their ranges, as shown in Table 5-1. Results of the simulations were interpreted in terms of the four performance measure indices. Statistical analysis, using JMP software was performed to understand the significant importance of each parameter and to rank them based on their significant impact.

Table 5-6. Select input parameters and their ranges for GSA of fine-grained subgrade model.

Parameters	Range
w_L	5 to 40
$e_{Subgrade}$	0.6 to 1.4
P_r	0.01 to 0.1 m/hour
P_d	5 to 15 hours
E_r	0.0001 to 0.001
GWL	1 to 5m
$K_{s,base}$	12 to 160 m/hour
$K_{s,subbase}$	4 to 40 m/hour
Th_{base}	0 to 0.5 m
$Th_{subbase}$	0 to 0.3 m
$M_{R\text{-}opt,base}$	200 to 300 MPa
$M_{R\text{-}opt,subbase}$	100 to 200 MPa
$M_{R,AC}$	700 to 7000 MPa
Th_{AC}	0.05 to 0.5 m

5.3.1 Sensitivity of δ_p to Select Parameters

Table 5-7 presents results of analyses for sensitivity of δ_p to variations of the select parameters. Similar to the coarse-grained subgrade model results, Th_{AC} may have the most significant impact on the peak surface deflection during a moisture variation event and under a given traffic load. Unlike the coarse-grained subgrade model, the results indicate that evaporation rate may have a significant impact on δ_p while δ_p is not significantly affected by the variations of aggregate base and subbase hydraulic conductivity. This is due to initial assumption that aggregate base and subbase layers consist of relatively highly permeable material. However, the results indicate that the use of these permeable layers and a change in their thicknesses can significantly impact δ_p.

Table 5-7. Summary of the analysis of the sensitivity of δ_p to select input parameters for fine-grained subgrade model.

Ranking	Source	Log (worth)	t Ratio	p value
1	Th_{AC}	160.15	-95.4	<.0001
2	P_r	46.66	57.14	<.0001
3	$M_{R,AC}$	41.64	-52.13	<.0001
4	Th_{Base}	40.98	-39.67	<.0001
5	$e_{Subgrade}$	32.84	-37.41	<.0001
6	*Initial GWL*	20.88	-35.25	<.0001
7	P_d	18.42	-10.44	<.0001
8	$Th_{Subbase}$	10.56	-6.8	<.0001
9	$M_{R\text{-}OPT,Subbase}$	4.40	-4.14	<.0001
10	E_r	4.20	-4.07	<.0001
11	w_L	2.94	-3.27	0.0010
12	$M_{R\text{-}OPT,Base}$	2.29	2.81	0.0051
13	$Ks_{subbase}$	0.53	1.06	0.291
14	$K_{s,Base}$	0.52	1.03	0.3055

5.3.2 Sensitivity of δ_p/δ_0 to Select Parameters

Table 5-8 presents results of analyses for sensitivity of δ_p/δ_0 to variations of the select parameters for the fine-grained subgrade model. Similar to the coarse-grained model, results indicate high sensitivity of δ_p/δ_0 to input parameter governing the precipitation and hydrology of the subgrade. In addition, results indicate that δ_p/δ_0 in fine-grained subgrade model can significantly be affected by the evaporation rate. δ_p/δ_0 is less sensitive to stiffness of pavement layers compared to other parameters listed in Table 5-8.

Table 5-8. Summary of the analysis of the sensitivity of δ_p/δ_0 to select input parameters for fine-grained subgrade model.

Ranking	Variable	Log (worth)	t Ratio	p value
1	w_L	348.65	-53.09	<.0001
2	P_r	181.712	33.19	<.0001
3	P_d	82.621	20.59	<.0001
4	Th_{AC}	55.069	-16.4	<.0001
5	E_r	19.933	-11.19	<.0001
6	$e_{Subgrade}$	19.345	-9.44	<.0001
7	Th_{Base}	9.764	9.3	<.0001
8	$Th_{Subbase}$	6.547	5.19	<.0001
9	*Initial GWL*	3.71	3.91	<.0001
10	$K_{s,Base}$	3.63	3.73	0.0002
11	$Ks_{subbase}$	2.456	-2.95	0.0033
12	$M_{R\text{-}OPT,Subbase}$	2.424	2.91	0.0037
13	$M_{R,AC}$	1.811	2.43	0.0153
14	$M_{R\text{-}OPT,Base}$	0.619	1.18	0.2367

5.3.3 Sensitivity of t_p to Select Parameters

Results of analyses for sensitivity of t_p to variations of the select parameters indicate that climatic related data may have the most substantial impact on t_p (Table 5-9). Further, t_p is expected to be significantly affected by the thicknesses of aggregate base and subbase layers.

Table 5-9. Summary of the analysis of the sensitivity of t_p to select input parameters for fine-grained subgrade model.

Ranking	Variable	Log (worth)	t Ratio	p value
1	P_r	245.115	39.12	<.0001
2	E_r	141.436	-27.71	<.0001
3	P_d	114.124	24.43	<.0001
4	Th_{Base}	68.488	-18.33	<.0001
5	$Th_{Subbase}$	33.105	-12.37	<.0001
6	$w_{L,\ Subgrade}$	28.394	11.39	<.0001
7	$e_{Subgrade}$	9.044	-6.16	<.0001
8	$M_{R,AC}$	2.075	2.64	0.0084
9	Th_{AC}	1.653	-2.29	0.0222
10	*Initial GWL*	1.231	1.89	0.0587
11	$M_{R\text{-}OPT,Base}$	1.103	-1.76	0.0788
12	$M_{R\text{-}OPT,Subbase}$	0.992	1.64	0.1019
13	$K_{s,\ subbase}$	0.954	-1.59	0.1112
14	$K_{s,Base}$	0.914	1.55	0.122

5.3.4 Sensitivity of t_R to Select Parameters

Table 5-10 presents the summary of the sensitivity of t_R to variations of the select parameters evaluated in this study. Results indicate that subgrade liquid limit and precipitation rate may have the most significant impact on t_R. Also, unlike the coarse-grained model, evaporation rate may play a significant role in accelerating the recovery of surface deflection in pavements with fine-grained subgrade.

Table 5-10. Summary of the analysis of the sensitivity of t_R to select input parameters for fine-grained subgrade model.

Ranking	Variable	Log (worth)	t Ratio	p value
1	$w_{L,Subgrade}$	145.202	-28.78	<.0001
2	P_r	109.695	24.28	<.0001
3	E_r	48.835	-15.35	<.0001
4	P_d	32.818	12.37	<.0001
5	$e_{Subgrade}$	32.557	12.31	<.0001
6	$Th_{Subbase}$	8.641	-6.01	<.0001
7	Th_{Base}	6.708	-5.23	<.0001
8	*Initial GWL*	4.911	4.39	<.0001
9	$M_{R,AC}$	3.103	3.36	0.0008
10	$Ks_{subbase}$	3.026	3.31	0.0009
11	Th_{AC}	1.891	-2.49	0.0129
12	$K_{s,Base}$	0.702	1.29	0.1985
13	$M_{R\text{-}OPT,Base}$	0.217	0.51	0.6066
14	$M_{R\text{-}OPT,Subbase}$	0.02	0.06	0.9547

CHAPTER 6: SENSITIVITY ANALYSIS SUMMARY AND CONCLUSIONS

6.1 SUMMARY

This study presented sets of sensitivity analysis of the SDM estimations to input variables. Results of the sensitivity analyses shed light on sensitivity of pavement performance during periods of excessive moisture with respect to various climatic, geotechnical and pavement related system parameters. The pavement performance was interpreted in terms of four key performance measures: (1) peak surface deflection during moisture variation and under a certain traffic load, (2) the ratio of peak surface deflection and the surface deflection before precipitation event, (3) time to reach peak surface deflection, and, (4) required time for recovery of pavement system. A summary of key findings is provided herein:

- The performance of the pavement during a moisture variation event and the significance of input parameters are highly dependent on the permeability of subgrade soil.
- Regardless of the type of subgrade soil, climate data including precipitation rate and duration play a significant role in estimation of pavement performance. Accurate estimation of these parameters is of critical importance for a reasonable prediction of pavement performance during moisture variation.
- For pavements with subgrade of relatively low permeability and poor drainage system, evaporation rate may have a significant impact on pavement system performance during and after a moisture variation event.
- Thickness and mechanical properties of AC layer may significantly impact the peak surface deflection during excessive moisture conditions; however, they may have a minimal impact on the extent of the impact of moisture variation relative to the initial condition and the required time for recovery of the pavement.
- Thickness of compacted granular base and subbase layers with relatively high permeability can significantly impact the performance of pavement systems during and after excessive moisture variation. This impact is expected to be more substantial in pavements with subgrade of relatively lower permeability.
- For pavements with relatively permeable granular base and subbase layers, variation of the layers' hydraulic conductivity may not substantially impact the performance of pavement systems with fine-grained subgrade; however, it may substantially impact the performance of pavement systems with coarse-grained subgrade.
- Hydraulic properties of subgrade soil including hydraulic conductivity and water retainability can substantially impact its behavior during moisture variations. For soils with relatively high permeability (such as, clean sand), a decrease in permeability can adversely impact pavement performance while for subgrades with relatively very low permeability (i.e., clay), reduction in permeability may improve the pavement capacity during moisture variation.

- GWL may have a complex impact on the performance of pavements systems during moisture variations. While an increase in the depth of ground water may lower peak surface deflection experienced during moisture variation, it may increase the recovery time.

The significant importance of each parameter relies on the performance measure for design or evaluation of the pavement section prone or subjected to moisture variation. Table 6-1 qualitatively presents the relative importance of input parameters for evaluation of flexible pavement performance measures based on LSA and GSA presented in this study.

Table 6-1. A qualitative summary of the intensity of the impact of input parameters on the performance measure indices.

Variable	Performance measure index							
	$(\delta_p)_{coarse}$	$(\delta_p)_{fine}$	$(\delta_p/\delta_0)_{coarse}$	$(\delta_p/\delta_0)_{fine}$	$(t_P)_{coarse}$	$(t_P)_{fine}$	$(t_R)_{coarse}$	$(t_R)_{fine}$
$D_{10,\ Subgrade}$	Very significant impact	NA	Very significant impact	NA	Significant impact	NA	Significant impact	NA
$w_{L,Subgrade}$	NA	Moderate impact	NA	Very significant impact	NA	Significant impact	NA	Very significant impact
$e_{Subgrade}$	Moderate impact	Significant impact	Very significant impact	Significant impact	Significant impact	Significant impact	Significant impact	Very significant impact
P_r	Very significant impact	Significant impact	Very significant impact	Very significant impact	Very significant impact	Very significant impact	Very significant impact	Very significant impact
P_d	Moderate impact	Significant impact	Significant impact	Very significant impact	Very significant impact	Very significant impact	Very significant impact	Very significant impact
E_r	Minimal impact	Significant impact	Moderate impact	Significant impact	Minimal impact	Very significant impact	Minimal impact	Very significant impact
Initial GWL	Moderate impact	Significant impact	Significant impact	Significant impact	Very significant impact	Significant impact	Very significant impact	Significant impact
$K_{s,base}$	Very significant impact	Moderate impact	Significant impact	Moderate impact	Minimal impact	Minimal impact	Minimal impact	Minimal impact
$K_{s,subbase}$	Significant impact	Moderate impact	Significant impact	Moderate impact	Minimal impact	Minimal impact	Minimal impact	Moderate impact
Th_{base}	Very significant impact	Moderate impact	Very significant impact	Significant impact	Moderate impact	Significant impact	Moderate impact	Significant impact
$Th_{subbase}$	Significant impact	Significant impact	Moderate impact	Significant impact	Minimal impact	Significant impact	Minimal impact	Significant impact
$M_{R\text{-}opt,base}$	Very significant impact	Significant impact	Significant impact	Moderate impact	Minimal impact	Minimal impact	Minimal impact	Minimal impact
$M_{R\text{-}opt,subbase}$	Significant impact	Significant impact	Moderate impact	Moderate impact	Minimal impact	Minimal impact	Minimal impact	Minimal impact
$M_{R,AC}$	Very significant impact	Significant impact	Very significant impact	Moderate impact	Minimal impact	Moderate impact	Minimal impact	Moderate impact
Th_{AC}	Very significant impact	Very significant impact	Very significant impact	Very significant impact	Minimal impact	Moderate impact	Minimal impact	Moderate impact
Wheel load	Very significant impact	Very significant impact	Minimal impact	Minimal impact	Minimal impact	Minimal impact	Minimal impact	Minimal impact

Very significant impact
Significant impact
Moderate impact
Minimal impact

6.2 FUTURE WORK

The insight gained from sensitivity analysis is being utilized in the development of a load restriction decision tool-kit for assessment of pavement capacity and to make traffic allowance decisions during and after periods of excessive moisture. The developed platform will be calibrated and validated using information from MnROAD (and other agency data if made available to researchers) on pavement sub-surface moisture states and pavement surface deflections (from FWD testing).

REFERENCES

Chapuis, R. P. (2004). “Predicting the saturated hydraulic conductivity of sand and gravel using effective diameter and void ratio.” *Canadian Geotechnical Journal*, NRC Research Press Ottawa, Canada , 41(5), 787–795.

van Genuchten, M. T. (1980). “A Closed-form Equation for Predicting the Hydraulic Conductivity of Unsaturated Soils.” *Soil Science Society of America Journal*, Wiley, 44(5), 892–898.

Ghayoomi, M., Dave, E., and Mousavi, S. (2019). “Mechanistic Load Restriction Decision Platform for Pavement Systems Prone to Moisture Variations National Road Research Alliance MnDOT Contract 1034192 Task 2: Literature Review.”

Mbonimpa, M., Aubertin, M., Chapuis, R. P., and Bussière, B. (2002). “Practical pedotransfer functions for estimating the saturated hydraulic conductivity.” *Geotechnical and Geological Engineering*, 20(3), 235–259.

Mousavi, S., Ghayoomi, M., and Dave, E. (2020). *Mechanistic Load Restriction Decision Platform for Pavement Systems Prone to Moisture Variations National Road Research Alliance MnDOT Contract 1034192 Task 3: System Dynamics Framework Development*.

Saltelli, A., Ratto, M., Andres, T., Campolongo, F., Cariboni, J., Gatelli, D., Saisana, M., and Tarantola, S. (2008). *Global Sensitivity Analysis: The Primer*. *John Wiley & Sons*.

Tang, Y., Reed, P., Wagener, T., Van Werkhoven, K., and Wagener, T. (2007). *Comparing sensitivity analysis methods to advance lumped watershed model identification and evaluation*. *European Geosciences Union*.

Wei, T. (2013). “A review of sensitivity analysis methods in building energy analysis.” *Renewable and Sustainable Energy Reviews*, Pergamon.

Zapata, C. E., Witczak, M. W., Houston, W. N., and Andrei, D. (2007). “Incorporation of Environmental Effects in Pavement Design.” *Road Materials and Pavement Design*, Taylor & Francis Group , 8(4), 667–693.

APPENDIX

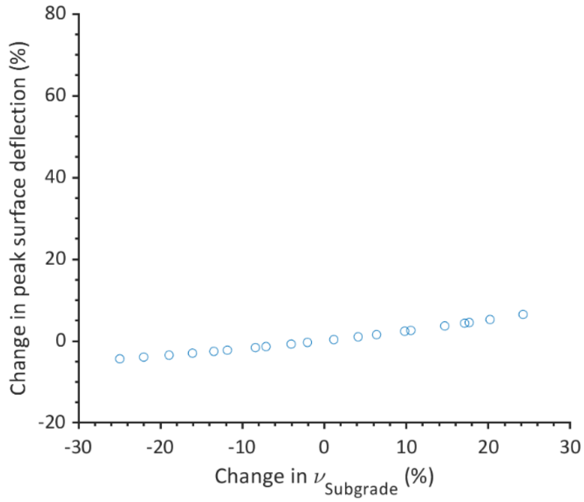

Figure A-1. Sensitivity of peak surface deflection to the variations of subgrade Poisson's ratio for coarse-grained subgrade model.

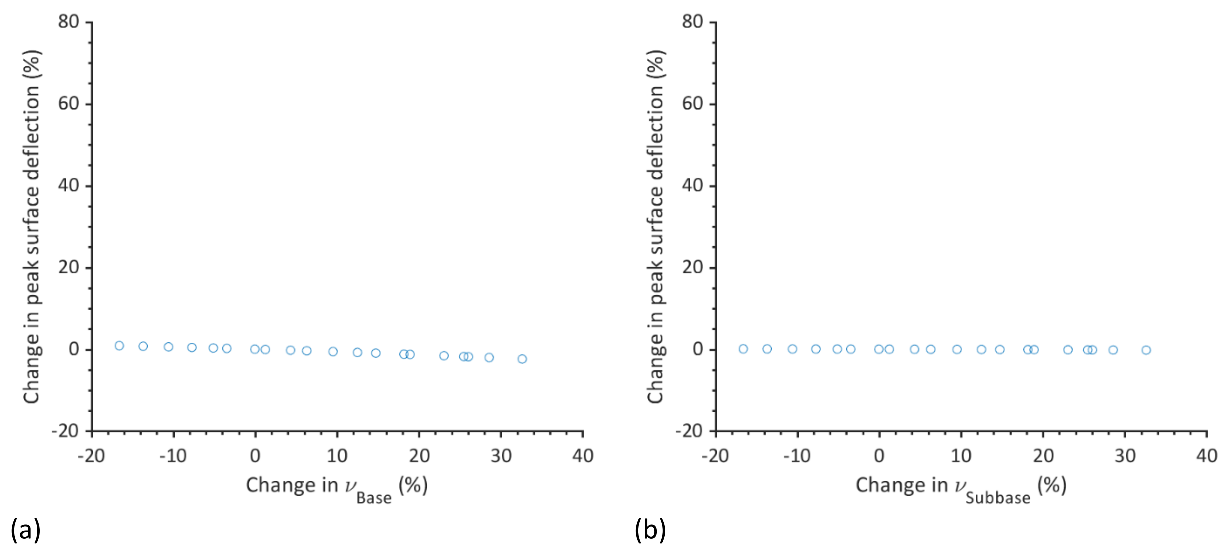

Figure A-2. Sensitivity of peak surface deflection to the variations of (a) base and (b) subbase Poisson's ratio for coarse-grained subgrade model.

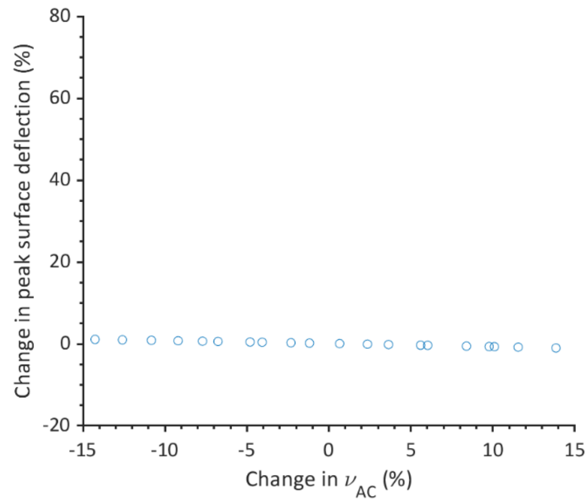

Figure A-3. Sensitivity of peak surface deflection to the variations of AC Poisson's ratio for coarse-grained subgrade model.

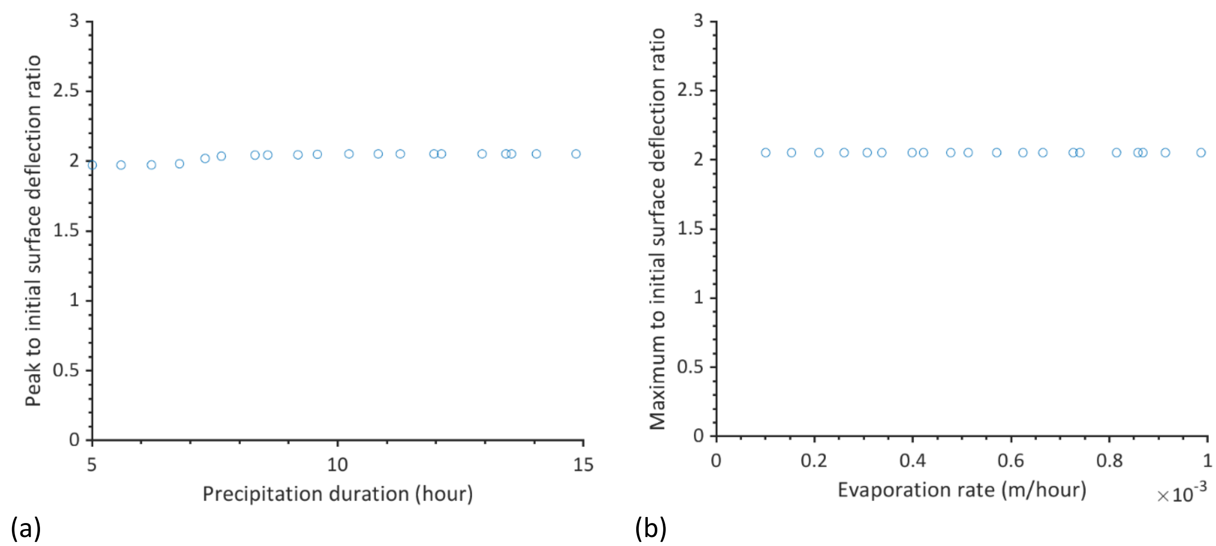

Figure A-4. Sensitivity of δ_p/δ_0 to variations in (a) precipitation duration and (b) evaporation rate for coarse-grained subgrade model.

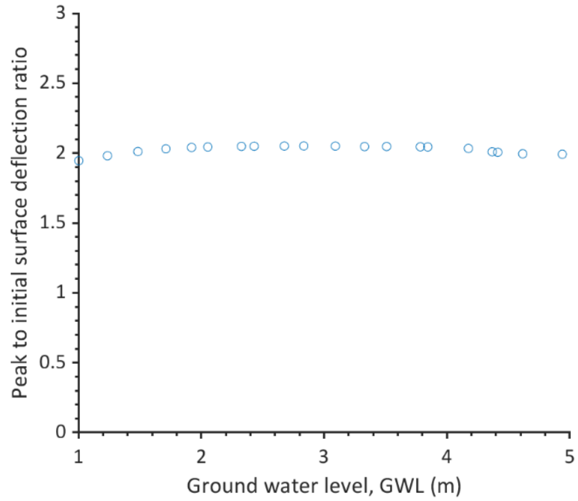

Figure A-5. Sensitivity of δ_p/δ_0 to variations in initial GWL for coarse-grained subgrade model.

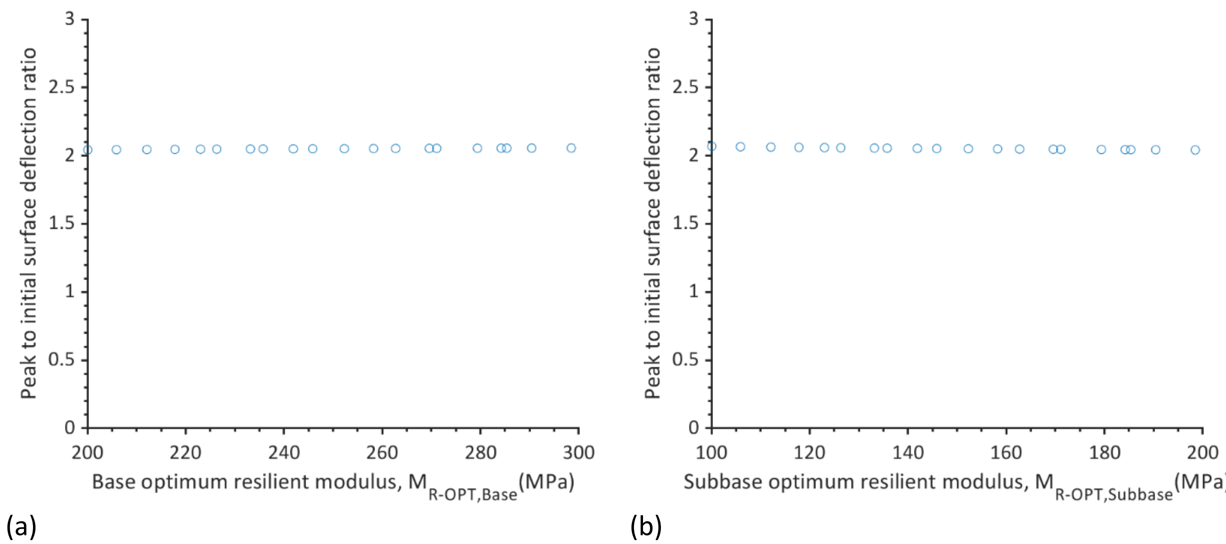

Figure A-6. Sensitivity of δ_p/δ_0 to variations in (a) aggregate base and (b) subbase optimum resilient moduli for coarse-grained subgrade model.

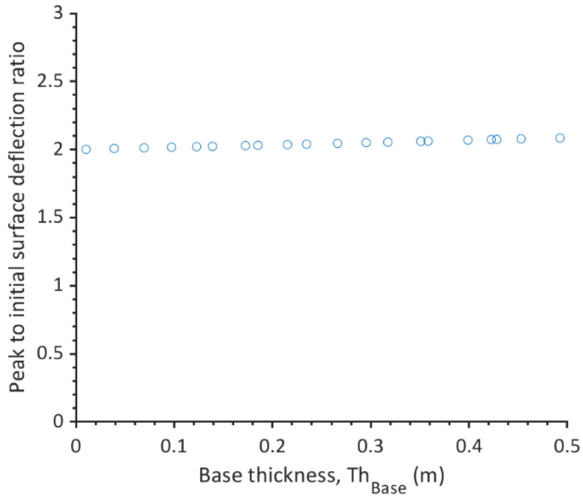

(a)

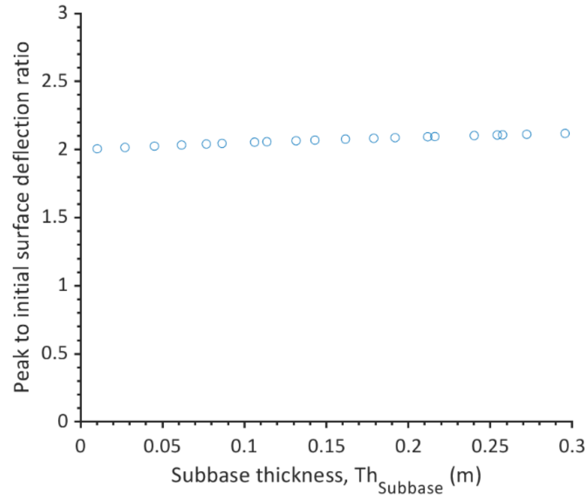

(b)

Figure A-7. Sensitivity of δ_p/δ_0 to variations in (a) aggregate base and (b) subbase thicknesses for coarse-grained subgrade model.

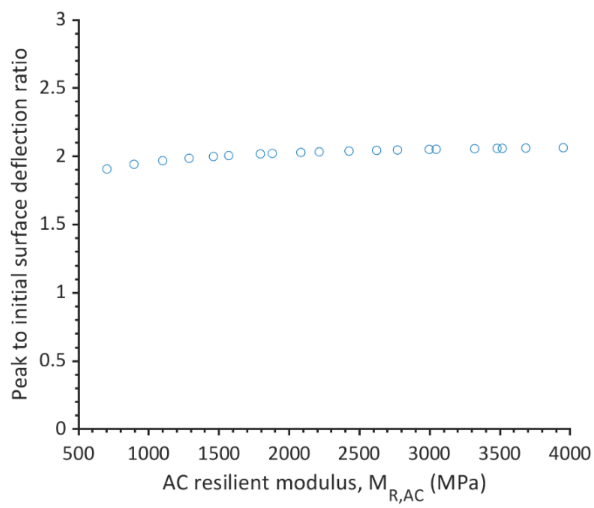

Figure A-8. Sensitivity of δ_p/δ_0 to variations in AC resilient modulus for coarse-grained subgrade model.

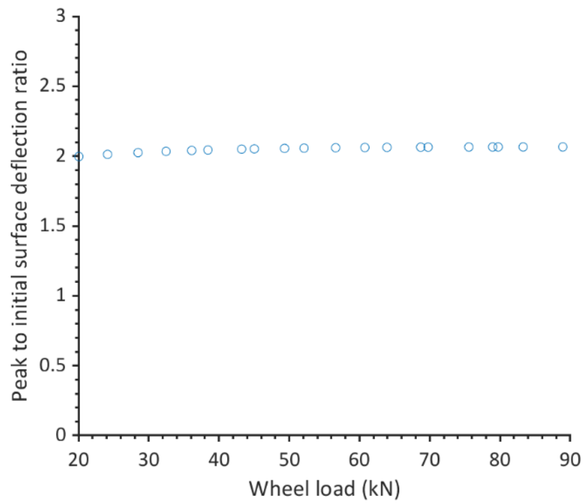

Figure A-9. Sensitivity of δ_p/δ_0 to variations in wheel load for coarse-grained subgrade model.

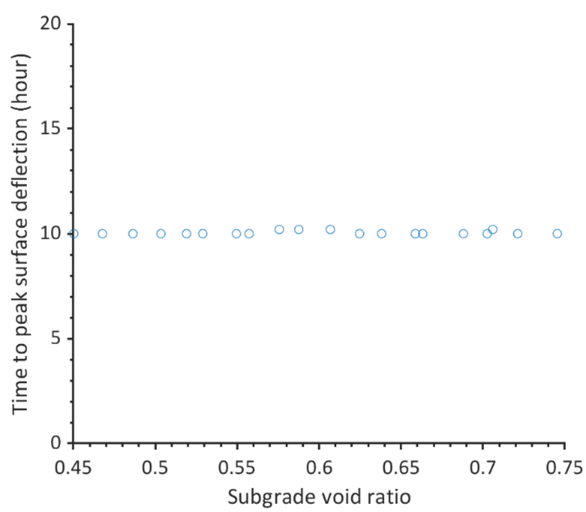

Figure A-10. Sensitivity of t_P to variations in subgrade void ratio for coarse-grained subgrade model.

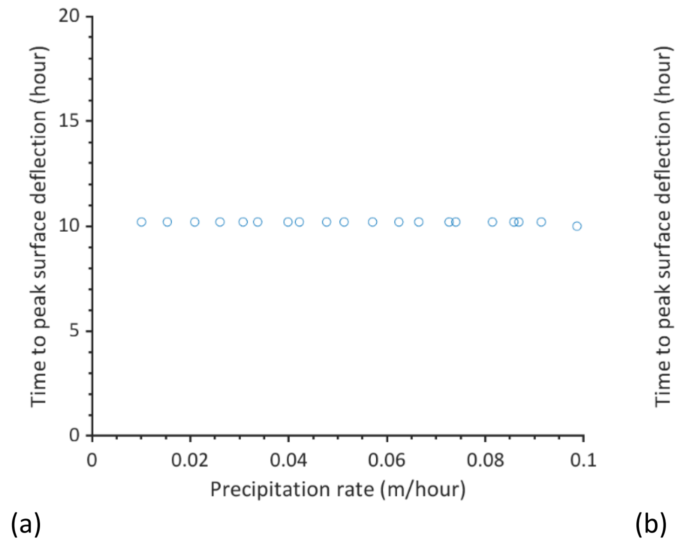

Figure A-11. Sensitivity of t_P to variations in precipitation (a) rate and (b) duration for coarse-grained subgrade model.

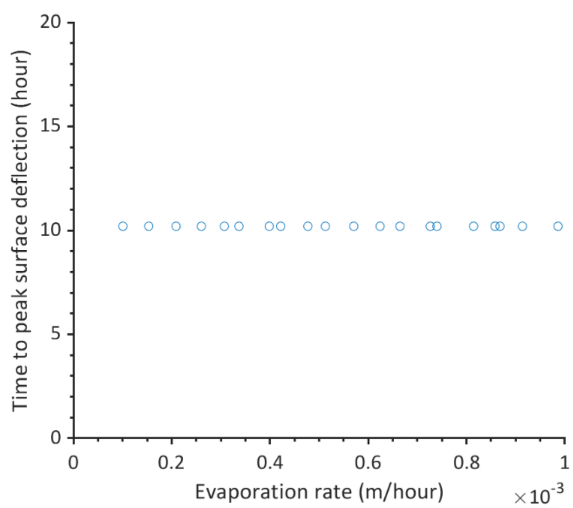

Figure A-12. Sensitivity of t_P to variations in evaporation rate for coarse-grained subgrade model.

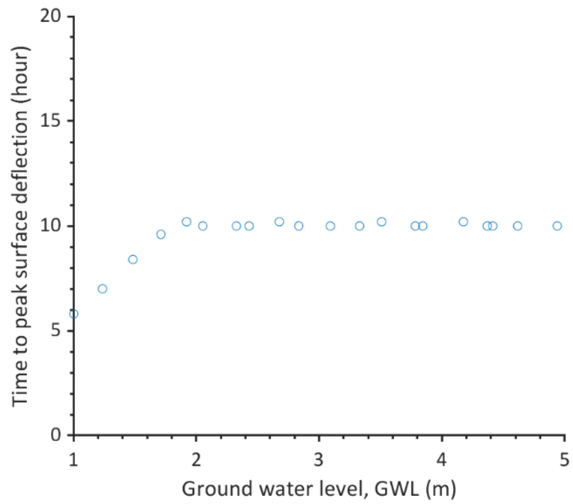

Figure A-13. Sensitivity of t_P to variations in initial GWL for coarse-grained subgrade model.

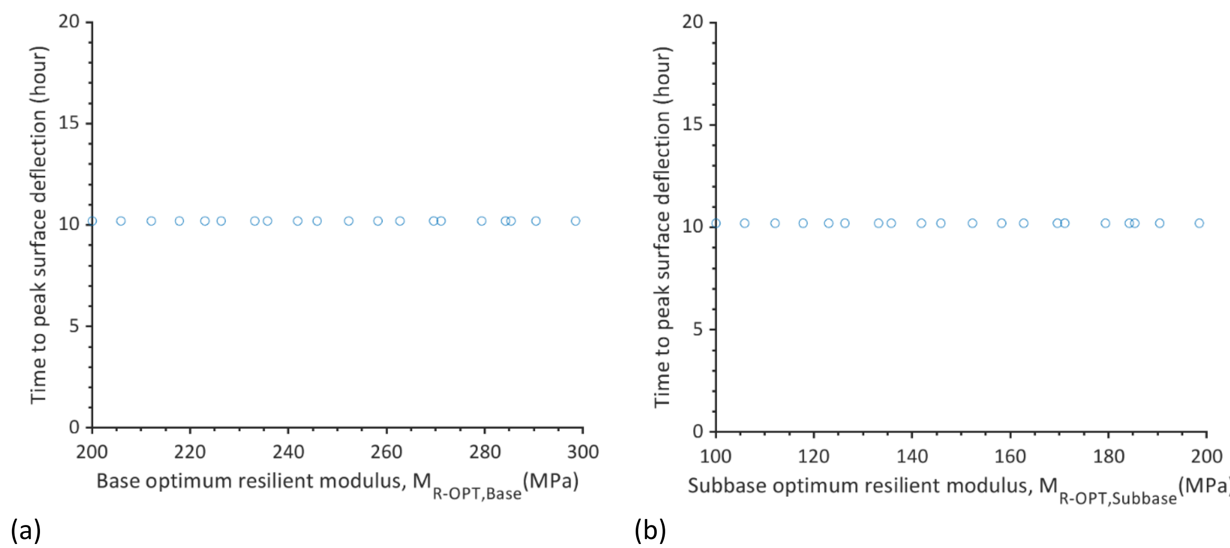

Figure A-14. Sensitivity of t_P to variations in (a) aggregate base and (b) subbase optimum resilient moduli for coarse-grained subgrade model.

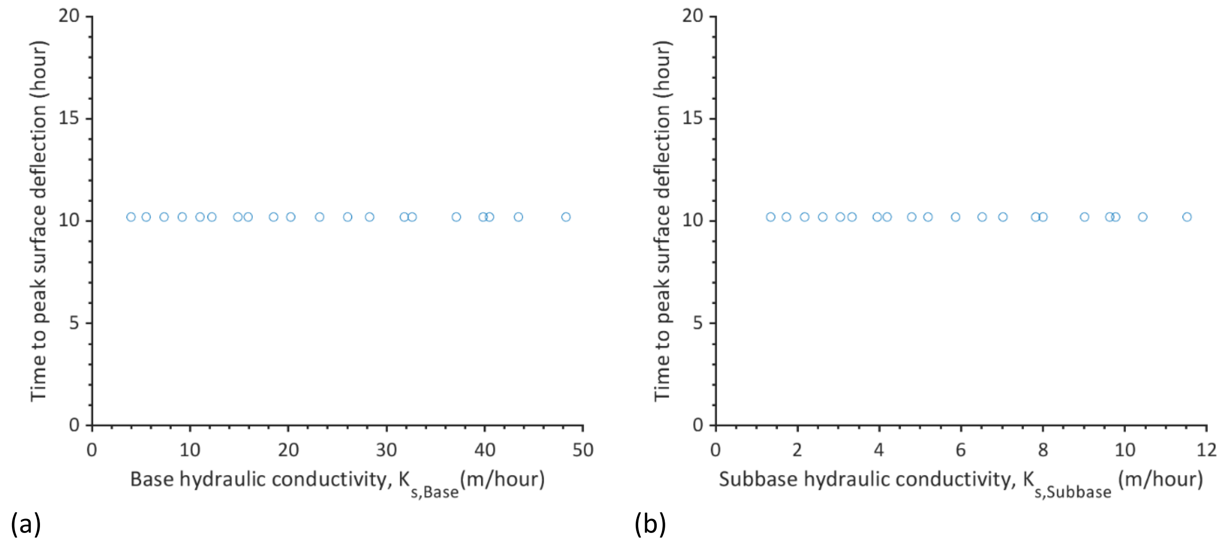

Figure A-15. Sensitivity of t_P to the variations of (a) aggregate base and (b) subbase hydraulic conductivities for coarse-grained subgrade model.

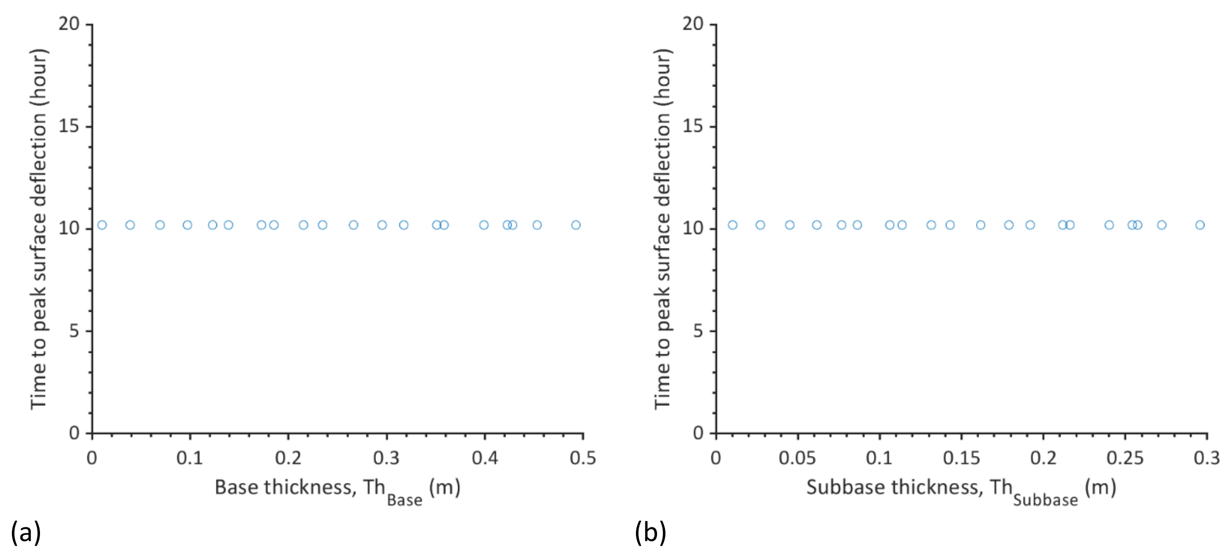

Figure A-16. Sensitivity of t_P to variations in (a) aggregate base and (b) subbase thicknesses for coarse-grained subgrade model.

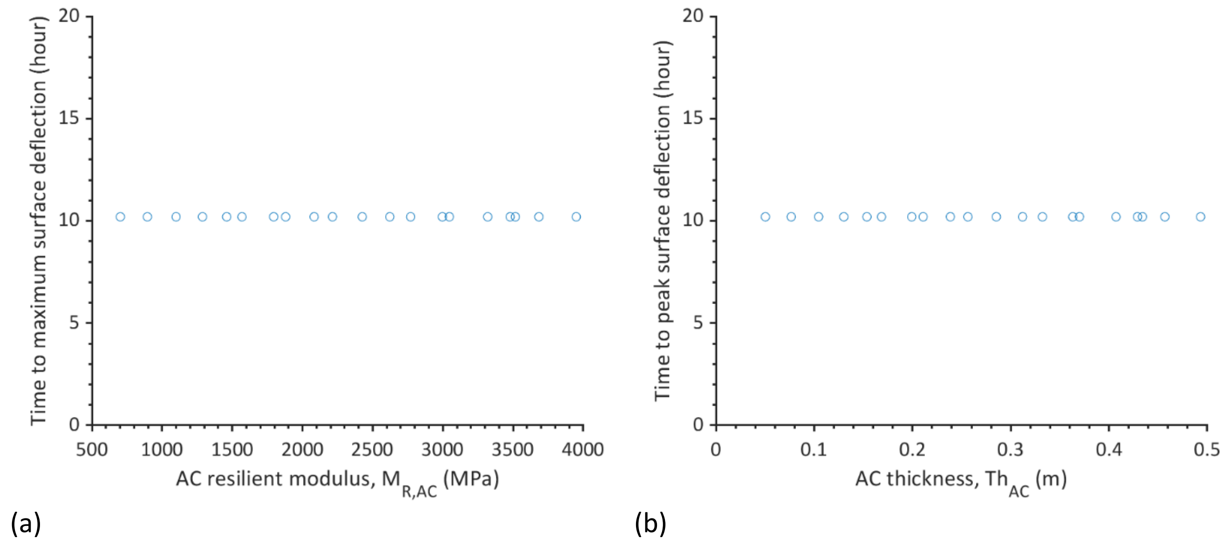

Figure A-17. Sensitivity of t_P to variations in AC (a) resilient modulus and (b) thickness for coarse-grained subgrade model.

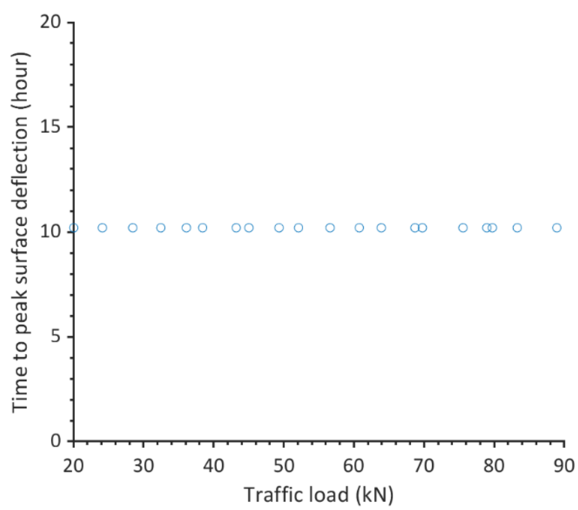

Figure A-18. Sensitivity of t_P to variations in wheel load for coarse-grained subgrade model for coarse-grained subgrade model.

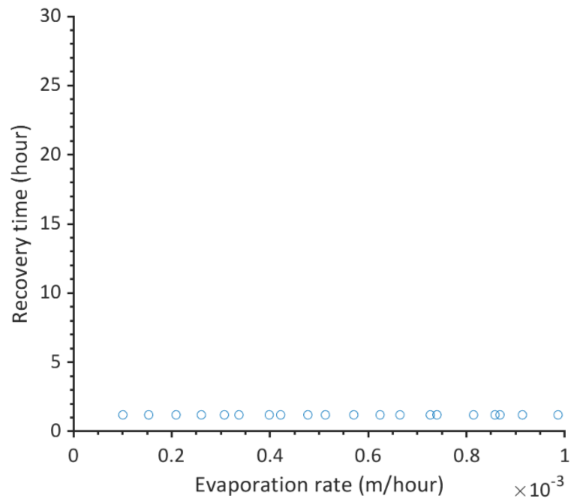

Figure A-19. Sensitivity of t_R to variations in evaporation rate for coarse-grained subgrade model.

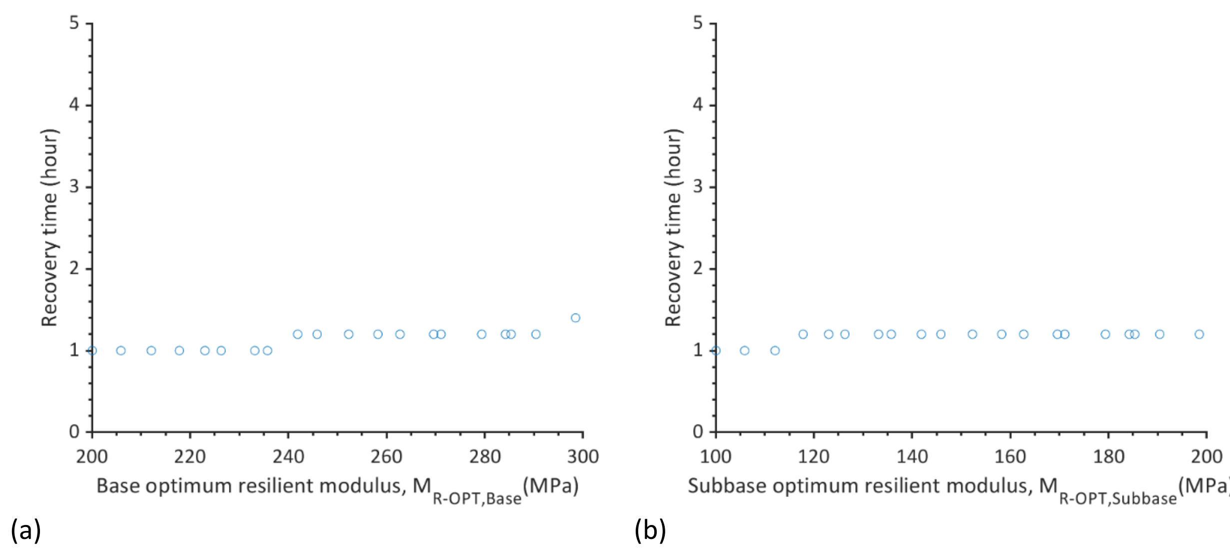

Figure A-20. Sensitivity of t_R to variations in (a) aggregate base and (b) subbase optimum resilient moduli for coarse-grained subgrade model.

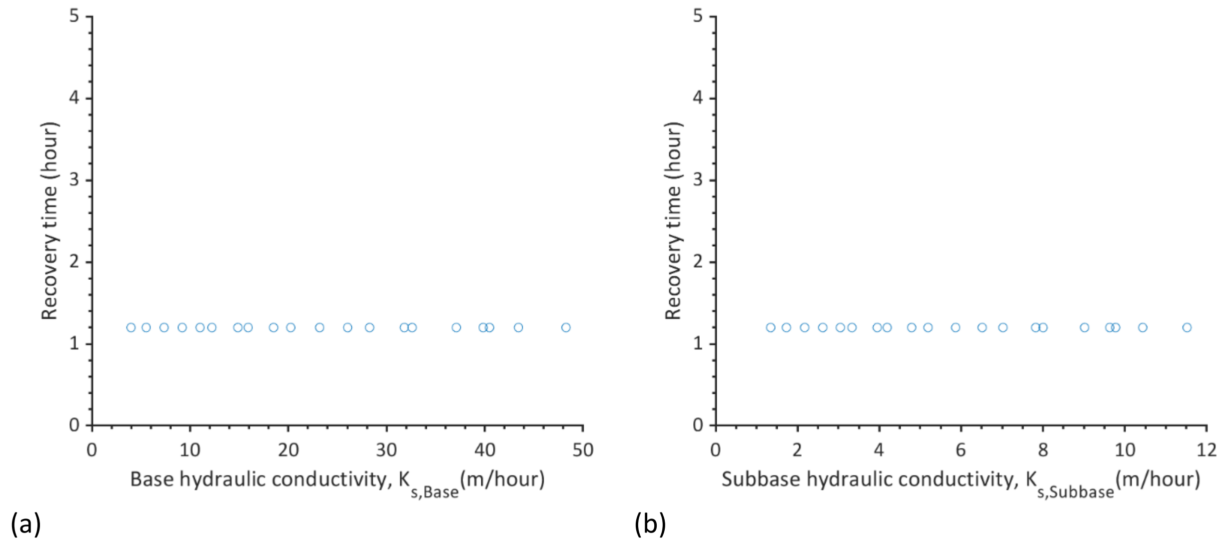

Figure A-21. Sensitivity of t_R to the variations of (a) aggregate base and (b) subbase hydraulic conductivities for coarse-grained subgrade model.

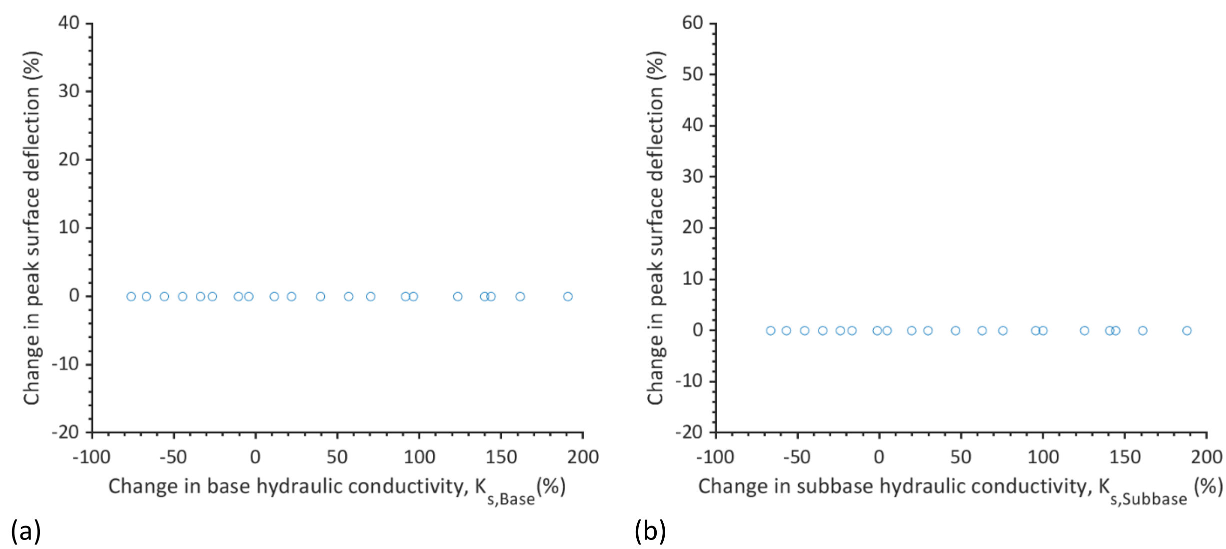

Figure A-22. Sensitivity of peak surface deflection to the variations of (a) aggregate base and (b) subbase hydraulic conductivities for fine-grained subgrade model.

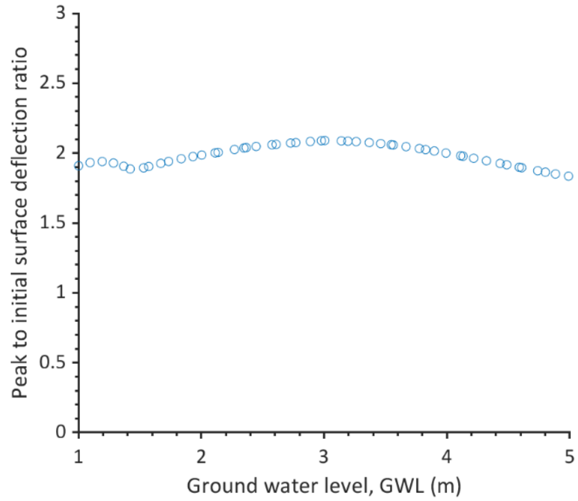

Figure A-23. Sensitivity of δ_p/δ_0 to variation in initial GWL for fine-grained subgrade model.

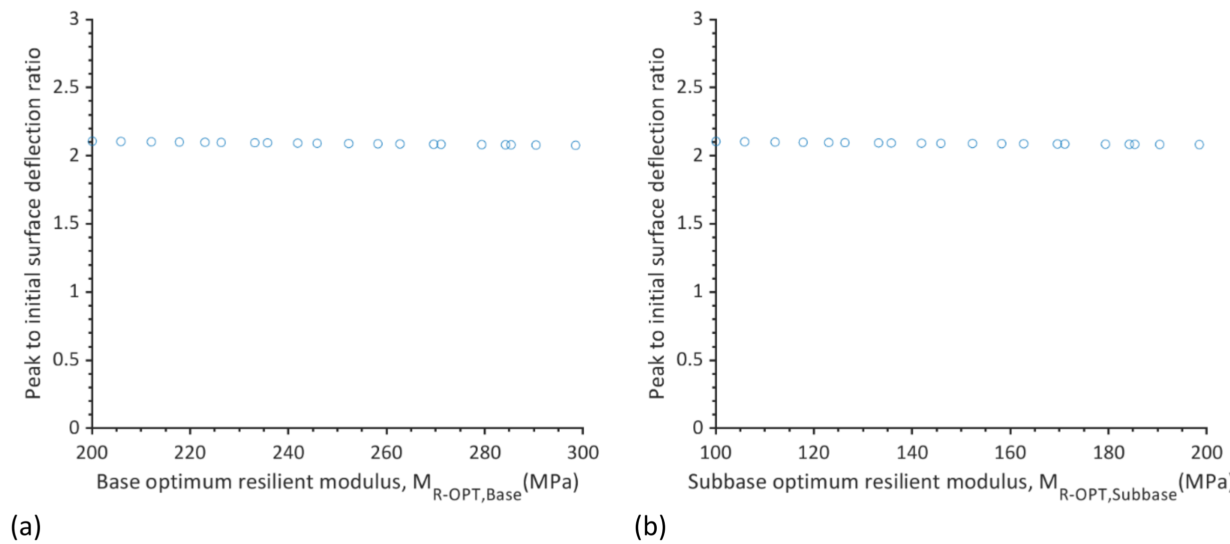

Figure A-24. Sensitivity of δ_p/δ_0 to variations in (a) aggregate base and (b) subbase optimum resilient moduli for fine-grained subgrade model.

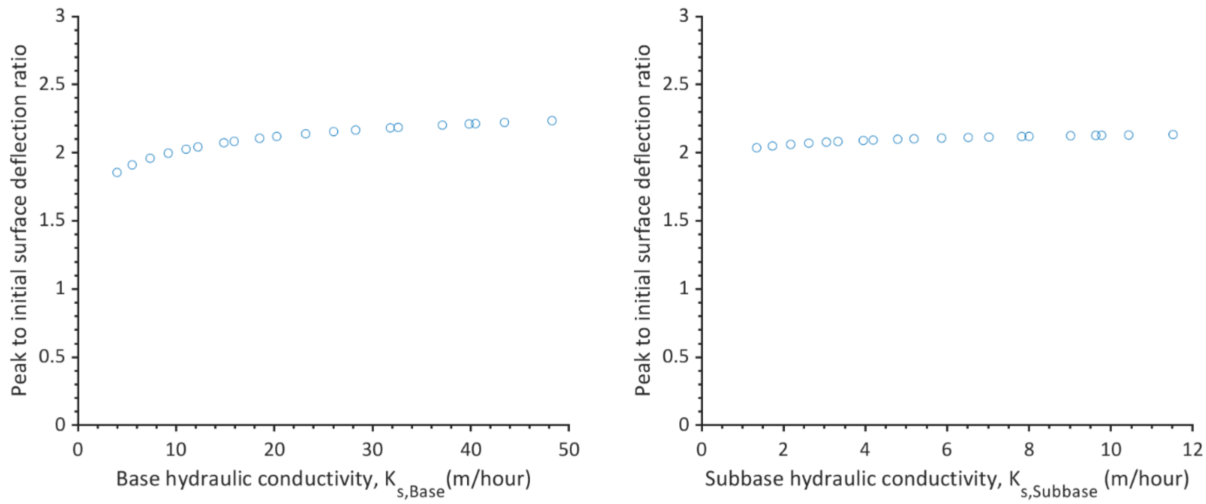

(a) (b)

Figure A-25. Sensitivity of δ_p/δ_0 to the variations of (a) aggregate base and (b) subbase hydraulic conductivities for fine-grained subgrade model.

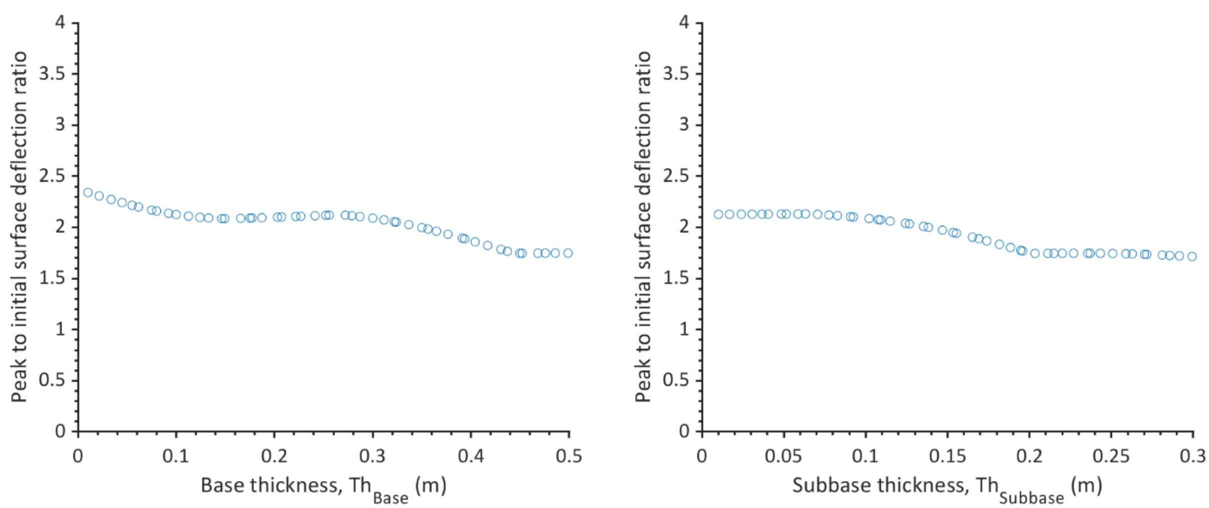

(a) (b)

Figure A-26. Sensitivity of δ_p/δ_0 to variations in (a) aggregate base and (b) subbase thicknesses for fine-grained subgrade model.

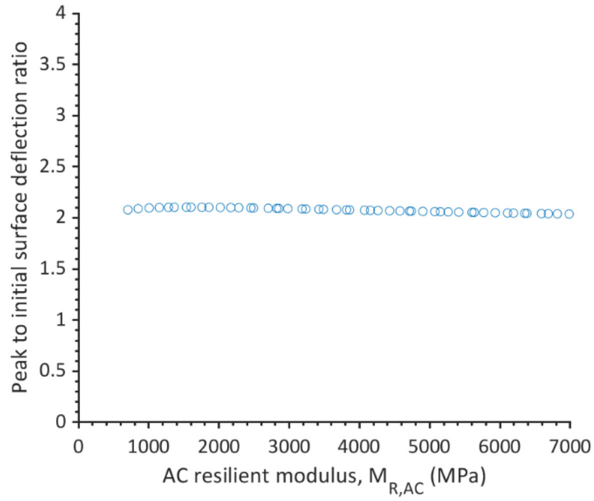

Figure A-27. Sensitivity of δ_p/δ_0 to variations in AC resilient modulus for fine-grained subgrade model.

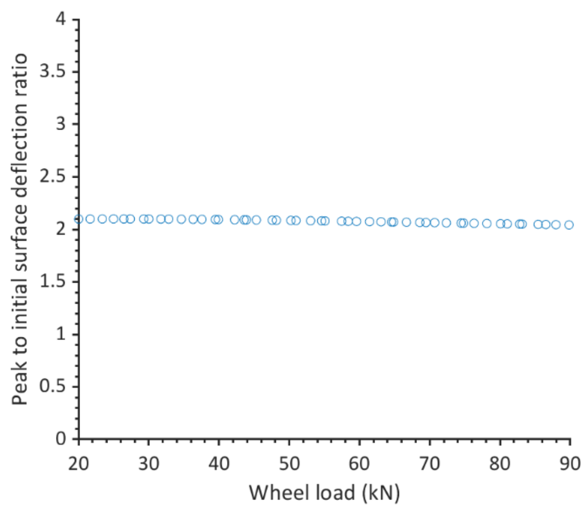

Figure A-28. Sensitivity of δ_p/δ_0 to variations in wheel load for fine-grained subgrade model.

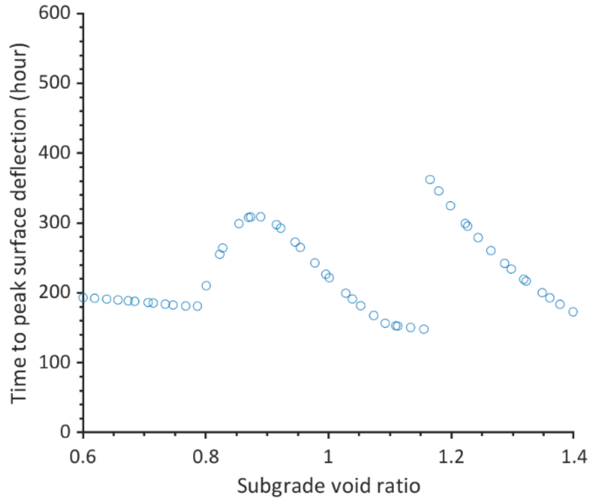

Figure A-29. Sensitivity of t_P to variations in subgrade void ratio for fine-grained subgrade model.

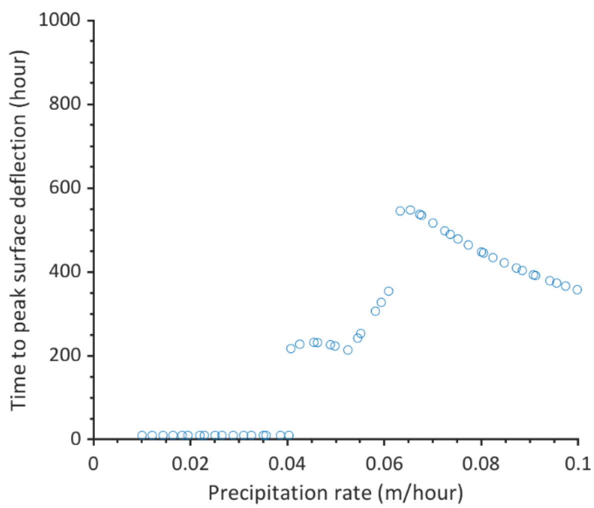

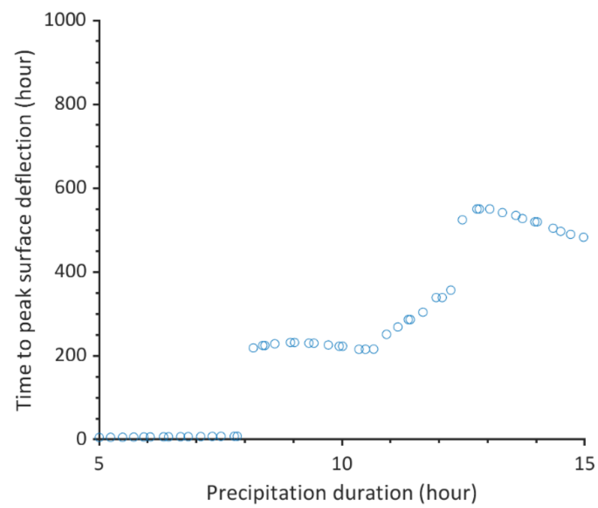

Figure A-30. Sensitivity of t_P to variations in precipitation (a) rate and (b) duration for fine-grained subgrade model.

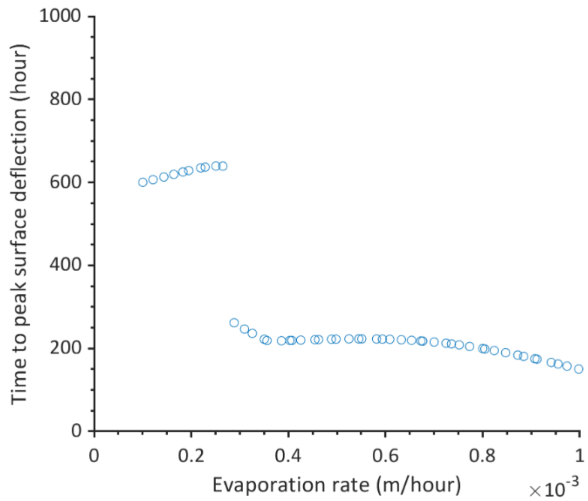

Figure A-31. Sensitivity of t_P to variations in evaporation rate for fine-grained subgrade model.

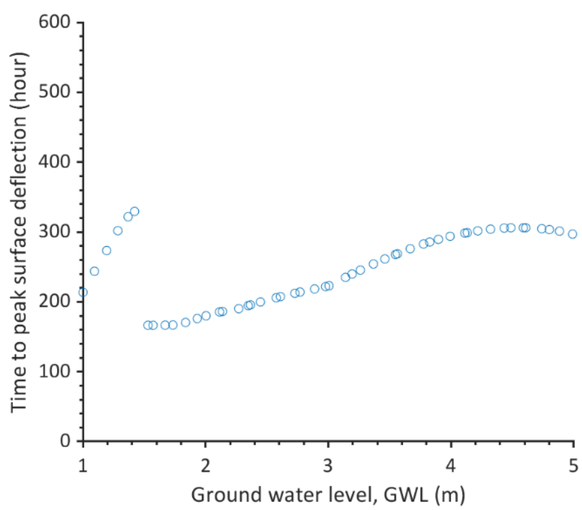

Figure A-32. Sensitivity of t_P to variations in initial GWL for fine-grained subgrade model.

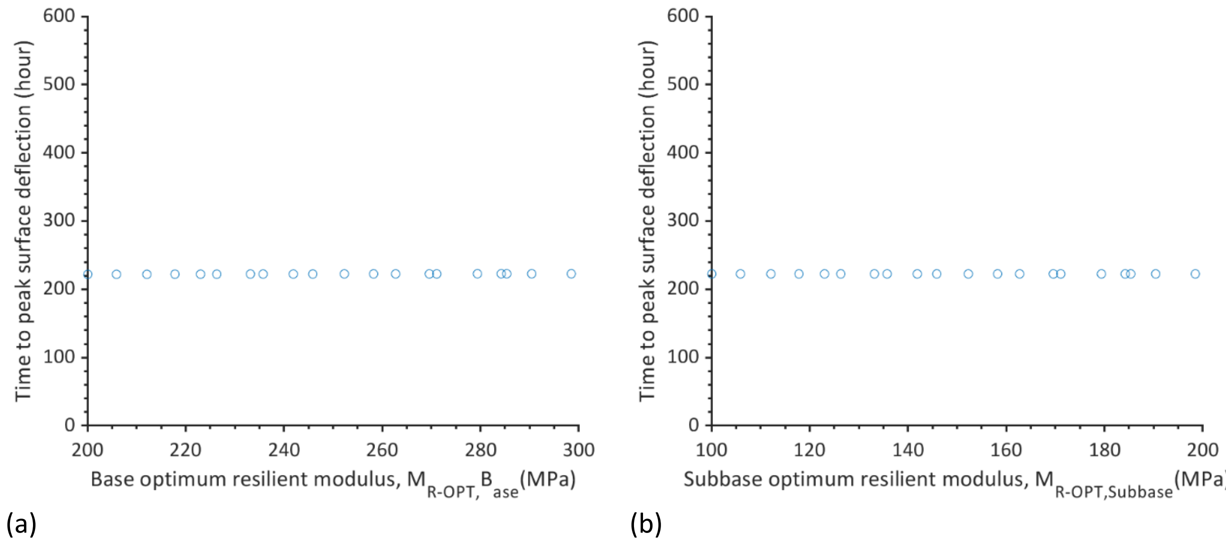

Figure A-33. Sensitivity of t_P to variations in (a) aggregate base and (b) subbase optimum resilient moduli for fine-grained subgrade model.

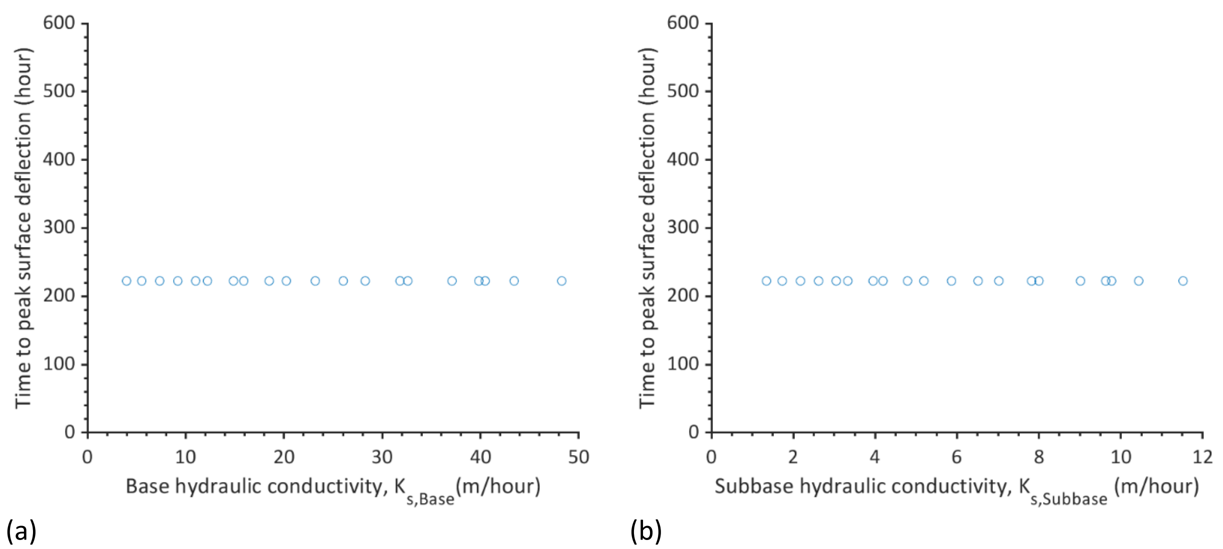

Figure A-34. Sensitivity of t_P to the variations of (a) aggregate base and (b) subbase hydraulic conductivities for fine-grained subgrade model.

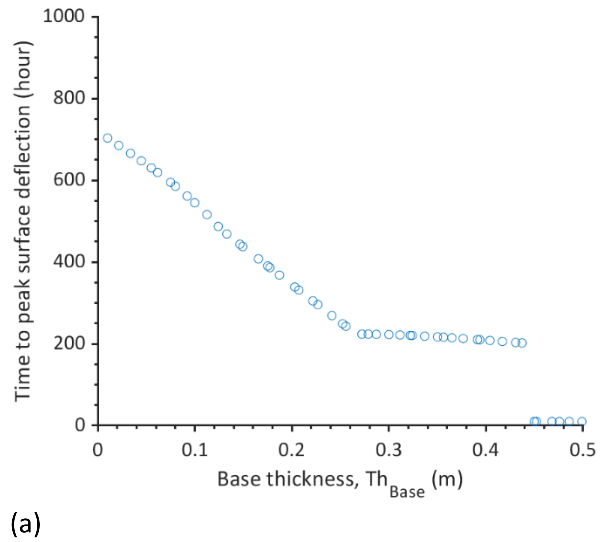

Figure A-35. Sensitivity of t_P to variations in (a) aggregate base and (b) subbase thicknesses for fine-grained subgrade model.

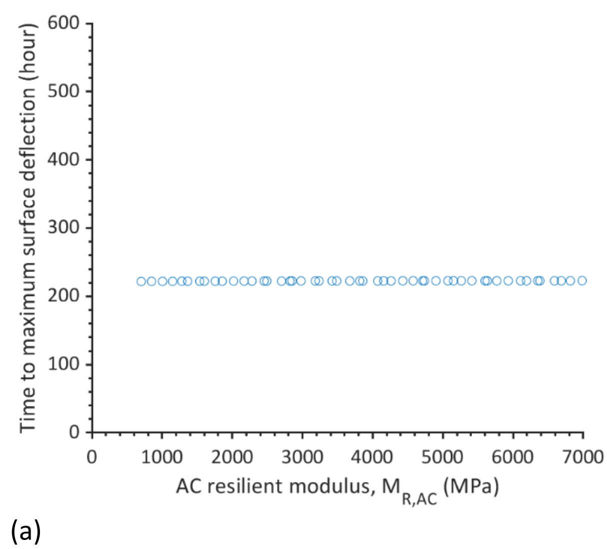

Figure A-36. Sensitivity of t_P to variations in AC (a) resilient modulus and (b) thickness for fine-grained subgrade model.

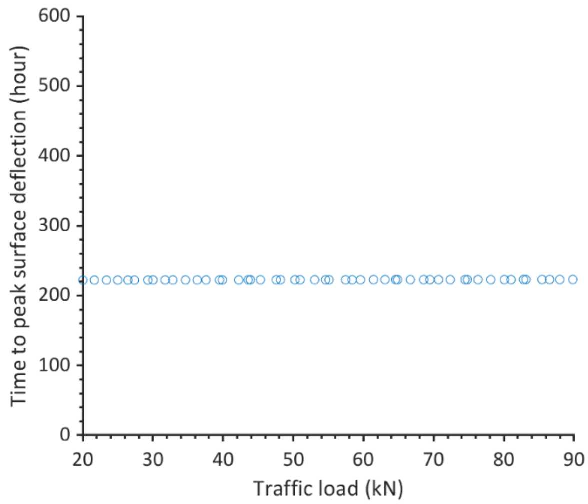

Figure A-37. Sensitivity of t_P to variations in wheel load for coarse-grained subgrade model for fine-grained subgrade model.

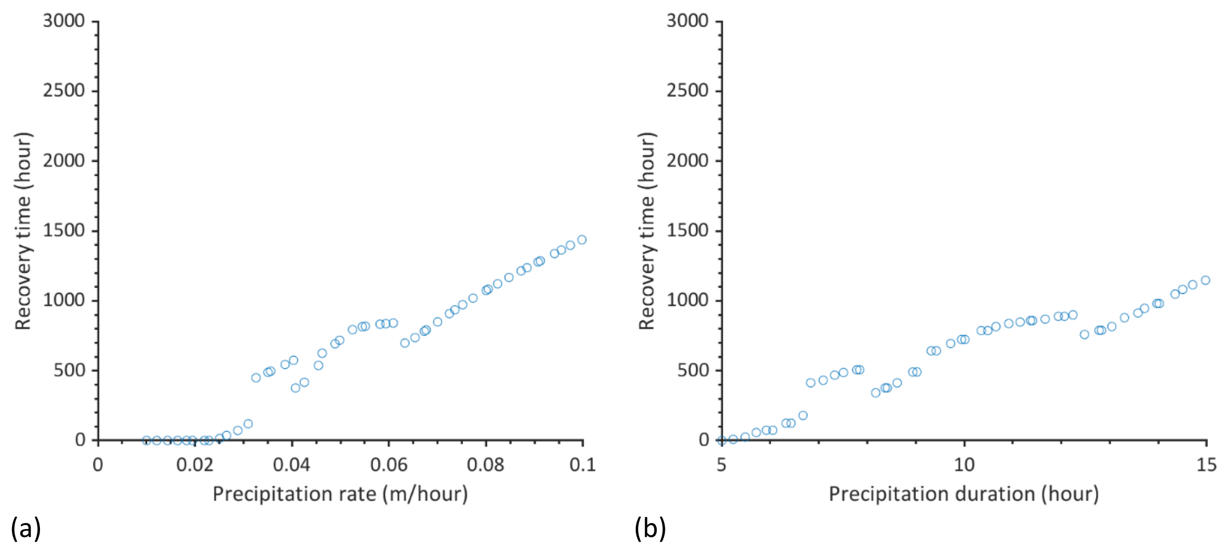

Figure A-38. Sensitivity of t_R to variations in precipitation (a) rate and (b) duration for fine-grained subgrade model.

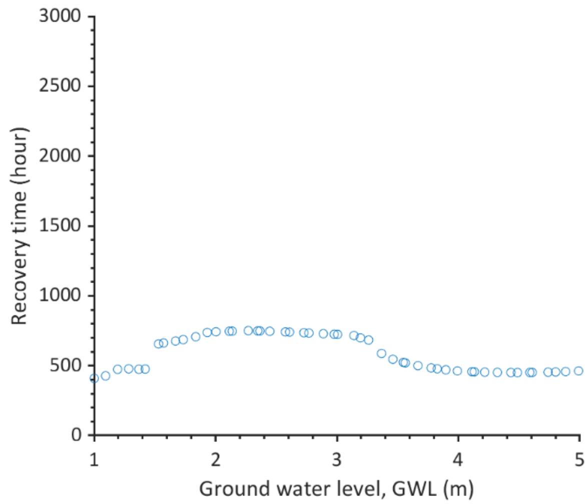

Figure A-39. Sensitivity of t_R to variations in initial GWL for fine-grained subgrade model.

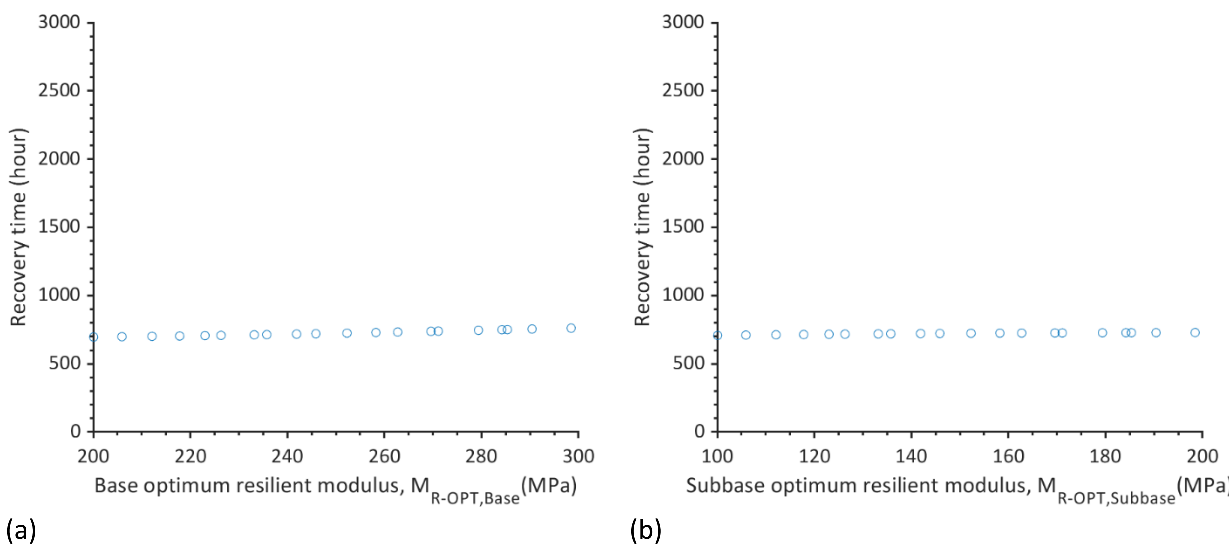

Figure A-40. Sensitivity of t_R to variations in (a) aggregate base and (b) subbase optimum resilient moduli for fine-grained subgrade model.

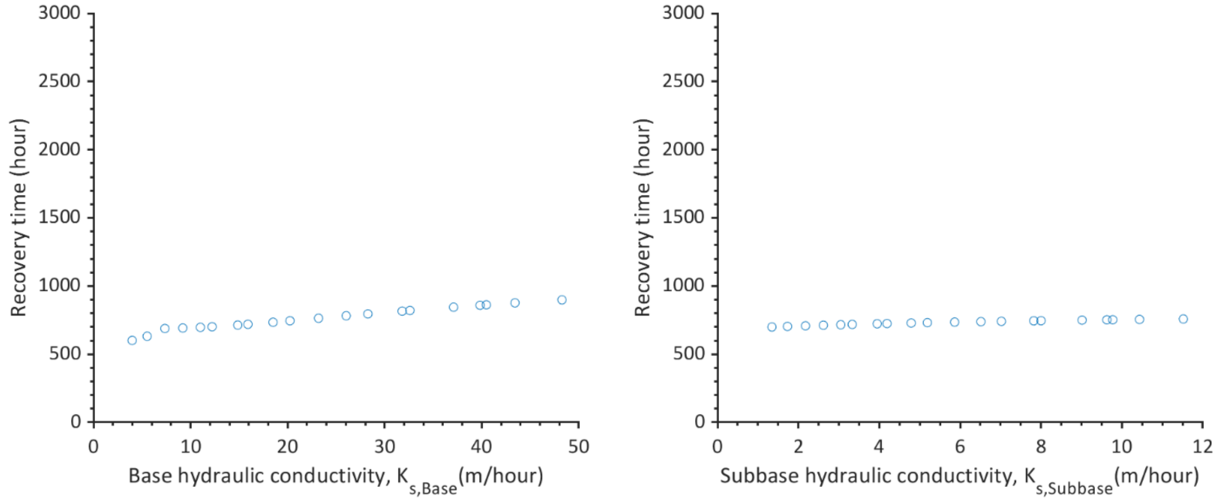

(a) (b)

Figure A-41. Sensitivity of t_R to the variations of (a) base and (b) subbase hydraulic conductivities for fine-grained subgrade model.

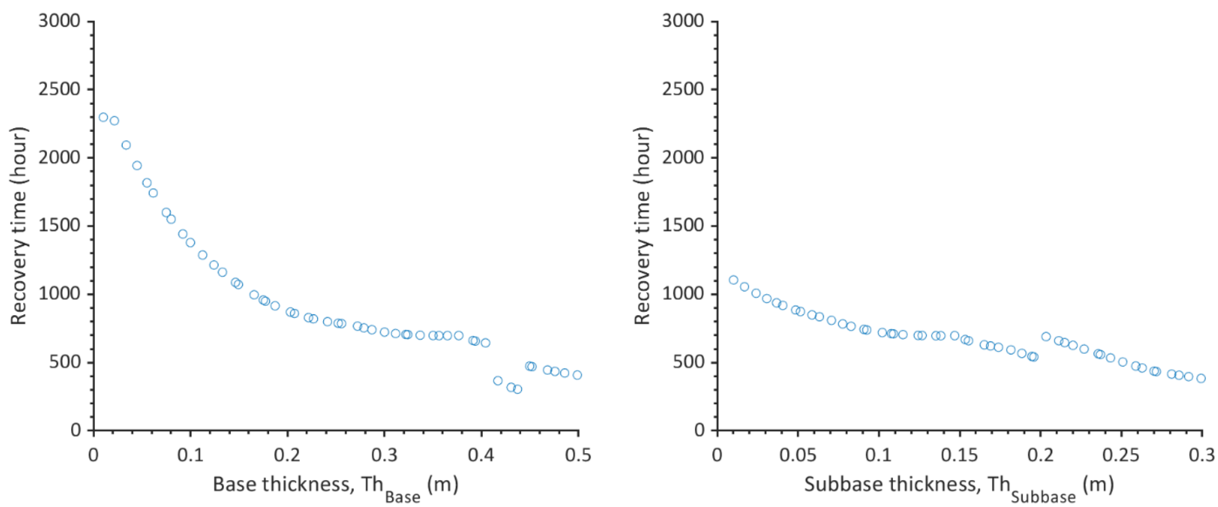

(a) (b)

Figure A-42. Sensitivity of t_R to variations in (a) base and (b) subbase thicknesses for fine-grained subgrade model.

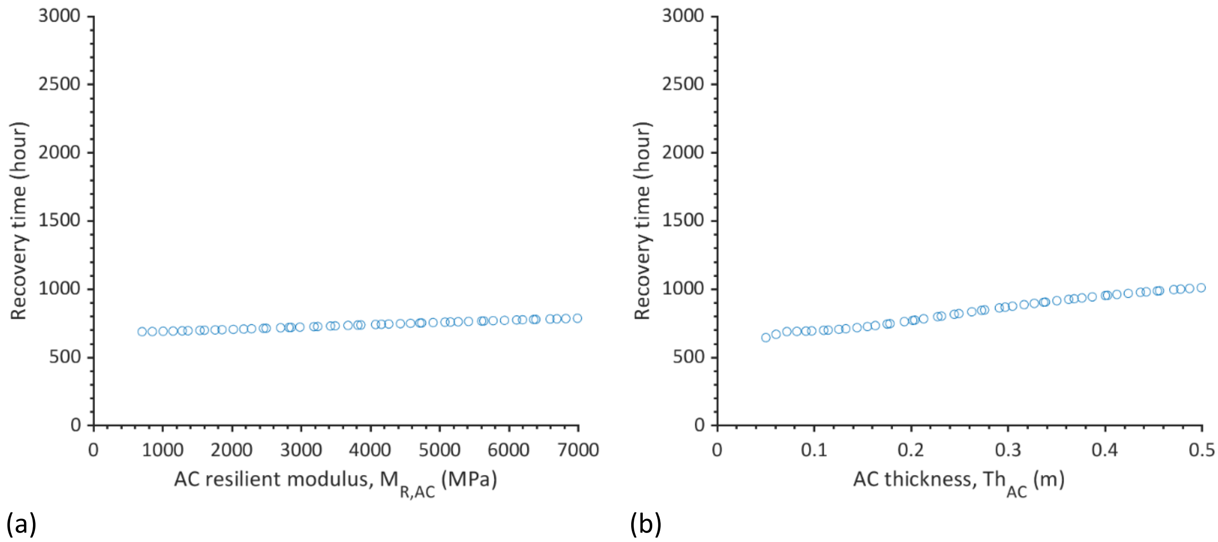

Figure A-43. Sensitivity of t_R to variations in AC (a) resilient modulus and (b) thickness for fine-grained subgrade model.

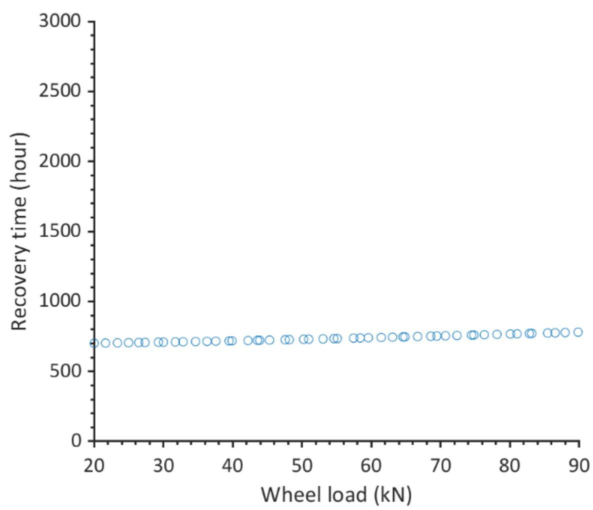

Figure A-44. Sensitivity of t_R to variations in wheel load for coarse-grained subgrade model for fine-grained subgrade model.